POLITECNICO
MILANO 1863

SCUOLA DI INGEGNERIA INDUSTRIALE
E DELL'INFORMAZIONE

A data-driven model for feedstock blending optimization in anaerobic co-digestion scenarios

TESI DI LAUREA MAGISTRALE IN
CHEMICAL ENGINEERING – INGEGNERIA CHIMICA

Author: **Alessia Goracci**

Student ID:	945882
Advisor:	Giulia Luisa Bozzano
Co-advisor:	Federico Moretta
Academic Year:	2020-21

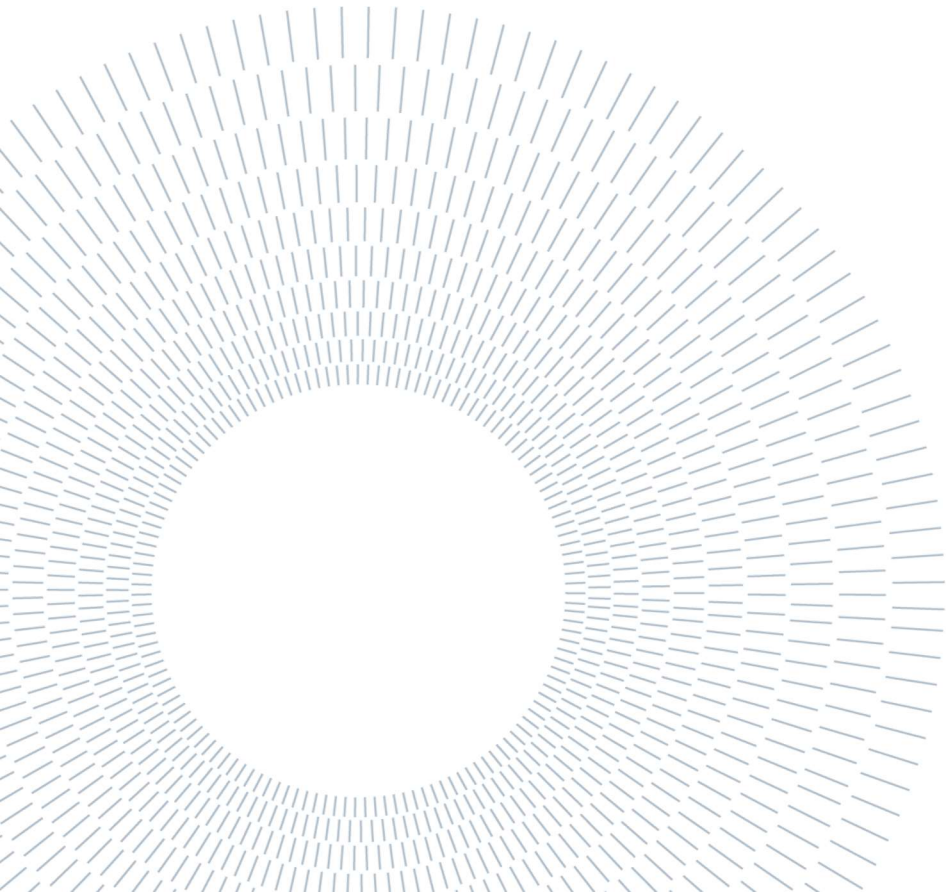

Abstract

The increasing energy demand and the growing environmental concerns have lately encouraged the exploitation of fossil-free, renewable energy sources. In this context, anaerobic digestion represents an interesting technology since it allows the production of biogas starting from substances made of waste (e.g., animal manure, agro-industrial and organic waste types, sludges), achieving at the same time their valorization and disposal. Single substrate digestion frequently leads to an under-exploitation of the raw material due to poor feedstock characteristics, resulting in low methane production. On the other hand, it has been demonstrated that the methane yield could be significantly increased by properly combining two or more substrates, performing an anaerobic co-digestion. Throughout the years, many studies have been carried out to understand how different raw materials should be combined to maximize their co-digestion performances; however, an easy-to-use and quick technology able to predict their best blending conditions does not exist in literature. Consequently, the purpose of this project is to create a model that with few, simple inputs is able to estimate with good precision the optimal blending ratios of mixtures of substrates to maximize the methane yield of their co-digestion. The extremely large number of possible raw materials and the high variability of their compositions depending on their source reflect the high complexity of the problem; thus, the starting point has been the creation of a database where data about commonly used substrates have been collected from literature. These data have been then analysed and exploited to build a data-driven optimization model that, through the maximization of an objective function representing the biomethane potential (BMP) of a mixture, is able to calculate the optimal composition of the feedstock. This model, initially based on lab-scale batch tests, has also been improved to make it suitable for industrial-scale scenarios, so that the optimal feedstock blending of batch and CSTR-based digesters is calculated taking into account supply chain factors such as substrates availability and storage capabilities of the plant. In addition, an Excel dashboard linked with a Python™ algorithm has been developed to make calculations more practical in view of an industrial usage. The optimization model has been validated by the comparison of its results with the ones of experimental batch tests available in literature and with

industrial data that have been provided by two companies. After validation, this innovative model has demonstrated to yield satisfactory and practical findings.

Key-words: anaerobic co-digestion; biogas; feedstock; optimization; model; data-driven; software; programming.

Abstract in lingua italiana

La crescente domanda di energia e l'interesse nella transizione ecologica hanno incoraggiato negli ultimi anni lo sfruttamento di fonti di energia alternative rispetto a quelle di origine fossile. In questo contesto, la digestione anaerobica ha guadagnato particolare attenzione in quanto permette la produzione di biogas a partire da scarti di varia natura (letame animale, rifiuti agro-industriali e organici, fanghi di depurazione), permettendone allo stesso tempo lo smaltimento e la valorizzazione. La digestione di un singolo tipo di substrato porta spesso a basse rese in biometano in quanto l'alimentazione potrebbe presentare caratteristiche non ottimali. È stato invece dimostrato che rese maggiori possono essere ottenute alimentando due o più substrati, effettuando in questo caso una co-digestione anaerobica. Negli anni sono stati effettuati numerosi studi riguardo come diversi substrati dovrebbero essere combinati per ottenere la massima resa possibile; tuttavia, in letteratura non esistono modelli in grado di fornire in maniera semplice e veloce le migliori condizioni di miscelazione. Lo scopo di questo progetto, quindi, è quello di creare un modello che, con pochi e semplici input, riesca a predire in quali rapporti certi substrati debbano essere miscelati in modo da ottenere la massima resa possibile in biometano. Il grande numero di possibili materie prime e l'alta variabilità delle loro composizioni a seconda dell'origine riflettono la complessità di questo problema; il punto di partenza è stato quindi raccogliere in un database un gran numero di dati riguardo i substrati più comuni. Grazie all'analisi di questi dati, è stato costruito un modello di ottimizzazione data-driven che, attraverso la massimizzazione di una funzione rappresentante il potenziale di biometano (BMP) della miscela, è in grado di calcolare la composizione ottima del feedstock. Questo tool, inizialmente costruito sulla base di batch test in scala di laboratorio, è stato poi migliorato per renderlo adeguato all'applicazione su scala industriale, in modo da calcolare il blending ottimo dell'alimentazione di digestori anaerobici industriali di tipo batch e CSTR, tenendo anche in considerazione fattori relativi alla supply chain quali la disponibilità delle materie prime e la capacità di stoccaggio dei rifiuti dell'impianto. In più, è stata anche creata una dashboard su Excel, connessa ad un algoritmo scritto nel linguaggio Python™, in modo da rendere i calcoli più pratici in vista di un utilizzo a livello industriale. I risultati del modello sono

stati validati grazie al confronto con quelli di sperimentazioni in scala di laboratorio, disponibili in letteratura, e con dati industriali che sono stati forniti da due aziende del settore. A seguito della sua validazione, è possibile affermare che questo modello innovativo è in grado di fornire risultati soddisfacenti e affidabili.

Parole chiave: co-digestione anaerobica; biogas; alimentazione; ottimizzazione; modello; data-driven; software; programmazione.

Contents

1. Introduction: Anaerobic Digestion and co-Digestion

Anaerobic digestion (AD) is a process through which a variety of substrates is degraded to produce mainly methane and carbon dioxide – which together represent the biogas – and a liquid-solid residue called digestate. Substrates that can be used are typically waste such as manure, agricultural and organic waste, sludges which are this way recovered as renewable energy sources. On the other hand, up to now, due to the complexity of the process itself, there is not much information about its optimization and often methane yields result to be low with respect to the potential of the raw materials. One of the possible causes of low yields lays on an inappropriate feedstock composition, which may cause process inhibition. A possible solution to obtain optimal feedstock conditions is the anaerobic co-digestion (AcoD) of two or more substrates, which may allow to obtain a balance of macro and micronutrients, optimal properties, and synergistic effects.
This chapter aims at giving an overview of the anaerobic digestion and co-digestion processes and describing the purpose of this project.

1.1 Anaerobic Digestion

1.1.1 Reactions

Anaerobic digestion consists of the degradation of substrates through anaerobic bacteria, which leads to the production of biogas – composed mainly of methane (50-70%) and carbon dioxide (30-50%) – and a digestate, which is often used in agriculture as fertilizer [1,2].

The anaerobic digestion of substrates involves four main stages:

- *Hydrolysis*: stage during which carbohydrates, proteins and lipids undergo hydrolysis reactions with the help of extracellular enzymes and are turned into simpler molecules such as amino acids, sugars and long-chain fatty acids. It is

often considered as the "rate-determining step" of the anaerobic digestion process, and great attention is turned towards the speeding up of this stage.

- *Acidogenesis*: during this stage the hydrolysed compounds are further converted to a mixture of short-chain volatile fatty acids (VFAs) and other minor products such as ethanol and lactate. Amino acids breakdown also leads to the production of ammonia, which, at sufficiently high concentrations, is known to be an inhibitor of anaerobic digestion.
- *Acetogenesis*: process during which VFAs and other intermediates are turned into acetate, carbon dioxide and hydrogen.
- *Methanogenesis*: final stage during which methanogenic bacteria convert the acetogenesis products to methane. This stage is carried out following mainly two routes: the main route, through which about 70% of the total biomethane is produced, involves acetoclastic bacteria that turn acetate into methane and carbon dioxide; the other route involves hydrogenotrophic bacteria which produce methane through a redox reaction of hydrogen and carbon dioxide.

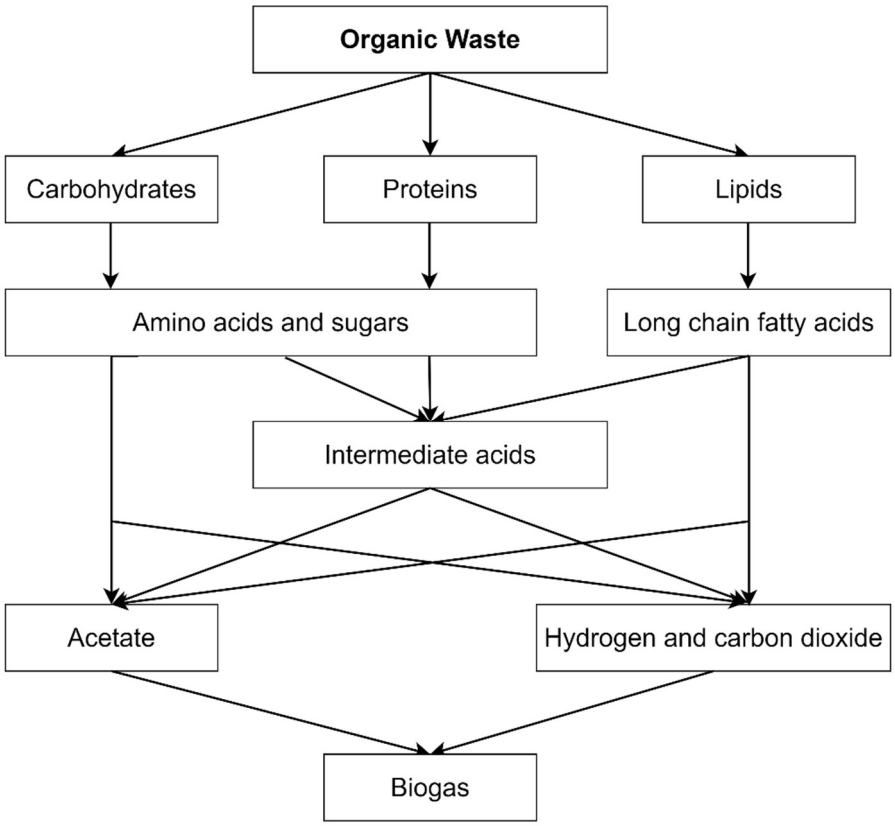

Figure 1.1: The simplified scheme of pathways in anaerobic digestion [1]

Anaerobic bacteria are usually already present in the initial matter and the digestion process takes place spontaneously in absence of oxygen. Process performances, however, depend on many factors, involving mainly the characteristics of the feedstock and of the microbial community, and the operating conditions.

1.1.2 Classification of Anaerobic Digestion Processes

At industrial level, anaerobic digestion can be carried out through both a discontinuous and continuous layout, and the process can also be classified depending on the operating conditions [3].

In first place, AD can be classified depending on the temperature at which the digester is operated, and the related digestion time. Three temperature conditions can be identified:

- *Psychrophilic conditions:* temperature of about 20°C and digestion times comprised between 30 and 90 days.
- *Mesophilic conditions:* temperature of about 35°C and digestion times of 20-30 days.
- *Thermophilic conditions:* temperature of about 55 °C and digestion times of 14-16 days.

Increasing the digester's temperature, the reactions' kinetics is sped up, and residence times are reduced. Consequently, psychrophilic conditions are rarely used due to the extremely high reaction times. Working at high temperatures, however, implies high energy costs, and it has been demonstrated that in thermophilic conditions the process is less stable than in mesophilic conditions, leading to a reduction of the methane content in the produced biogas: this happens because most of the microorganisms are more active in mesophilic conditions, while they deactivate at higher temperatures. Therefore, mesophilic conditions represent are the most employed ones [2,4].

Another distinction for anaerobic processes is based on the concentration of solids in the digester. Defining Total Solids (TS) as the amount of dry solid matter contained in the feedstock, three process types can be defined:

- *Wet digestion:* TS < 10%
- *Semi-dry digestion:* 10 % < TS < 20 %
- *Dry digestion:* TS > 20%

The most widespread processes at industrial level are the wet and, less often, semi-dry digestion. Indeed, high solids amount may cause inhibition due to VFAs accumulation, resulting in a general reduction of the methane yield for dry digestion

processes; moreover, the management of the influent might be difficult due to high viscosities. Further details about this parameter will be given in Section 2.3.

1.2 Anaerobic co-Digestion

Anaerobic co-digestion consists of the simultaneous digestion of two or more substrates. This technology has gained lot of attention nowadays because it gives the possibility to significantly improve process performances. Indeed, the digestion of a single substrate might lead to poor performances in terms of substrate utilization and methane yield due to the lack of some nutrients or non-optimal parameters. By co-digesting different substrates that show "complementary" characteristics, instead, methane yield and process stability can be significantly improved, and synergistic effects may be observed too. On the other hand, an improper choice of co-substrates could lead to a system imbalance and create antagonistic effects, reducing the methane generation with respect to the mono-digestion [2,4].

1.3 Feedstocks for AD and AcoD

The feedstock for anaerobic digestion can be defined as any substrate – ranging from readily degradable to complex high-solids wastes – which can be turned into biogas and a digestate following the reactions described in Section 1.1.1.

Historically, AD has been associated with the treatment of animal manure and wastewater active sludge; however, after the 70s, the increasing demand for new waste management strategies and the necessity of renewable energy forms, broadened the field of applications for this technology and new substrates started to be exploited: for example, wastes such as harvest remains, energy crops, garden wastes, algal biomasses, food wastes, municipal wastes, industrial wastes and wastewaters are currently used as possible feedstocks [5].

As mentioned in the previous section, anaerobic co-digestion involves the use of mixtures of complementary substrates as feedstocks, which brings economic advantages since it allows to recover many typologies of wastes coming from nearby waste sources (such as farms, industries, wastewater treatment plants). However, to have a considerable increment of performances, the different substrates should be mixed in appropriate ratios so that the methane yield can be significantly improved with respect to the mono-digestion, avoiding antagonistic effects too. Many research studies have demonstrated that some of the parameters characterizing the feedstock should be kept within defined ranges to obtain high methane yields, and mixtures of substrates should respect such constraints to obtain good performances.

1.4 Aim and Innovativeness of the Project

Summarizing, to improve the performances of AcoD processes, it is necessary to understand how to properly combine different substrates to maximize the methane yield.

In the last years, numerous studies have been carried out to find the optimal blending conditions of mixtures of substrates by carrying out experimental tests, however the results that were obtained from such kind of experimentations are not general and are only representative of the analysed mixture. On the other hand, some attempts to build mathematical models able to predict the optimal feedstock blending have been done in the past: a control system involving a linear programming algorithm has been developed to perform a continuous optimization of the composition, loading rate and retention time during the operation of existing plants [6–8]; moreover, a model based on an ant-colony approach have been proposed to perform a blending optimization accounting also for the distance and the transport of the waste from the source to the plant [9,10] – further details about these two models are shown in Chapter 3. These models, however, are both intended to be applied as on-line control systems and involve the measurement of hardly measurable variables. The purpose of this work, instead, is the development of an easy-to-use and quick tool that with few, simple inputs can estimate with good precision the optimal blending ratios of mixtures of substrates, aiming at supporting industrial realities with decision-making processes related to the feedstock management.

The topic is extremely innovative and complex, due to the wide number of possible raw materials that can be co-digested and the high variability of their compositions according to their source. This project, therefore, aims first at generalizing as possible the feedstock properties through the building of a database, and then at understanding how different substrates interact with each other through the development of a model able to return the best blending conditions of available wastes, allowing to maximize the methane yield through a better exploitation of raw materials.

2. Feedstock Properties

To understand how to optimize the feedstock composition, it is important to identify the parameters and properties that mostly characterize the influent.

2.1 Macronutrients content

Substrates are mainly composed of proteins, carbohydrates, and lipids, which are progressively turned into methane and carbon dioxide following the reactions described in Section 1.1.1.

Compounds like proteins, fats, sugars, starch and easily degradable carbohydrates are digested in a relatively short time by anaerobic bacteria thanks to their high biodegradability; conversely, the presence of lignocellulosic components – represented by hardly degradable polysaccharides such as lignin, cellulose, and hemicellulose – make the digestion difficult and reduce the overall biodegradability of the organic matter.

A balance between nutrients to obtain a good biodegradability is fundamental in AcoD, which can be obtained by feeding complementary substrates and possibly taking advantage of pre-treatments of lignocellulosic matters.

Other macronutrients that may affect digestion are inorganic compounds such as heavy metals and contaminants such as antibiotics, deriving mainly from animals' diets [5]. AcoD represents a beneficial technology also from this point of view since it allows the dilution of these compounds by other substrates, reducing their impact on methane yield.

2.2 Micronutrients content

AD is carried out thanks to the presence of anaerobic bacterial species, then the micronutrients content of the substrate is an extremely important factor. Substrates fed to the digester usually already contain the bacteria needed for digestion,

however, different substrates may contain different quantities and types of microbial species: livestock wastes, for example, usually contain high concentrations of micronutrients, while agro-industrial and food waste may show a lack in microbial concentrations [11]. Therefore, also in this case, by mixing complementary feedstocks the process performances could be improved.

2.3 Total Solids and Volatile Solids

As mentioned in Section 1.1.2, Total Solids (TS, [% w/w]) represent the mass percentage of dry matter contained in a certain feedstock. Depending on the substrate, the quantity of TS may vary from few point percentages to near 100%, and often substrates need to be diluted to reach the desired solids concentration in the digester. Volatile Solids (VS, [%TS w/w]) represent instead the organic fraction of the TS: the higher this parameter, the higher the organic content of the substrate that could potentially be converted to methane. Substrates with dry organic content lower than 60 %TS are rarely considered as valuable [5]. This parameter doesn't account for the *real* biodegradability of the substrate, neglecting the fact that not all the organic matter can be degraded within the digestion time due to the presence of lignocellulosic compounds and ashes.

Generally, the higher the TS inside the digester, the higher the methane productivity per unit volume of the reactor (measured in $[m^3_{CH4}/m^3_{reactor}/d]$); however, increasing solids concentration, an over-accumulation of VFAs could be observed, inhibiting the methanogenesis and lowering the efficiency of the process in terms of methane production per mass of VS added (i.e., methane yield, $[m^3_{CH4}/kg_{VS}/d]$) [12]. In addition, high solids content makes the management of the influent more difficult due to high viscosities, causing poor heat transfer and uneven distribution during stirring, making it necessary to adopt more complex reactor designs [2]. Therefore, to improve the substrate utilization, at expenses of higher reactor volumes, many research studies have demonstrated that wet digestion (TS < 10%) is the most convenient option, and an optimal TS within this range usually exists. For example, the experimental study of [12] showed how, for mixtures of municipal solid wastes and sewage sludge in a mass ratio of 60:40, optimal conditions for methane yields were achieved for a concentration of TS of 5% and any further increase would imply a methane yield reduction.

2.4 C/N ratio

The ratio between organic carbon and nitrogen in the feedstock is a dimensionless parameter that is commonly used to characterize its nutrients and stresses the fact that

not only the organic carbon content but also nitrogen content represents a crucial factor in biogas production [1].

To obtain good methane yields, it has been demonstrated that this parameter should be maintained in a range between 20 and 40: below this range substrates result rich in proteins – that are the main nitrogen source – , whose degradation causes an increase in ammonia concentration that may inhibit the digestion process due to an impediment of microbial growth; above this range, instead, the substrate results rich in carbon sources, leading to the production of high concentrations of VFAs, which are another cause of inhibition due to methanogenic bacteria deactivation [4].

C/N ratio is one of the main parameters affecting the anaerobic digestion process, however substrates are often characterized by non-optimal C/N. Therefore, many studies have been carried out about the maximization of the methane yield by co-digesting substrates so that the global carbon to nitrogen ratio falls within the optimal range. For example, the research study of [13] investigated the possibility of improving the methane yield of a mixture of dairy manure (DM), chicken manure (CM) and wheat straw (WS) through the optimization of the C/N ratio: using a Central Composite Design associated to Response Surface Methodology to carry out experiments, the conclusion was that the maximum methane production is achieved with a mixture containing 32.5%w/w of DM, 48.1%w/w of CM and 19.5% w/w of WS, characterized by a global C/N ratio of 27.2 – which falls within the aforementioned optimal range. Similarly, [14] performed Biomethane Potential (BMP) tests of ternary mixtures of sugar beet root waste, cow dung and poultry manure and concluded that maximum methane yield was obtained with an overall C/N ratio of 26.24.

Like VS, this parameter is calculated by considering the total amount of organic carbon, of which just a part is biodegradable. To exclude the carbon that is not affected by microorganisms, an *available* carbon to nitrogen ratio has been proposed by [15].

2.5 pH

pH is another important parameter since it influences the solubilization of organic matter and contributes to the creation of a favorable environment for microbes [4].

The microorganism species acting in the AD process are characterized by different optimal pH ranges: hydrolytic and acidogenic bacteria prefer a pH within the range 5.5-6.5, while the optimal pH for methanogenic bacteria is near 7. All things considered, many researchers have found out that maintaining a pH between 6.8 and 7.5 is usually preferable in AD processes, therefore the pH of the feedstock should be inside this optimal range. Many research studies that support this statement have been

carried out: for example, [16] investigated the effect of initial pH on the co-digestion of food waste and rice straw using a Central Composite Design, obtaining an optimal methane yield at a C/N ratio of 30 and an initial pH of 7.3.

2.6 Organic Loading Rate and Hydraulic Retention Time

In continuous digesters, the organic loading rate (OLR, $[kg_{VS}/m^3/d]$) represents the amount of dry organic solids fed to the reactor per unit volume and unit time, while the hydraulic retention time (HRT, $[d]$) represents the average time that the influent spends inside the reactor (generally mesophilic digestion is accomplished with HRT within 20-30 days).

The HRT depends on the volume of the digester and on the inlet volumetric flow rate (defined as Q, $[m^3/d]$), and their relationship can be expressed as in Equation 2.1 [1]:

$$HRT = \frac{V_{reactor}}{Q} \tag{2.1}$$

The OLR is strictly connected to the HRT and to the TS and VS content inside the digester: supposing to deal with a CSTR with fixed volume, higher OLRs correspond to shorter HRTs and higher TS content. Similarly to TS, if the ORL is too high overloading is observed, leading to an accumulation of VFAs and performances reduction. The OLR, then, should be maintained within an optimal range [4], and many research studies have been carried out for the determination of the best OLRs for the mono and co-digestion of a variety of substrates. For example, [17] studied the co-digestion of a mixture of rice straw and cow manure at a massive ratio of 50:50 varying OLR from 3 to 12 $kg_{VS}/m^3/d$: the conclusion was that the best performances were achieved at 6 $kg_{VS}/m^3/d$, while at higher values the process was inhibited by accumulation of VFAs. Similarly, the study of [18] identified an optimal OLR range of 5-6 $kg_{VS}/m^3/d$ for the digestion of a mixture of rice husk and food waste.

2.7 Biodegradability

The biodegradability (BD) represents the fraction of organic matter that is available for degradation and can be effectively converted to methane. Indeed, the organic fraction of substrates, represented by VS, may be composed both by readily degradable components such as simple carbohydrates, proteins, and lipids, and by hardly degradable fractions, represented by the lignocellulosic components, whose bioavailability is typically low. Generally, the higher the biodegradability, the higher the methane production.

Many definitions of biodegradability can be found in literature, which are now reported:

1. Ratio between the Biological Oxygen Demand (BOD) and the Total Chemical Oxygen Demand (COD_t) [19]:

$$BD_{BOD} = \frac{BOD}{COD_t} \tag{4.2}$$

The COD_t represents the amount of oxygen present in a sample that can be consumed in a reaction with oxidising agents, thus it is a measure of the organic fraction of the substrate. The BOD, instead, represents the degradable fraction of the COD_t, and thus a measure of the *biodegradable* organics present in a substrate [1]. If divided by the COD_t, therefore, the obtained value represents the biodegradability of the substrate.

2. Percentage of removed VS [20–22]:

$$BD_{VS} = \frac{VS_{feedstock} - VS_{digestate}}{VS_{feedstock}} \tag{4.3}$$

The biodegradability can be defined as the percentage of VS that is consumed – i.e., turned into methane – during the digestion process. Therefore it can be expressed as the difference between the VS at the initial and final condition, divided by the VS of the feedstock.

3. Percentage of removed COD_t [20,21]:

$$BD_{COD} = \frac{COD_{t,feedstock} - COD_{t,digestate}}{COD_{t,feedstock}} \tag{4.4}$$

The biodegradability can also be defined as the COD_t reduction between the initial and final condition, divided by the initial COD_t in the feedstock. The meaning of this expression is analogue to the one of BD_{VS}.

4. Ratio between the Experimental Biomethane Potential (EBMP) and the Theoretical Biomethane Potential (TBMP) of the feedstock [14,23,24]:

$$BD_{BMP} = \frac{EBMP}{TBMP} \tag{4.5}$$

Finally, the biodegradability can be defined as the ratio between the cumulative methane yield obtained through a Biomethane Potential (BMP) test and the cumulative yield calculated by theoretical methods. Both TBMP and EBMP are expressed in $[mL/g_{VS}]$.

2.7.1 Theoretical Biomethane Potential

The theoretical biomethane potential (TBMP) represents the theoretical methane yield that could be achieved if the feedstock would be completely degraded, and if the use of the substrate by microorganisms as an energy source is assumed as insignificant [25]. Several methods can be used to calculate the TBMP, among which two are the most used: one based on the elemental composition of substrates ($TBMP_{el}$), and one based on organic fractions composition ($TBMP_{org}$).

2.7.1.1 Elemental Composition Method

One of the main formulas used for the estimation of the TBMP is the Buswell equation [26], which is based on the assumption that the organic matter, expressed with the general chemical formula $C_cH_hO_o$, is completely degraded to methane and carbon dioxide through an approximate redox reaction involving water, represented by the following empirical equation:

$$C_cH_hO_o + \left(c - \frac{h}{4} - \frac{o}{2}\right)H_2O \longrightarrow \left(\frac{c}{2} + \frac{h}{8} - \frac{o}{4}\right)CH_4 + \left(\frac{c}{2} - \frac{h}{8} + \frac{o}{4}\right)CO_2$$

This equation is derived by balancing the total conversion of the organic material $C_cH_hO_o$ to CH_4 and CO_2 with H_2O as the only external source, i.e. under anaerobic conditions [27].

Such equation has been improved by Boyle by including in the chemical formula of the organic matter nitrogen and sulfur, that are assumed to be entirely converted to NH_3 and H_2S, and to negatively affect anaerobic digestion [28,29]. In this case, for a generic organic matter $C_cH_hO_oN_nS_s$, the empirical reaction is represented as:

$$C_cH_hO_oN_nS_s + \left(c - \frac{h}{4} - \frac{o}{2} + \frac{3n}{4} + \frac{s}{2}\right)H_2O \longrightarrow \left(\frac{c}{2} + \frac{h}{8} - \frac{o}{4} - \frac{3n}{8} - \frac{s}{4}\right)CH_4 + \left(\frac{c}{2} - \frac{h}{8} + \frac{o}{4} + \frac{3n}{8} + \frac{s}{4}\right)CO_2 + nNH_3 + sH_2S$$

Considering this last reaction, the theoretical methane yield TBMP can be calculated with the empirical formula shown in Equation 4.7.

$$TBMP_{el} = \frac{\left(\frac{c}{2} + \frac{h}{8} - \frac{o}{4} - \frac{3n}{8} - \frac{s}{4}\right) \cdot 22415}{12c + h + 16o + 14n + 32s} \tag{4.7}$$

The term 22415 is the coefficient that allows to obtain the desired unit of measure (mL/g_{VS}). This formula doesn't account for the content of non-degradable components such as lignin, considering the substrate as completely degradable: the real methane yield, then, is for sure lower than the TBMP.

2.7.1.2 Organic Fractions Composition Method

Another method for the calculation of the TBMP takes advantage of the knowledge of the organic fractions of lipids, carbohydrates, and proteins, using Equation 4.8 [30] for the calculation of the TBMP:

$$TBMP_{org} = 415 \cdot \%Carbohydrates + 496 \cdot \%Proteins + 1014 \cdot \%Lipids \quad (4.8)$$

The coefficients appearing in this equation represent the $TBMP_{el}$ calculated with the general chemical formulas for carbohydrates ($C_6H_{10}O_5$), proteins ($C_5H_7O_2N$) and lipids ($C_{57}H_{104}O_6$), obtained with the modified Buswell formula.

The drawbacks of this formula are that the fractions of carbohydrates, lipids and proteins must be quantified by analytical techniques, which are time-consuming and expensive; plus, also in this case, the fraction of poorly available carbon isn't considered – since carbohydrates include lignocellulosic compounds.

Generally, the elemental analysis method gives slightly higher results with respect to the ones calculated with the organic fractions analysis method, however it could be said that both methods give similar results [23]. Therefore, in the building of the database, it has been decided to report just the $TBMP_{el}$ of substrates, which is the most used method in literature and which, from now on, will be simply called $TBMP$.

2.7.2 Experimental Biomethane Potential

The BMP of substrates can be experimentally calculated by performing lab-scale batch tests. The BMP evaluated with such assays represents the ultimate cumulative methane yield that substrates give in "optimal" conditions, using appropriate solids concentrations and substrate/inoculum ratios to create the best environment for methane production, as well as appropriate digestion times. Despite the usefulness and inexpensiveness of BMP tests, they don't follow a universally accepted protocol and they aren't currently standardized, so they might give quite different results even for the same type of substrate. The variabilities that can be observed in BMP tests are due to possible differences in operating conditions, the substrate/inoculum ratio, the inoculum source, the substrates concentration and composition; moreover, the experimental setups might differ in their gas measurement and analytical techniques. Therefore, the EBMPs resulting from these kind of tests should be carefully compared and discussed [31].

2.7.3 Choice of Biodegradability Definition

All the four definitions of Biodegradability are effective in giving a measure of the biodegradable fraction of a substrate. However, since one of the goals of this thesis is

to build a database based on data available in literature, the first three definitions are difficult to be used. The first and third definition of biodegradability, BD_{BOD} and BD_{COD}, often cannot be calculated because information about the BOD and COD_t of the substrates and digestate are quite rare in literature, since their determination requires dedicated experimental tests. Similarly, BD_{VS} requires information about the VS content in digestate, which is rarely reported in literature.

The definition of biodegradability based on Experimental and Theoretical BMPs (BD_{BMP}) is the most convenient one since these information are often available in scientific articles and, if properly analysed and averaged on a wide number of data, general mean values for these quantities can also be obtained for each substrate. The convenience of this parameter will be also demonstrated in Chapter 4, where significant correlations between the BD_{BMP} and other parameters will be derived. Consequently, from now on, the BD_{BMP} will be simply called BD.

3. Previous Studies

As mentioned in Section 1.4, two research studies about the development of feedstock optimization models have been carried out in the last years. This chapter aims at describing these models and then disclosing how they differ from the one developed in this project.

2.8 Control System based on Linear Programming Optimization

The study carried out by [7,8] proposes a control system based on linear programming for anaerobic digesters to perform an on-line optimization of the feeding composition, to obtain higher methane productivities and higher COD removal efficiencies.

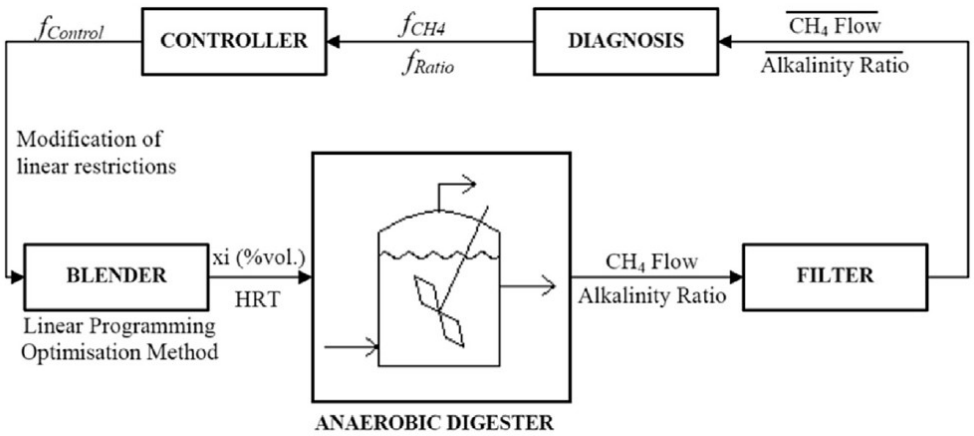

Figure 3.1: Proposed closed-loop control system architecture

As shown in Figure 3.1, the architecture of the control strategy comprises four blocks, executed as a loop and connected to the digester: (1) Substrate Blender, (2) Filter, (3) Diagnosis, (4) Controller.

The Blender block contains a linear programming method that involves the maximization of an objective function, subjected to a set of linear restrictions on some selected parameters. The objective function represents the methane production (measured in $[g_{COD}/L/d]$) expected in a continuous AcoD system and is calculated as in Equation 3.1.

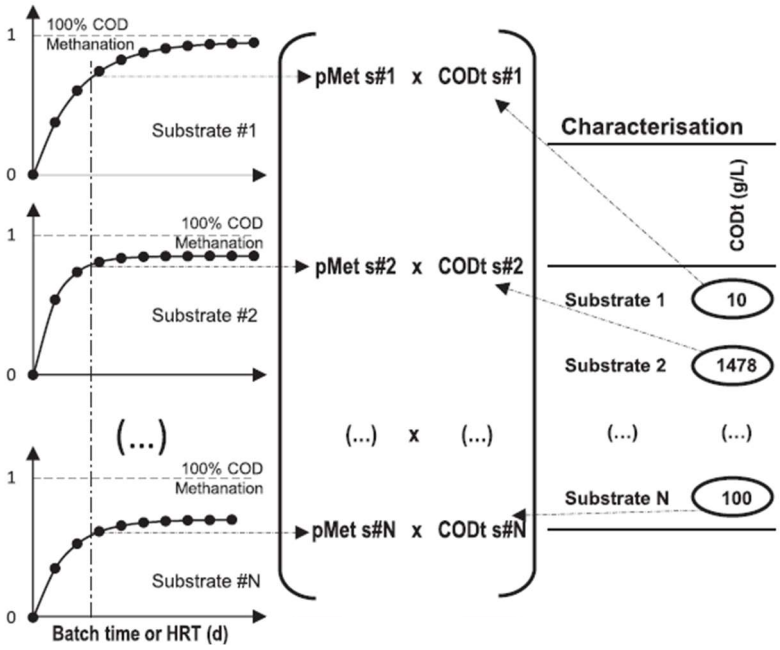

Figure 3.2: Visual representation of the building of the objective function

$$\max f_{objective} = \frac{\sum_{i=1}^{N} pMet_i \cdot CODt_i \cdot x_i}{HRT} \tag{3.1}$$

As shown in Figure 3.2, the expression of the methane production is built by exploiting experimental information from batch BMP assays and the knowledge of the physic-chemical properties of the single substrates: $pMet_i$ represents the percentage of methanogenic conversion of a substrate i obtained in a BMP test at a time equal to the HRT, assuming that the expected methanation of each substrate in a continuously-operated digester working at a certain HRT would be similar to the one obtained in a batch assay; $CODt_i$ represents the total Chemical Oxygen Demand of substrate i; x_i represents the volumetric fraction of substrate i in the blend.

The maximization of this function involves two steps, performed on MATLAB: first, using the *'linprog'* function, the blends of substrates maximizing the objective function at varying HRTs are calculated; secondly, the function *'fminbnd'* is used to find the HRT that optimizes the methane productivity. Such maximization is subjected to linear restrictions that define a maximum and a minimum value for the following parameters: (i) organic loading rate (OLR); (ii) total Kjeldahl nitrogen (TKN); (iii) moisture or liquid fraction; (iv) lipid content; (v) total alkalinity; (vi) Na^+ concentration; (vii) K^+ concentration; (viii) H_2S content in biogas; (ix) effluent COD content. The optimal ranges for these parameters should be appropriately selected according to the operating conditions, the stage of operation (start-up, dynamic or steady-state operations), the substrates' nature and the objective of the digestion (biogas or digestate's use), and they can be modified during the operation. For example, Table 3.1 shows a possible list of optimal ranges for the nine parameters at the start-up.

Linear restriction	**Minimum**	**Maximum**
OLR [gCOD/L/d]	0	2.5
TKN [gN/L]	0.2	4
Liquid fraction [kg liquid/kg wet]	0.85	1.00
Lipids [g/L]	0	10
Alkalinity [$gCaCO_3$/L]	2	8
Na^+ [g/L]	0	3
K^+ [g/L]	0	3
Biogas quality [ppm H_2S]	0	10000
Digestate quality [gCOD/L]	0	6

Table 3.1: Initial values of the substrate blending optimization restrictions [8]

The linear programming, in addition, informs about the restrictions that are actively limiting and that could be modified to potentially move the operation towards a new optimum with a higher methane yield.

After the Blending block, a Filter module calculates the average values of the physic-chemical parameters monitored in the reactor and used as diagnosis indicators during a specific period. In particular, the chosen diagnosis indicators are the alkalinity ratio (*Ratio*) and methane flow (F_{CH4}), whose average values are defined by Equations 3.2 and 3.3.

$$\overline{Ratio} = \frac{\frac{\int IA\ dt}{\int dt}}{\frac{\int TA\ dt}{\int dt}} \tag{3.2}$$

$$\overline{F_{CH4}} = \frac{\int F_{CH4}(t)\ dt}{\int dt} \tag{3.3}$$

IA stands for intermediate alkalinity, which represents the alkalinity due to VFA, and TA stands for the total alkalinity, which represents the alkalinity due to both VFA and bicarbonate. The integration time is ¼ of the current HRT, which is the time period when the controller is executed.

Then, the Diagnosis block informs about the stability of the process and methane production performance, comparing the average values of alkalinity and methane flow with reference values, considered as thresholds of process stability: *Ratio**, which is assumed equal to 0.4, and F^*_{CH4}, set equal to 15 $m^3_{CH4}/m^3/d$. Two stability factors can be defined:

$$f_{ratio} = \begin{cases} \left(1 - \frac{\overline{Ratio}}{Ratio^*}\right)^{\frac{1}{2}} & if\ \overline{Ratio} \leq Ratio^* \\ \left(\frac{Ratio^*}{\overline{Ratio}}\right)^5 - 1 & if\ \overline{Ratio} > Ratio^* \end{cases} \tag{3.4}$$

$$f_{CH4} = \frac{\propto \cdot F^*_{CH4}}{\overline{F_{CH4}} + \propto \cdot F^*_{CH4}} \quad (\propto = 0.1, shape\ factor) \tag{3.5}$$

After that, the Controller block calculates at the end of each period (¼ HRT) a control indicator, $f_{control}$, as the product of f_{ratio} and f_{CH4} when the system is stable, or equal to f_{ratio} when the system is unstable and f_{ratio} is negative. The value of $f_{control}$ is comprised between [-1,1] and determines the extent of the control action that modifies the operational restrictions of the linear programming problem (in the Blender module).

$$f_{control} = \begin{cases} f_{ratio} \cdot f_{CH} & if\ f_{ratio} > 0 \\ f_{ratio} & if\ f_{ratio} \leq 0 \end{cases} \tag{3.6}$$

Then, $f_{control}$ modifies the boundaries of the most active restriction following Equation 3.7.

$$Limit_{NEW} = Limit_{ACTUAL} + f_{control} \cdot (Limit_{HIGHER} - Limit_{LOWER}) \tag{3.7}$$

When the system is stable, $f_{control}$ is positive, so the control promotes the use of feedings with higher methane production potential by relaxing the limits of the most active restriction. When $f_{control}$ is negative, instead, instability is observed, and the control promotes the use of feedings with lower methane production to prevent the system from possible acidification.

This control model was validated with simulations using an ADM1-based AcoD model and then with continuous experiments performed at pilot scale in an Upflow Anaerobic Sludge Blanket – Anaerobic Filter (UASB-AF) reactor and the conclusions were that this substrate blending control strategy was proven capable of changing operating conditions to increase methane productivities and to recover the system from transient acidifications.

2.9 Blending Optimization using Ant Colony Approach

This research works of [9,10] aim at building a new co-digestion optimization tool based on an enhanced version of the Ant Colony Approach (ACO) algorithm to simultaneously optimize the feedstock composition and the logistics – focusing on the transport route and substrate availability – associated with each component. Therefore, the objective function, in this case, involves both substrate biochemical characterization (for biogas production maximization) and logistics characterization (for route optimization).

The problem statement considers a set of substrate generators $w \in \{1, \dots, N\}$, located at different distances d_w (measured in km) from the anaerobic digester; each generator has a certain capacity to store its waste until it is transported to the anaerobic digester.

Each substrate is characterized by a volume V_w and a set of parameters C_w^c, where:

- C_w^1 is the Chemical Oxygen Demand concentration (COD, measured in $[g/m^3]$)
- C_w^2 is the ratio of COD to total nitrogen concentration (COD/TN, dimensionless)
- C_w^3 is the alkalinity concentration (Alk, measured in $[g/m^3]$)
- C_w^4 is the toxicity level (Tox, dimensionless)

Each volume V_w can be selected as a substrate contribution to be transported to the digester, and it must respect the volumetric possibilities V_w^s (with $s \in \{1, \dots, l_w\}$, where l_w represents the number of different volumetric configurations) of the waste generator, that are determined as a multiple of a number (e.g., 1000) such that $1000 l_w = V_w^s$. The selection of each volumetric possibility is determined by the corresponding value of a binary decision variable y_w^s, where $y \in \{0,1\}$, with $y_w^s = 0$ when the substrate w is not selected, and $y_w^s = 1$ when it is selected. Also, it must be

noted that for each waste generator there are l_w different volumetric configurations, but only one is selected at a time, so that the Equation 3.8 is satisfied.

$$\sum_{s=1}^{lw} y_w^s = 1 \quad \forall\, w \in \{1, \dots, N\} \tag{3.8}$$

The conveyance of the selected volumes implies a distance d_w with a social impact I_w and an economic cost X_w. $I_w = 1, \dots, 3$ is a dimensionless parameter that depends on different criteria such as route traffic density or proximity to pedestrian/sensitive areas, and it is assigned qualitatively accounting for all these factors. X_w is defined in $[€/km]$ and represents the cost of substrate transport.

The blend of all transported substrates, which represents the digester's input, must also fulfil a certain set of restrictions: the maximum acceptable total volume V; the optimal range of COD/TN ratio $[C_{min}^2, C_{max}^2]$; the optimal alkalinity range $[C_{min}^3, C_{max}^3]$; the toxicity threshold $Tox < C_{max}^4$.

The optimization problem, in this case, consists of the minimization of an objective function expressed as follows:

$$B = \frac{1}{\sum_{w=1}^{N} \sum_{s=0}^{lw} y_w^s V_w^s T_w \left[(\sum_{c=1}^{3} F_w^c) \rho_q + \frac{\rho_x}{X_w d_w I_w} \right]} \tag{3.9}$$

Where y_w^s is the binary decision variable; V_w^s is the substrate contribution of generator w, measured in $[L]$; T_w is the substrate toxicity level (dimensionless); F_w^c is a set of coefficients corresponding to the substrate composition (dimensionless); ρ_q is the quality coefficient (dimensionless); ρ_x is the logistics coefficient (dimensionless); X_w is the economic cost of transport in $[€/km]$; d_w the distance in $[km]$; I_w is the social impact (dimensionless).

The coefficients F_w^c (c=1,…,3) and T_w are related to the value of the parameters C_w^c of the single substrates:

- F_w^1 is related to the COD content of the substrate:

$$F_w^1 = 0.00001 \cdot C_w^1 - 0.01 \tag{3.10}$$

- F_w^2 is related to the ratio COD/TN, whose optimum value is comprised between 20 and 60:

$$F_w^2 = e^{-\left(\frac{(C_w^2 - 4\ )^2}{450}\right)} \tag{3.11}$$

- F_w^3 is related to the alkalinity concentration, whose optimal range is 3000-6000 g/m^3:

$$F_w^3 = e^{-\left(\frac{(C_w^3 - 4500)^2}{8 \cdot 10^6}\right)} \tag{3.12}$$

- F_w^4 is related to the toxicity level:

$$T_w = e^{-\left(\frac{(C_w^4)^2}{0.6}\right)} \tag{3.13}$$

The objective function in Equation 3.9 contains a term related to the quality composition of the substrate, and a term related to the transport: the two coefficients ρ_q and ρ_x represent the relative importance of the two terms, allowing to state whether the priorities are more focused on the maximization of biogas production or logistics.

The minimisation of this function is performed running an ACO algorithm, which executes an iterative procedure that uses a population of ants, initially placed in a random location of the search space of the solution. To build the solution, each ant traces a path through the search space following a probabilistic rule known as *state transition*, which is defined by Equation 3.14:

$$p_{ws}^m(t) = \frac{[\tau_{ws}(t)]^\alpha [\eta_{ws}(t)]^\beta}{\sum_{l=0}^{lw} [\tau_{wl}(t)]^\alpha [\eta_{wl}(t)]^\beta} \tag{3.14}$$

At iteration t, $p_{ws}^m(t)$ represents the probability that the *m-th* ant chooses the volume V_w^s; $\tau_{ws}(t)$ is the pheromone trail; α is the importance assigned to the pheromone trail; $\eta_{ws}(t)$ is the specific heuristic information, defined by Equation 3.15; β is the importance assigned to the heuristic information.

$$\eta_{ws}(t) = \frac{V_w^s \sum_{c=1}^{3} F_w^c}{d_w} \tag{3.15}$$

The pheromone trail $\tau_{ws}(t)$ is updated at each iteration following Equation 3.16.

$$\tau_{ws}(t+1) = \rho \tau_{ws}(t) + \Delta {\tau_{ws}}^{best} \tag{3.16}$$

The quantity ρ (comprised between 0 and 1) is the persistence of the pheromone in the trails at iteration t, and $\Delta {\tau_{ws}}^{best}$ is the amount of pheromone added to the trail of the ant that has achieved the best solution B^* at iteration t:

$$\Delta {\tau_{ws}}^{best} = B^* \tag{3.17}$$

The rest of the paths followed by ants that have not achieved the best solution do not increase their pheromone trails, and at the beginning of iteration $t+1$ their amounts are those corresponding to iteration t decreased by the value of the persistence ρ. This way, only the pheromone trails of the ants that have achieved the best solutions increase. For all iterations, all pheromone trails have values in the range $[\tau_{min}, \tau_{max}]$.

This model was validated by using real data from an actual sanitation network composed of 12 wastewater treatment plants and 7 industries, where waste are produced, in the area of the *Besòs* river basin in Catalonia. Therefore, the methodology

was applied to a set of 19 substrate generators, distinguishing between two scenarios – O1 and O2 – in which 0% and 50% weights are given to the logistics importance term ρ_x: hence, in scenario O1 the optimization is only focused on the quality of the blend, while in O2 the quality of the blend and the logistics are given the same importance.

The result of this study was that the ACO algorithm allows an optimized logistic planning proposal in terms of average volume extracted from each waste generator, and allows to estimate average travels per month, biogas production and the resulting OPEX. Consequently, it represents a very complete algorithm that permits to optimize the co-digestion from many points of view, and if applied along with an online digester monitoring and diagnosis system it should assure system stability and control.

2.10 Remarks about the previous studies and the current project

The model developed by [7,8] consist of a control system that can be applied for an on-line monitoring of existing plants. The definition of the model exploits the results of batch tests made specifically on the supplied substrates and requires the in-line measurement of physic-chemical parameters such as the COD – which appears in the objective function – and the alkalinity of the effluent.

The work of [9,10] is also meant for the on-line monitoring of biogas plants, focusing the attention on logistics optimization besides biomethane production, which makes it interesting from this point of view. Indeed, also in this project factors related to the supply chain such as substrates availability and storage capabilities of plants will be considered.

The aim of this thesis, however, is different from the ones of these two works. Indeed, they are both intended to be applied as on-line control systems and involve the use of analytical techniques and laboratory experiments for the measurement of variables. The purpose of this work, instead, is the development of a tool that with few inputs, possibly available in a specially built database, can estimate with good precision the optimal blending ratios of substrates to maximize the methane potential of their mixture, complying also with supply chain requirements at industrial level. Such kind of tool could enable industrial realities to understand how to better exploit their raw materials by changing their blending ratios, or possibly to predict the effect of adding a new substrate to the ones that are already fed to an existing digester, without the need to perform laboratory-scale analysis.

The first goal of this project, therefore, is the building of a database where data about the most common substrates are gathered and statistically analysed. Then, such data are used to build correlations between parameters and develop a data-driven optimization model.

4. Database Building and Data Analysis

The first aim of this project is to build a database where data about a large number of substrate properties are collected from literature. Due to the many factors that affect the composition of substrates, even feedstocks of the same nature may show different characteristics depending on their source, thus it is impossible to describe them in an absolute way. However, common features can be identified in similar substrates, and their parameters are characterized by a distribution. Consequently, to obtain general, reliable values for each parameter of a certain substrate, an averaging process should be carried out, together with the calculation of standard deviations to express the parameters variability. The main reasons to build a database are that it makes it possible not to necessarily carry out laboratory experiments to obtain values of substrate properties, moreover it can be used to build correlations and data-driven models.

After having created the database, it has been possible to analyse data and identify correlations between parameters. The feedstocks that have been considered for the database are among the most common substrates that are employed in anaerobic digestion, about which much information is found in literature.

4.1 Parameters

During a preliminary collection of data, a large number of parameters were initially considered: TS, VS, content of C, N, P, H, O [%TS], C/N ratio, total Chemical Oxygen Demand (COD_t), soluble Chemical Oxygen Demand (COD_s), Biological Oxygen Demand (BOD), Volatile Fatty Acids (VFA) content, Total Ammonium Nitrogen (TAN) content, Alkalinity, pH, percentages [%TS] of lipids (LIP), proteins (PROT), sugars, starch and easily degradable carbohydrates (collected in the same quantity named SSEDC), lignin (LIG), cellulose (CEL), hemicellulose (HCEL) and ash (ASH), Theoretical Biomethane Potential (TBMP) Experimental Biomethane Potential (EBMP), and Biodegradability (BD).

In the final version of the database some of these parameters were not reported due to their poor availability. In particular, information about COD_t, COD_s and BOD of substrates are difficult to find in literature, since they are obtained by carrying out specific tests and are rarely reported in scientific articles, making it impossible to obtain reliable mean values. Similarly, scarce information is generally available for the VFA, TAN and Alkalinity contents. On the other hand, it has been decided not to include information about the C, N, P, H, O contents of the substrates and their pH because their role in this technology development is quite irrelevant.

The parameters that have been finally reported – and their unit of measure – are the following:

- Total Solids – TS [% w/w]
- Volatile solids – VS [%TS w/w]
- C/N ratio – dimensionless
- Lipids content – LIP [%TS]
- Proteins content – PROT [%TS]
- Sugars, starch and easily degradable carbohydrates content – SSEDC [%TS]
- Lignin content – LIG [%TS]
- Cellulose content – CELL [%TS]
- Ash content – HCELL [%TS]
- Theoretical Biomethane Potential – TBMP [$mL_{CH}\ /g_{VS}$]
- Experimental Biomethane Potential – EBMP [$mL_{CH}\ /g_{VS}$]
- Biodegradability – BD, dimensionless

The definition of BD, as mentioned in Section 2.7.3, is the ratio between the Experimental Biomethane Potential (EBMP) and the Theoretical Biomethane Potential (TBMP):

$$BD = \frac{EBMP}{TBMP} \tag{4.1}$$

The TBMP comes from the elemental analysis of the substrate, while the EBMP comes from batch assays to assess the biomethane potential of the substrates. The database reports the TBMPs and EBMPs evaluated by previous studies reported by scientific articles. The BMP tests often follow different protocols for their experimental setup: in general, they are performed with a concentration of VS comprised between 5 and 15 [g_{VS}/L], a substrate/inoculum ratio between 0.5-2 and in mesophilic conditions (35-37°C).

4.2 Database

The database has been built by first defining four macro-categories, containing each a certain number of substrates:

1. *Manure*
2. *Agro-Industrial Waste*
3. *Organic Waste*
4. *Sludges*

The substrates comprised in each macro-category are shown in Figure 4.1. Data about the chosen parameters for each substrate were collected from over eighty papers and used to build the so-called *Complete Database*, which will be entirely shown in Section 4.2.1. Then, data about each substrate were averaged to obtain mean values for each parameter – characterized by a certain standard deviation –, which were used to build the *Primary Averaged Database*, described in Section 4.2.2: indeed, after a re-elaboration of averaged data – in order to infer missing data and to obtain coherent values of component percentages (whose sum have to be 100 %TS) – the obtained values can be considered as reliable for the creation of an averaged database. After that, the same reasoning was done to perform another averaging process for each macro-category, leading to the building of a *Secondary Averaged Database*, described in Section 4.2.3.

A schematic procedure for this process is reported in Figure 4.1.

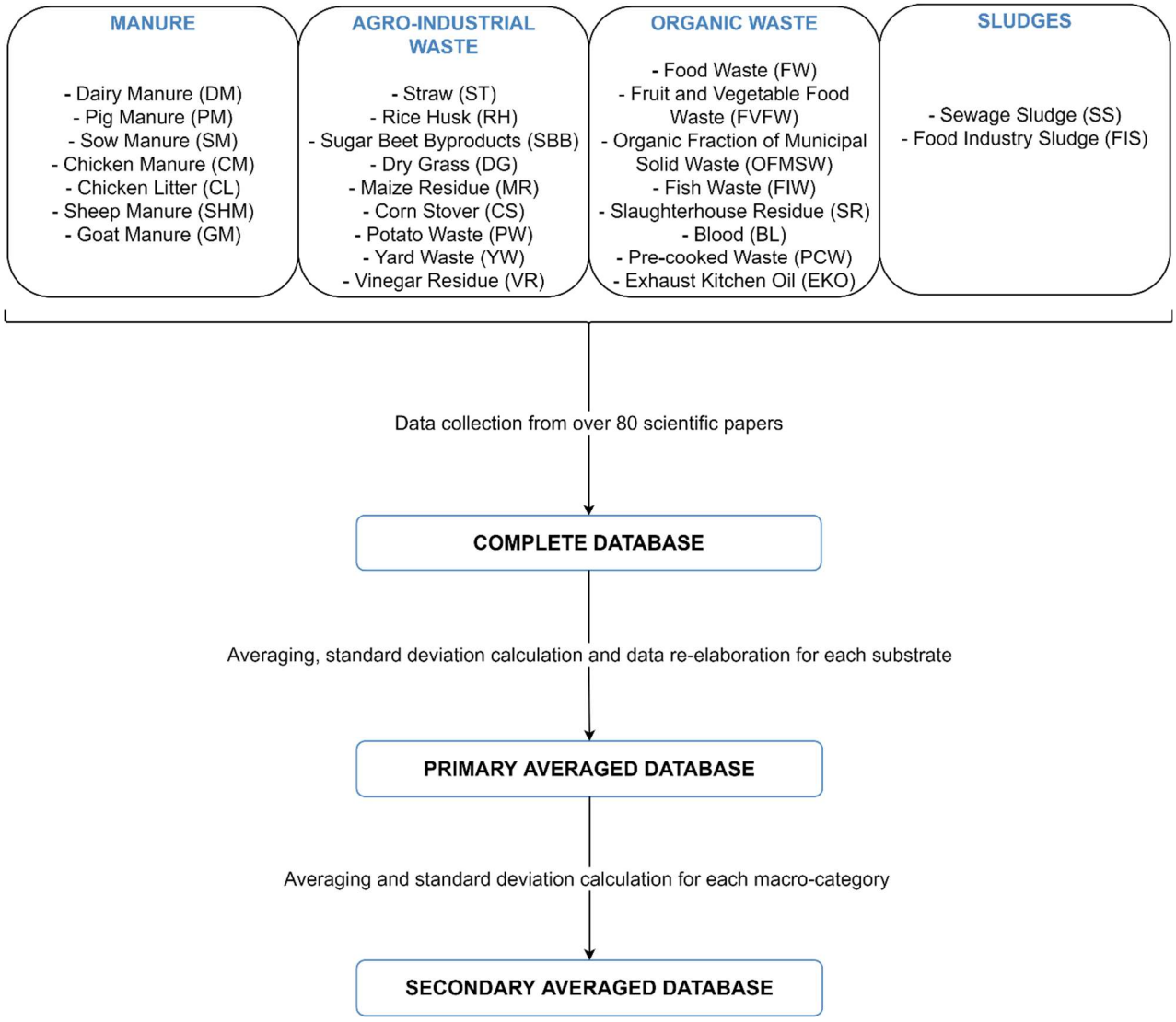

Figure 4.1: Schematic representation of the building process of the Complete Database, Primary Averaged Database and Secondary Averaged Database

4.2.1 Complete Database

In this paragraph, the *Complete Database* for each substrate is reported and commented.

4.2.1.1 Manure

- Dairy Manure (DM)

Substrate	TS [%]	VS [%TS]	C/N [-]	LIP [%TS]	PROT [%TS]	SSEDC [%TS]	LIG [%TS]	CELL [%TS]	HCELL [%TS]	ASH [%TS]	TBMP [mL/gVS]	EBMP [mL/gVS]	BD [-]
DM	14.40	78.60	22.10									177.40	
	8.50	80.00	13.00	3.87	10.32	42.97	5.57	13.92	7.50	15.85		165.00	
	16.00	82.90	19.40								336.64	252.27	0.75
	23.40	74.60	12.40										
	14.00	68.70	16.00										
	12.40	82.26		13.24	4.69	13.57	11.35	7.90	4.69	44.56	473.43	242.70	0.51
	26.62	72.76	17.83	2.26	7.99	32.02	4.72	14.58	18.23	20.20		175.84	
	26.64	79.80	14.19								490.00	323.00	0.66
											551.41	360.00	0.65
	11.56	81.57					11.91	16.58	7.97		525.10	197.00	0.38
	17.36	55.76					6.49	15.58	3.56		522.70	223.60	0.43
	38.50	74.81	23.40	0.00	17.00	5.60	17.40	19.50	15.20	25.30	505.00		
	10.94	73.01		3.63	7.55		10.41	17.51	23.26			222.08	
	18.16	64.42		2.16	8.79		16.24	19.84	21.54			153.01	
	16.91	60.62	25.00	2.56	8.59		9.33					204.00	

Table 4.1: Complete Database of Dairy Manure (DM) [5,13,14,17,19,21,23,24,26,29–32]

Dairy manure is typically collected by a scraper system, and often straw – used as bedding material – is present too, resulting in slight variations of the TS and of the content of lignocellulosic compounds (lignin, cellulose, and hemicellulose). The high variability in composition, C/N ratio, TS and VS content depends on many factors such as the animal housing system, the location, animals' age, and diet [5]. The C/N ratio of DM is generally quite low, typical of manures, due to the high proteins content, which is one of the main nitrogen carriers. The high lignin, cellulose and hemicellulose content are due to the presence of straw, while lipids content is quite low and shows a high variability. The EBMP is extremely variable too since it depends on the composition and on the method used to carry out the BMP tests.

- Pig Manure (PM)

Pigs are usually kept in feedlots with open floors where the excrements are collected through slots or scraper systems [5]. According to the housing system, the TS is highly variable, and PM can be collected both as a liquid slurry (TS = 1÷5 %) or with a higher dry matter content. Similarly, also all the other parameters may change according to the same factors mentioned in the previous paragraph.

Substrate	TS [%]	VS [%TS]	C/N [-]	LIP [%TS]	PROT [%TS]	SSEDC [%TS]	LIG [%TS]	CELL [%TS]	HCELL [%TS]	ASH [%TS]	TBMP [mL/gVS]	EBMP [mL/gVS]	BD [-]
PM	5.50	75.00	6.50	6.41	14.92	35.75	4.58	11.03	12.59	14.72		225.00	
	36.60	54.00	8.49										0.63
	21.56	78.60	13.10										
	20.00	74.80	13.00										
	1.73	67.63		8.67	6.36	53.18							
	27.16	74.10	17.00								554.03		
	22.10	71.76	13.12										
	3.32	65.36	5.30		17.17								
	31.22	74.54	10.89	5.15	14.58	32.13	1.66	6.00	15.01	25.46		330.00	
	1.88	67.55	13.89								754.00	558.00	0.74
			10.33								641.88	487.90	0.76
	16.20	72.84					0.38	3.76	0.97		449.60	417.20	0.93
	30.40	72.40	15.80	0.00	13.20	15.70	4.30	11.30	27.70	27.80	468.00	322.00	0.69
	19.40	82.88		7.89	24.73		6.88	10.47	17.88			443.55	
	31.02	86.81	12.00	9.40	26.80		3.81					323.00	

Table 4.2: Complete Database of Pig Manure (PM) [5,6,14,21,23,26,29–36]

As all manures, the C/N ratio of PM is very low, indeed the proteins content is high. Lignin, cellulose, and hemicellulose contents are quite high due to the presence of lignocellulosic compounds such as straw coming from the housing system. The lipids content is also quite high and the EBMP is generally higher than for DM.

- Sow Manure (SM)

Substrate	TS [%]	VS [%TS]	C/N [-]	LIP [%TS]	PROT [%TS]	SSEDC [%TS]	LIG [%TS]	CELL [%TS]	HCELL [%TS]	ASH [%TS]	TBMP [mL/gVS]	EBMP [mL/gVS]	BD [-]
SM	4.90	77.96					10.34	21.41	15.36		537.50	213.80	0.40
	10.94	82.45					9.58	23.22	14.79		531.00	248.80	0.47
	37.20	75.83		2.10	14.86		16.19	12.86	15.52			177.73	
	31.89	81.93		13.09	18.00	32.87					529.00	250.00	0.47
	29.68	81.01		14.64	14.16	31.88					536.00	260.00	0.49
	31.70	74.55		17.51	17.51	30.89					524.00	317.00	0.60
	28.92	74.78	10.30				1.08	18.48	26.64				

Table 4.3: Complete Database of Sow Manure (SM) [24,31,37,38]

Sows' manure, especially when gestating, is usually distinguished from PM due to some differences in their composition and on their methane production, which is usually lower for SM.

From Table 4.3 it can be noted that few information about the C/N ratio has been found in literature and just one datum has been included in the database; this value is reasonable and similar to other manures, therefore it will be used in the Secondary Averaged Database as the mean value itself, with a standard deviation equal to zero. Similarly, no information about ash content have been found.

- Chicken Manure (CM)

Substrate	TS [%]	VS [%TS]	C/N [-]	LIP [%TS]	PROT [%TS]	SSEDC [%TS]	LIG [%TS]	CELL [%TS]	HCELL [%TS]	ASH [%TS]	TBMP [mL/gVS]	EBMP [mL/gVS]	BD [-]
CM	20.00	75.00	6.50									475.00	
	26.80	62.30	8.84									126.90	
	47.06	82.65	11.20								381.90		
			6.35										
	32.36	72.62	6.01				5.08	24.29	4.90				
	20.96	67.98	11.92								486.00	290.00	0.60
	25.90	75.29	10.60	0.00	20.50	9.70	1.60	20.00	23.20	25.00	468.00	295.00	0.63
	47.50	70.02	10.00	1.01	27.00		5.07					259.00	
	29.90	75.92	10.90								617.00	291.00	0.47
	24.90	77.91	10.10	0.00	15.60	17.10	2.30	20.00	23.20	21.90	476.90	291.10	0.61

Table 4.4: Complete Database of Chicken Manure (CM) [5,13,23,26,32,39–43]

Chickens are usually kept in open feedlots holding up to several hundred thousand animals. Keeping chickens in open feedlots typically causes a significant contamination of manure with sand and bedding materials such as straw [5], then CM is usually characterized by high TS contents (20÷50%) and high quantities of ash and lignocellulosic compounds.

From Table 4.4 it can be noted that the C/N ratios are the lowest among all the manures: this is because CM is characterized by high concentrations of ammonia and proteins. The lipids content is generally the lowest among manures, and the EBMP is quite low as well.

- Chicken Litter (CL)

Substrate	TS [%]	VS [%TS]	C/N [-]	LIP [%TS]	PROT [%TS]	SSEDC [%TS]	LIG [%TS]	CELL [%TS]	HCELL [%TS]	ASH [%TS]	TBMP [mL/gVS]	EBMP [mL/gVS]	BD [-]
CL	77.20	50.65	13.02										
	66.20	70.85		2.70	28.44		4.61		19.85				
			8.78								544.05	437.60	0.80
	66.28	69.61	8.15		24.70	19.65				20.13		113.20	
	40.50	71.36	10.00										
	66.00	61.00										245.00	
				0.40	31.20		9.20	21.80	16.80	12.40			
				0.39	14.40		9.60	30.20	18.80	12.30			
				0.29	20.60		8.20	22.80	28.60	12.20			

Table 4.5: Complete Database of Chicken Litter (CL) [30,44–49]

Compared to chicken manure, the litter contains a higher quantity of bedding materials such as straw and wood shavings, which are typical lignocellulosic matters. Therefore, CL contains more carbon and less nitrogen with respect to CM and can be

classified as an independent substrate. The composition of CL may considerably vary according to the bedding materials and animals' diet.

From Table 4.5 it can be observed that the TS is generally very high, due to the high solids content, and that the mean C/N ratio, lignin content, cellulose content and hemicellulose content are higher than those of CM. On the other hand, the lipids, proteins and SSEDC contents are quite similar than those of CM. The higher quantity of lignocellulosic compounds leads to a lower mean value of the EBMP, and thus a lower biodegradability.

- Sheep Manure (SHM)

Substrate	TS [%]	VS [%TS]	C/N [-]	LIP [%TS]	PROT [%TS]	SSEDC [%TS]	LIG [%TS]	CELL [%TS]	HCELL [%TS]	ASH [%TS]	TBMP [mL/gVS]	EBMP [mL/gVS]	BD [-]
SHM	38.96	71.71	11.79								507.00	305.00	0.60
	22.27	83.92	14.59				8.59	11.63	13.27	16.08			
	53.58	82.42	13.51								346.54	135.98	0.39
	25.39	58.42		1.26	10.18		15.21	16.67	26.12			150.55	

Table 4.6: Complete Database of Sheep Manure (SHM) [26,31,50, 51]

Few information has been found about sheep manure, which are reported in Table 4.6. As all manures, SHM is characterized by a low C/N ratio and by the presence of bedding materials, which lead to a quite high TS and lignin content.

Only one datum was found for lipids, proteins, and ash content, then, during the averaging process, the mean value will correspond to the datum itself and the standard deviation is assumed as zero. No data about SSEDC components were found.

- Goat Manure (GM)

Substrate	TS [%]	VS [%TS]	C/N [-]	LIP [%TS]	PROT [%TS]	SSEDC [%TS]	LIG [%TS]	CELL [%TS]	HCELL [%TS]	ASH [%TS]	TBMP [mL/gVS]	EBMP [mL/gVS]	BD [-]
GM	79.86	83.55	18.02	3.96	0.09	35.51	4.96	13.40	16.67	25.41		204.30	
	35.26	57.01		2.45	10.18		14.58	13.33	19.51			169.86	
	81.63	78.68	20.00	3.33	14.70		13.68					159.00	
	62.30	84.75	15.70				17.60			10.00	290.00	274.00	0.94
	64.90	84.20								10.50	313.40	206.00	0.66

Table 4.7: Complete Database of Goat Manure (GM) [29,31,32,52,53]

Similarly to SHM, few data about goat manure have been found, generally characterized by quite high TS (from about 35% to 80%), low C/N ratios and high lignin content, which stresses the fact that GM usually contains high quantities of bedding materials.

4.2.1.2 Agro-Industrial Waste

- Straw (ST)

Substrate	TS [%]	VS [%TS]	C/N [-]	LIP [%TS]	PROT [%TS]	SSEDC [%TS]	LIG [%TS]	CELL [%TS]	HCELL [%TS]	ASH [%TS]	TBMP [mL/gVS]	EBMP [mL/gVS]	BD [-]
ST	86.10	90.60	81.10									121.20	
	82.90	96.24	81.50										
	91.42	97.47					18.38			5.73			
			84.22										
	88.95	94.40	92.72				6.53	44.44	32.59				
	87.59	92.31	60.90								447.00	0.00	0.00
	93.60	96.73					6.41	47.97	28.38		447.70	289.50	0.65
	90.50	86.10	99.80	0.00	2.50	6.60	7.60	42.20	27.20		456.00	245.00	0.54
	93.72	95.26	47.50								333.06		
	94.09	80.50	43.00										
	92.90	84.60	44.10	0.00	5.60	2.50	10.80	40.50	25.20		455.00	281.00	0.62
	84.00	93.00										120.00	

Table 4.8: Complete Database of Straw (ST) [13,16,17,24,26,40,41,44,45,48,54]

This substrate comprises different species of straws, particularly wheat straw and rice straw, which have similar characteristics and can be generalized in the same category. Since straw is a dry substrate, it is generally characterized by a very high TS and a high organic content. The percentages of lipids, SSEDC and proteins are usually low, leading to high C/N ratios, while the principal components are lignin, cellulose, and hemicellulose. Since the lignocellulosic content is very high, the EBMP is usually low, and highly depend on the operating conditions of the batch test and on eventual pre-treatments (the experimental methane yield can vary from a minimum of 0 to a maximum 289.5 mL/gVS).

- Rice Husk (RH)

Substrate	TS [%]	VS [%TS]	C/N [-]	LIP [%TS]	PROT [%TS]	SSEDC [%TS]	LIG [%TS]	CELL [%TS]	HCELL [%TS]	ASH [%TS]	TBMP [mL/gVS]	EBMP [mL/gVS]	BD [-]
RH	90.00	81.09	38.48										
	90.20	82.40	103.5	0.00	2.50	20.80	15.80	38.70	19.20		485.00	49.00	0.10
			80.56				13.00	29.40	17.70				

Table 4.9: Complete Database for Rice Husk (RH) [18,23,55]

Only few data have been found about rice husk, however this substrate is very important since it is an abundant by-product of rice cultivation and is characterized by a very low degradability, therefore it could be interesting to see how its methane production would improve with AcoD. Similarly to straw, the TS content is very high, and the major components are lignin, cellulose and hemicellulose. Furthermore, being the proteins content very low, the C/N ratio can reach very high values.

- Sugar Beet By-Products (SBB)

Substrate	TS [%]	VS [%TS]	C/N [-]	LIP [%TS]	PROT [%TS]	SSEDC [%TS]	LIG [%TS]	CELL [%TS]	HCELL [%TS]	ASH [%TS]	TBMP [mL/gVS]	EBMP [mL/gVS]	BD [-]
SBB	88.50	89.30	35.70				9.90	26.40	19.50			219.60	
	88.73	91.65	37.00										
	30.40	94.50	32.90	1.50	8.70					5.50		430.00	
	11.80	71.30	15.00	2.50	12.80					28.70		481.00	
	17.40	71.84		0.70	16.00					28.10	453.67	388.80	0.86
	18.95	71.61		0.80	6.90					28.40	553.00	428.17	0.77
	11.00	84.00	14.00								520.00		
											439.76	369.40	0.84
											447.40	412.50	0.92
											468.43	443.60	0.95

Table 4.10: Complete Database for Sugar Beet By-Products (SBB) [21,35,56–59]

This substrate comprises all the by-products that come from sugar beets cultivation and processing, like roots, leaves, exhausted pulp, and molasses. According to the composition of this substrate its parameters can considerably change: for example, the TS content and the C/N ratio are highly variable. Few information about the lignin, cellulose and hemicellulose content have been found, while no information about the SSEDC content have been found. The EBMPs of this category are usually very high.

- Dry Grass (DG)

Substrate	TS [%]	VS [%TS]	C/N [-]	LIP [%TS]	PROT [%TS]	SSEDC [%TS]	LIG [%TS]	CELL [%TS]	HCELL [%TS]	ASH [%TS]	TBMP [mL/gVS]	EBMP [mL/gVS]	BD [-]
DG	84.60	95.86	42.17										
	87.82	86.18	57.03				5.51	42.21	28.45				
	93.01	97.29		0.00	0.68	0.00	8.08	47.48	41.06	2.71	362.32	122.20	0.34
	93.40	94.24					5.98	35.99	22.89		461.40	306.30	0.66
	91.30	95.70	109.0	0.00	2.50	7.10	11.30	43.10	31.70	4.30	448.00	246.00	0.55

Table 4.11: Complete Database for Dry Grass (DG) [19,23,24,41,44]

In this substrate different types of grass have been included, such as switchgrass, meadow grass and hay grass, which are characterized by similar compositions. Similarly to straw, DG is characterized by high TS, high C/N ratios, high quantities of lignocellulosic compounds and quite low EBMP.

- Maize Residue (MR)

MR comprises by-products from maize cultivation and processing such as fresh maize, maize plant and silage.

Substrate	TS [%]	VS [%TS]	C/N [-]	LIP [%TS]	PROT [%TS]	SSEDC [%TS]	LIG [%TS]	CELL [%TS]	HCELL [%TS]	ASH [%TS]	TBMP [mL/gVS]	EBMP [mL/gVS]	BD [-]
MR	38.75						2.40	23.74	37.68		452.30	399.40	0.88
	29.92						2.98	26.86	35.92		443.80	405.30	0.91
	27.89						1.81	22.31	36.73		445.20	360.50	0.81
			60.00										
			59.10				1.90	32.80	44.10				
	40.50	96.30			7.90	40.70							
	38.60	96.37			8.20	41.40							
	38.50	96.36			8.20	45.70							
	39.10	96.16			7.80	43.50							
	38.50	96.62			8.00	38.40							
	38.30	96.34			7.70	42.10							
				2.70									
				4.70	10.41					5.36			

Table 4.12: Complete Database for Maize Residue (MR) [24,60–63]

The C/N ratio is usually about 60, and the main components are generally SSEDC, cellulose and hemicellulose, while lignin content is quite low. The EBMPs of MR are usually quite high.

- Corn Stover (CS)

Substrate	TS [%]	VS [%TS]	C/N [-]	LIP [%TS]	PROT [%TS]	SSEDC [%TS]	LIG [%TS]	CELL [%TS]	HCELL [%TS]	ASH [%TS]	TBMP [mL/gVS]	EBMP [mL/gVS]	BD [-]
CS	86.02	94.04	88.35	6.60	1.49	38.16	2.30	24.24	21.24	5.96		217.70	
	84.90	90.60	54.00	0.00	5.00	3.20	10.30	42.30	29.80	9.40	469.00	241.00	0.51
	94.48	91.83	63.50				7.10	38.81	29.50		564.00	311.00	0.55
	88.80	94.14	63.20	0.00	4.40	8.50	9.40	42.30	29.80	5.90	437.60	260.70	0.60
	80.00	93.00										180.00	

Table 4.13: Complete Database of Corn Stover (CS) [23,29,43,48,64]

Corn stover derives from maize cultivation too, and consists of dried leaves, stalks and cobs of maize plants. This makes it a lignocellulosic substrate similar to straw. Indeed, the C/N ratio is usually high, and the lignin, cellulose and hemicellulose contents are high as well.

- Potato Waste (PW)

Substrate	TS [%]	VS [%TS]	C/N [-]	LIP [%TS]	PROT [%TS]	SSEDC [%TS]	LIG [%TS]	CELL [%TS]	HCELL [%TS]	ASH [%TS]	TBMP [mL/gVS]	EBMP [mL/gVS]	BD [-]
PW	17.74	92.16		0.74	9.68	72.99	0.00	8.76	0.00	7.84		334.50	
	19.86	95.92	38.89								422.00	345.00	0.82
	14.40	96.81					20.69			0.58			
	9.10	96.00											
	11.50	90.07	40.78		14.78							349.00	
	8.10	88.21	28.59		15.72							348.00	

Table 4.14: Complete Database of Potato Waste (PW) [19,26,48,65,66]

This substrate comprises mainly fresh potato residues and potato peels. It is mainly composed of SSEDC, while all the other organic compounds represent the minority of the substrate; the C/N ratio is usually comprised between 30 and 40, then the EBMPs are generally quite high.

- Yard Waste (YW)

Substrate	TS [%]	VS [%TS]	C/N [-]	LIP [%TS]	PROT [%TS]	SSEDC [%TS]	LIG [%TS]	CELL [%TS]	HCELL [%TS]	ASH [%TS]	TBMP [mL/gVS]	EBMP [mL/gVS]	BD [-]
YW	72.50	83.30	25.90	0.00	10.00	21.70	10.50	21.00	20.10	16.70	503.00	183.00	0.36
	97.30	91.90	74.70				23.20	19.30	12.30	9.10	498.90	116.50	0.23
	16.69	88.03		1.52	9.39		6.35	27.87	31.18			220.53	
	27.00	89.00		6.23	4.45	38.27	11.57	19.58	8.90	11.00	504.00	237.00	0.47
	87.00	84.32	59.12				10.87	18.21	23.53				
	94.30	91.70	55.30				23.00	24.30	9.70				

Table 4.15: Complete Database of Yard Waste (YW) [23,31,67–70]

YW comprises house-garden grass and plants, leaves, tree trimming, and harvest remains. Usually the C/N ratio is high, and a high quantity of hardly degradable matter is contained, then the EBMP is usually quite low.

- Vinegar Residue (VR)

Substrate	TS [%]	VS [%TS]	C/N [-]	LIP [%TS]	PROT [%TS]	SSEDC [%TS]	LIG [%TS]	CELL [%TS]	HCELL [%TS]	ASH [%TS]	TBMP [mL/gVS]	EBMP [mL/gVS]	BD [-]
VR	92.40	91.80	22.90	0.00	11.90	11.20	12.40	23.30	33.00	8.20	468.00	253.00	0.54
	92.37	91.57	22.68				9.73	28.15	32.56		473.34	242.69	0.51
	96.60	94.38	18.68				9.20	22.96	38.90	5.62	433.94	203.91	0.47
	91.41	91.65	23.06				9.58	28.38	32.77				

Table 4.16: Complete Database of Vinegar Residue (VR) [23,71–73]

The vinegar residue is a typical solid by-product of the vinegar production process. It is characterized by a very high C/N ratio and a high content of lignocellulosic compounds. Few information has been found about lipids, proteins and SSEDC contents.

4.2.1.3 Organic Waste

- Food Waste (FW)

Food waste includes all the animal and vegetable food waste coming from houses, kitchens and supermarkets, thus it is a very abundant substrate. FW contains a high quantity of readily biodegradable organic materials, so anaerobic digestion is an ideal solution for energy recovery from it.

Substrate	TS [%]	VS [%TS]	C/N [-]	LIP [%TS]	PROT [%TS]	SSEDC [%TS]	LIG [%TS]	CELL [%TS]	HCELL [%TS]	ASH [%TS]	TBMP [mL/gVS]	EBMP [mL/gVS]	BD [-]
FW	27.90	94.27	18.10										
	16.60	94.52	18.83	4.74	19.33	19.50					550.87		
	27.45	91.99	16.81										
	19.69	67.75											
	27.60	68.88											
	26.30	86.30	20.30	35.50	16.00	2.90	4.30	15.20	9.20	16.90		541.00	
	41.00	84.00		21.00	10.08	43.68	1.68	10.08	5.88	7.60	582.00	572.00	0.98
	24.00	93.00		13.02	4.65	49.29	4.65	3.00	9.30	16.09	518.00	425.00	0.82
	22.17	80.60		33.82	16.88	21.60							
	16.93	90.02	21.82	16.50	13.00							264.00	
	24.91	92.77	18.24	23.00	17.30							276.00	
	21.14	93.33	19.03	27.60	16.40							306.00	
	22.71	91.24	18.90	30.40			1.80	4.12	9.68			507.00	
	29.00	95.00										290.00	
	23.90	91.30	16.30				0.60	2.00	2.40	9.70	543.50	526.80	0.97

Table 4.17: Complete Database of Food Waste (FW) [16,18,22,23,44,48,64,67,68,74–76]

It usually contains a high amount of lipids, proteins and SSEDC, which are easily degradable compounds, and a quite low quantity of lignin, cellulose and hemicellulose; the C/N ratio, however, is usually quite low and comprised between about 16 and 22 depending on the composition. Thanks to the high organic content the EBMP is usually high, making this substrate one of the most promising for AcoD.

- Fruit and Vegetable Food Waste (FVFW)

Substrate	TS [%]	VS [%TS]	C/N [-]	LIP [%TS]	PROT [%TS]	SSEDC [%TS]	LIG [%TS]	CELL [%TS]	HCELL [%TS]	ASH [%TS]	TBMP [mL/gVS]	EBMP [mL/gVS]	BD [-]
FVW	3.70	89.20	13.10	0.00	20.60	30.90	7.90	12.00	5.90	10.80	476.00	342.00	0.72
	4.40	89.32	22.66	5.59	12.52	13.85						338.37	
	4.50	89.11	16.27	5.30	12.46	30.30						363.00	
	7.86	91.60		1.28	16.31	40.85	0.00	33.16	0.00	8.40	397.13		
	7.94	84.89	17.21	1.09	11.80	24.50							
	10.80	78.00	6.84	1.36	26.90								

Table 4.18: Complete Database of Fruit and Vegetable Food Waste (FVFW) [19], [23], [78], [80], [81]

This substrate includes food waste of vegetable origin only. With respect to FW, the lipids content of FVFW is lower due to the absence of animal-based food residues, and the C/N ratio is often lower than FW. Consequently, the EBMP is generally lower than the one of FW.

- Organic Fraction of Municipal Solid Waste (OFMSW)

Substrate	TS [%]	VS [%TS]	C/N [-]	LIP [%TS]	PROT [%TS]	SSEDC [%TS]	LIG [%TS]	CELL [%TS]	HCELL [%TS]	ASH [%TS]	TBMP [mL/gVS]	EBMP [mL/gVS]	BD [-]
OFMSW	23.00	74.10	28.67										
	46.80	84.19	51.80								494.30	201.50	0.41
	29.40	77.21	16.50										
	18.40	61.41	11.40									314.00	
	46.30	75.38	27.00										
	37.40	90.11	13.30										
	15.00	88.67	36.36	8.50	6.87		8.50	15.50	9.50	11.50		320.00	
	21.10	82.46	12.80										
	25.90	95.37	17.00								460.00		
	28.30	77.74	14.00										
	42.20	71.09	21.00								412.00		
	52.83	63.52	25.00	4.36	8.26	21.60	11.69	16.01	3.30	34.79	557.00		
		93.00		11.00	15.00	48.30	5.00	9.00	5.10	6.60		430.00	
		93.00		31.00	17.00	25.10	4.90	10.00	5.00	7.00			
		92.00		19.00	16.00	36.20	5.00	11.00	5.10	7.70		490.00	
	29.40	95.30		19.00	18.10					4.70	549.00		

Table 4.19: Complete Database of OFMSW [12,20,79–83]

The OFMSW represents a household waste that generally includes food waste, garden waste, paper, and textile residues. Its composition varies depending on a range of factors, reflecting the population density, the location and season of production. Globally, an enormous amount of OFMSW is generated, most of which is burnt or landfilled; its uncontrolled decomposition contributes to climate change and pollution of soil, water, and air. Thanks to its high organic content anaerobic digestion is an environmentally friendly solution to recover OFMSW, preventing its related pollution.

Due to the extreme variability in its composition, all the parameters characterizing OFMSW can considerably vary depending on its source: the C/N ratio may vary from low values such as 11.4 to relatively high values as 51.8, then an average value with a certain distribution will be defined; the TS may considerably change depending on the moisture content of the waste; the organic composition is variable too. The EBMP is usually quite high due to the presence of a high amount of organic matter, however it is meanly lower than the one of FW since in this case the substrate contains a higher amount of hardly degradable fractions (e.g., lignin content).

- Fish Waste (FIW)

Fish waste consists of residues coming from fish processing, such as heads, tails, fish bones and viscera.

Substrate	TS [%]	VS [%TS]	C/N [-]	LIP [%TS]	PROT [%TS]	SSEDC [%TS]	LIG [%TS]	CELL [%TS]	HCELL [%TS]	ASH [%TS]	TBMP [mL/gVS]	EBMP [mL/gVS]	BD [-]
FIW	36.90	73.17		7.59	55.77	9.81							
	60.00	97.47		86.01	15.00		1.08	0.25	0.52				
	31.00	83.40	23.20	23.35	22.02						604.00	571.00	0.95
	26.60	86.40	24.70	23.16	26.96						601.00	516.00	0.86
	42.70	97.40	33.30	53.86	17.82						761.00	496.00	0.65
	30.00	69.80		5.24	20.45						484.00	312.00	0.64
	33.60	63.40		0.19	18.26						440.00	136.00	0.31
	34.30	84.50	20.40	21.46	23.66						590.00	445.00	0.75

Table 4.20: Complete Database of Fish Waste (FIW) [6,31,84]

This substrate contains a high quantity of lipids, and despite the high proteins content, it shows quite high C/N ratios, that fall into the optimal range of 20÷40. The lignocellulosic content is generally low, while no information is available about the ash content. The EBMP is generally high, which makes this substrate very promising for anaerobic digestion.

- Slaughterhouse Residue (SR)

Substrate	TS [%]	VS [%TS]	C/N [-]	LIP [%TS]	PROT [%TS]	SSEDC [%TS]	LIG [%TS]	CELL [%TS]	HCELL [%TS]	ASH [%TS]	TBMP [mL/gVS]	EBMP [mL/gVS]	BD [-]
SR	16.97	82.56		20.80	12.45		9.64	20.39	31.11			326.60	
	16.20	91.70		14.38	17.49		7.95	8.97	14.18			217.45	
	29.70	86.20	8.31	15.30	40.10						644.00	411.00	0.64
	29.70	85.39	21.59	4.00	15.10						517.00	357.00	0.69
				28.40	15.00					13.40			
				11.00	16.40					21.90			

Table 4.21: Complete Database of Slaughterhouse Residue (SR) [31,85,86]

SR represents the residues coming from meat processing – for example, viscera, intestine and digestive tract contents – of animals such as pigs, cows, chicken, sheep, goats, and rabbits. Few information are available about this substrate; just two values of C/N ratio were found, one of 8.21 and one of 21.59: this suggests that the C/N ratio may vary depending on the meat's nature, and it is generally quite low. Lipids and proteins content is generally high, and high contents of lignin, cellulose and hemicellulose are observed too, probably due to the presence of lignocellulosic bedding materials. No information about SSEDC was available. The EBMP is usually quite high.

- Blood (BL)

Blood is a slaughterhouse waste as well, but it is considered separately due to some characteristics that distinguish it from other slaughterhouse wastes.

Substrate	TS [%]	VS [%TS]	C/N [-]	LIP [%TS]	PROT [%TS]	SSEDC [%TS]	LIG [%TS]	CELL [%TS]	HCELL [%TS]	ASH [%TS]	TBMP [mL/gVS]	EBMP [mL/gVS]	BD [-]
BL	21.30	99.11	3.41								317.00	219.00	0.69
	22.33	21.34	3.36								321.00	231.00	0.72
	18.00	94.44	3.24	1.10	93.00		0.00	0.00	0.00		539.00		
	10.80	86.11	2.80	0.20									
	19.00									1.00			
	22.00	91.00		2.00									
	13.24	95.38	3.41	3.00	89.69						512.00	250.00	0.49
	19.70	95.60			96.50								
	17.90	93.85		0.30	88.60					2.45			
	18.00	94.44	3.24	1.10	93.00						538.00	443.00	0.82
	23.31	95.80	3.20	0.30	94.40								
	13.50		3.15								518.00	323.00	0.62

Table 4.22: Complete Database of Blood (BL) [61,85,87,88]

The C/N ratio of blood is extremely low, usually around 3: this because the most abundant component of Blood are proteins, which can even reach 96.5 %TS. No information about SSEDC is available, while the content of all the other compounds is generally low if compared to proteins. Although the C/N ratio is very low the EBMPs are quite high.

- Pre-Cooked Waste (PCW)

Substrate	TS [%]	VS [%TS]	C/N [-]	LIP [%TS]	PROT [%TS]	SSEDC [%TS]	LIG [%TS]	CELL [%TS]	HCELL [%TS]	ASH [%TS]	TBMP [mL/gVS]	EBMP [mL/gVS]	BD [-]
PCW	42.26	96.47		3.28	15.92	77.28	0.00	0.00	0.00	3.53		326.10	
	38.18	87.76		12.29	16.94	58.54	0.00	0.00	0.00	12.24	473.43	316.20	0.67
	41.50	95.00	22.68	1.36	13.80	57.90							

Table 4.23: Complete Database of Pre-Cooked Waste (PCW) [19,78]

This substrate involves precooked starchy food, such as pasta, generally rejected from the quality control line. Few information is available about PCW: only one datum was found for the C/N ratio, equal to 22.68; The SSEDC content represents the highest one, followed by proteins and lipids, while no lignocellulosic compounds are present. The EBMP is generally quite high.

- Exhaust Kitchen Oil (EKO)

This substrate represents exhaust oil – of both animal and vegetable origin – coming from kitchens. EKO is mainly composed of lipids, that represent nearly the 100 %TS, and the C/N ratio is usually quite high.

Substrate	TS [%]	VS [%TS]	C/N [-]	LIP [%TS]	PROT [%TS]	SSEDC [%TS]	LIG [%TS]	CELL [%TS]	HCELL [%TS]	ASH [%TS]	TBMP [mL/gVS]	EBMP [mL/gVS]	BD [-]
EKO	99.10	99.78		99.78	0.00	0.00	0.00	0.00	0.00	0.22	980.00	648.50	0.66
	75.40	95.00	48.50								629.00	586.00	0.93
	99.60	99.90		99.90	0.00	0.00	0.00	0.00	0.00	0.10		811.00	
	99.70	99.90		99.90	0.00	0.00	0.00	0.00	0.00	0.10		776.00	

Table 4.24: Complete Database of Exhaust Kitchen Oil (EKO) [19,23,26]

Due to these characteristics, both the TBMP and the EBMP are extremely high, then this substrate represents a sort of *"outlier"* with respect to the other substrates, and it won't be considered during the analysis of the database.

4.2.1.4 Sludges

- Sewage Sludge (SS)

Substrate	TS [%]	VS [%TS]	C/N [-]	LIP [%TS]	PROT [%TS]	SSEDC [%TS]	LIG [%TS]	CELL [%TS]	HCELL [%TS]	ASH [%TS]	TBMP [mL/gVS]	EBMP [mL/gVS]	BD [-]
SS	26.00	50.70	10.70										
	9.45	60.30	10.00	6.50	14.56	0.00					370.59		
	1.91	74.35											
	6.98	81.52	8.90								333.90	164.50	0.49
	30.70	88.21									527.00	342.00	0.65
	3.50	65.43	10.59	7.47	22.10	6.95						248.77	
	5.43	42.17	6.14	2.73	19.12								
	16.90	57.60	6.80				5.60	1.90	7.10	43.40	709.50	254.60	0.36
	33.00	69.70	10.00								298.00		
	1.60	75.00	5.40								305.60	200.39	0.66

Table 4.25: Complete Database of Sewage Sludge (SS) [12,20,22,26,67,74,75,77,80,89]

Sewage sludge represents the active sludge coming from wastewater treatment plants. This substrate is extremely abundant and contains pathogens such as viruses and bacteria, therefore it needs to be treated before being disposed and used, for example, as fertilizer. The quite high organic content allows it to be suitable for anaerobic digestion, even if C/N ratio is usually low and it is highly contaminated by heavy metals and ashes. Then, generally the EBMP is not so high. Its composition is very variable, it depends on the sludge source and few information is available.

- Food Industry Sludge (FIS)

This type of sludge can be distinguished from SS since it derives from the treatment of food industry wastewaters.

Substrate	TS [%]	VS [%TS]	C/N [-]	LIP [%TS]	PROT [%TS]	SSEDC [%TS]	LIG [%TS]	CELL [%TS]	HCELL [%TS]	ASH [%TS]	TBMP [mL/gVS]	EBMP [mL/gVS]	BD [-]
FIS	13.52	69.67	5.65								510.00	397.00	0.78
	7.65	89.80	11.35								493.00	415.00	0.84
	24.24	74.38	18.05								824.00	680.00	0.83
	39.14	95.58	53.40								824.00	706.00	0.86
	37.88	61.25	5.05								549.00	399.00	0.73
	9.10	94.50											
	11.30	75.00	7.63	3.15	31.90								
	0.60	66.67	5.50								197.50	80.20	0.41
	2.40	54.17	9.20								294.90	149.40	0.51
	3.80	89.47	9.20								411.80	246.81	0.60
	10.70	80.37	21.80										

Table 4.26: Complete Database of Food Industry Sludge (FIS) [26,48,78,89]

Actually, the quantity and the quality of the information collected about this substrate is quite poor, then it won't be considered for the building of the Primary Averaged Database, as it will be shown in the next section.

4.2.2 Primary Averaged Database

In order to build a first version of an averaged database, the data gathered for each substrate were averaged – except for BD – by using the Excel tool AVERAGE, while standard deviations were calculated using the tool STDEV.P. The mean value of the BD of the substrates, instead, was calculated with Equation 4.2 by dividing the mean EBMP for the mean TBMP.

$$BD_{mean} = \frac{EBMP_{mean}}{TBMP_{mean}} \tag{4.2}$$

The averaged values and their standard deviations are reported in Tables 4.27, 4.28 and 4.29.

Macro-Category	Substrate	Calculated quantity	TS [%]	VS [%TS]	C/N [-]	LIP [%TS]	PROT [%TS]	SSEDC [%TS]	LIG [%TS]	CELL [%TS]	HCELL [%TS]	ASH [%TS]	TBMP [mL/gVS]	EBMP [mL/gVS]	BD [-]
MAN	DM	AVG	18.24	73.56	18.15	3.96	9.28	23.54	10.38	15.68	12.74	26.48	486.33	224.66	0.46
		SD	7.77	8.14	4.37	3.97	3.53	14.75	4.19	3.55	7.28	10.96	65.46	60.27	-
	PM	AVG	19.15	72.73	11.62	6.25	16.82	34.19	3.60	8.51	14.83	22.66	573.50	388.33	0.68
		SD	11.48	7.60	3.37	3.13	6.48	13.31	2.10	3.06	8.63	5.70	113.24	100.83	-
	SM	AVG	25.03	78.36	10.30	11.84	16.13	31.88	9.30	18.99	18.08		531.50	244.56	0.46
		SD	11.21	3.17	0.00	5.84	1.65	0.81	5.39	3.92	4.95		4.88	42.71	-
	CM	AVG	30.60	73.30	9.24	0.34	21.03	13.40	3.51	21.43	17.10	23.45	485.96	289.71	0.60
		SD	9.63	5.61	2.08	0.48	4.67	3.70	1.58	2.02	8.63	1.55	75.37	93.97	-
	CL	AVG	63.24	64.69	9.99	0.95	23.87	19.65	7.90	24.93	21.01	14.26	544.05	265.27	0.49
		SD	12.15	7.97	1.87	1.01	5.93	0.00	1.97	3.75	4.52	3.39	0.00	133.21	
	SHM	AVG	35.05	74.12	13.30	1.26	10.18		11.90	14.15	19.70	16.08	426.77	197.18	0.46
		SD	12.40	10.21	1.15	0.00	0.00		3.31	2.52	6.43	0.00	80.23	76.47	
	GM	AVG	64.79	77.64	17.91	3.25	8.32	35.51	12.71	13.37	18.09	15.30	301.70	202.63	0.67
		SD	16.67	10.54	1.76	0.62	6.11	0.00	4.70	0.04	1.42	7.15	11.70	40.21	

Table 4.27: First version of the Primary Averaged Database for Manures

Macro-Category	Substrate	Calculated quantity	TS [%]	VS [%TS]	C/N [-]	LIP [%TS]	PROT [%TS]	SSEDC [%TS]	LIG [%TS]	CELL [%TS]	HCELL [%TS]	ASH [%TS]	TBMP [mL/gVS]	EBMP [mL/gVS]	BD [-]
AIW	ST	AVG	89.62	91.56	70.54	0.00	4.05	4.55	9.94	43.78	28.34	5.73	427.75	176.12	0.41
		SD	3.83	5.30	20.68	0.00	1.55	2.05	4.51	2.79	2.70	0.00	47.49	104.71	
	RH	AVG	90.10	81.75	74.18	0.00	2.50	20.80	14.40	34.05	18.45		485.00	49.00	0.10
		SD	0.10	0.66	26.92	0.00	0.00	0.00	1.40	4.65	0.75		0.00	0.00	
	SBB	AVG	38.11	82.03	26.40	1.38	11.10		9.90	26.40	19.50	22.68	452.45	421.92	0.93
		SD	32.48	9.50	9.41	0.72	3.55		0.00	0.00	0.00	9.92	9.42	33.82	
	DG	AVG	90.03	93.85	69.40	0.00	1.59	3.55	7.72	42.19	31.02	3.50	423.91	224.83	0.53
		SD	3.35	3.96	28.65	0.00	0.91	3.55	2.28	4.10	6.59	0.80	43.89	76.63	
	MR	AVG	36.67	96.36	59.55	3.70	8.32	41.97	2.27	26.43	38.61	5.36	447.10	388.40	0.87
		SD	4.22	0.14	0.45	1.00	0.87	2.27	0.47	4.03	3.23	0.00	3.72	19.87	
	CS	AVG	86.84	92.72	67.26	2.20	3.63	16.62	7.28	36.91	27.58	7.09	490.20	242.08	0.49
		SD	4.76	1.35	12.76	3.11	1.53	15.39	3.10	7.45	3.67	1.64	53.74	43.69	
	PW	AVG	13.45	93.20	36.09	0.74	13.39	72.99	10.35	8.76	0.00	4.21	422.00	344.13	0.82
		SD	4.32	3.27	5.36	0.00	2.65	0.00	10.35	0.00	0.00	3.63	0.00	5.75	
	YW	AVG	65.80	88.04	53.76	2.58	7.95	29.99	14.25	21.71	17.62	12.27	501.97	189.26	0.38
		SD	32.19	3.30	17.65	2.65	2.49	8.29	6.48	3.36	8.08	3.23	2.21	46.34	
	VR	AVG	93.20	92.35	21.83	0.00	11.90	11.20	10.23	25.70	34.31	6.91	458.43	233.20	0.51
		SD	2.01	1.17	1.82	0.00	0.00	0.00	1.27	2.57	2.66	1.29	17.45	21.13	

Table 4.28: First version of the Primary Averaged Database for Agro-Industrial Waste

Macro-Category	Substrate	Calculated quantity	TS [%]	VS [%TS]	C/N [-]	LIP [%TS]	PROT [%TS]	SSEDC [%TS]	LIG [%TS]	CELL [%TS]	HCELL [%TS]	ASH [%TS]	TBMP [mL/gVS]	EBMP [mL/gVS]	BD [-]
OW	FW	AVG	24.75	87.66	18.70	22.84	14.21	27.39	2.61	6.88	7.29	12.57	548.59	411.98	0.75
		SD	5.70	8.55	1.58	9.59	4.48	16.97	1.59	5.02	2.80	4.00	22.82	120.71	
	FVW	AVG	6.53	87.02	15.22	2.44	16.76	28.08	3.95	22.58	2.95	9.60	436.57	347.79	0.80
		SD	2.54	4.50	5.20	2.18	5.46	8.85	3.95	10.58	2.95	1.20	39.44	10.86	
	OFMSW	AVG	32.00	82.16	22.90	15.48	13.54	32.80	7.02	12.30	5.60	12.05	494.46	351.10	0.71
		SD	11.53	10.74	11.39	8.74	4.35	10.45	2.71	2.89	2.07	10.37	54.54	100.24	
	FIW	AVG	36.89	81.94	25.40	27.61	24.99	9.81	1.08	0.25	0.52		580.00	412.67	0.71
		SD	9.83	11.60	4.82	26.99	12.14	0.00	0.00	0.00	0.00		102.22	147.43	
	SR	AVG	23.14	86.46	14.95	15.65	19.42		8.80	14.68	22.65	17.65	580.50	328.01	0.57
		SD	6.56	3.31	6.64	7.62	9.37		0.85	5.71	8.47	4.25	63.50	70.63	
	BL	AVG	18.26	86.71	3.23	1.14	69.91		0.00	0.00	0.00	1.73	457.50	293.20	0.64
		SD	3.78	22.03	0.19	0.96	33.55		0.00	0.00	0.00	0.73	98.43	83.15	
	PCW	AVG	40.65	93.08	22.68	5.64	15.55	64.57	0.00	0.00	0.00	7.88	473.43	321.15	0.68
		SD	1.77	3.81	0.00	4.76	1.31	8.99	0.00	0.00	0.00	4.36	0.00	4.95	
	EKO	AVG	93.45	98.64	48.50	99.86	0.00	0.00	0.00	0.00	0.00	0.14	804.50	705.38	0.88
		SD	10.42	2.10	0.00	0.06	0.00	0.00	0.00	0.00	0.00	0.06	175.50	91.69	
SL	SS	AVG	13.55	66.50	8.57	5.57	18.59	3.47	5.60	1.90	7.10	43.40	424.10	242.05	0.57
		SD	11.59	13.42	2.00	2.05	3.10	3.47	0.00	0.00	0.00	0.00	148.88	59.90	
	FIS	AVG	14.58	77.35	14.68	3.15	31.90						513.03	384.18	0.75
		SD	12.81	13.22	13.93	0.00	0.00						209.91	211.78	

Table 4.29: First version of the Primary Averaged Database for Organic Waste and Sludges

As it can be observed in Tables 4.27, 4.28 and 4.29, some of the substrates show missing data (highlighted in red colour), which for the sake of completeness should be calculated. Moreover, the sum of the percentages of lipids, proteins, SSEDC, lignin, cellulose, hemicellulose, and ash should be equal to 100%TS, but after the averaging process their final sum could be lower or exceed this value. Therefore, a re-elaboration of data was done in two steps:

1) First, the attention was focused on the imputation of the missing mean values, which are present in:
   - Sow Manure (SM) – ash content
   - Sheep Manure (SHM) – SSEDC content
   - Rice Husk (RH) – ash content
   - Sugar Beet By-products (SBB) – SSEDC content
   - Fish Waste (FIW) – ash content
   - Slaughterhouse Residue (SR) – SSEDC content
   - Blood (BL) – SSEDC content
   - Food Industry Sludge (FIS) – SSEDC, lignin, cellulose, hemicellulose and ash contents

Since FIS shows five missing values, this substrate was excluded from the database due to the lack of data. Besides FIW, all the other substrates have only one missing data: ash content or SSEDC content. Then, since the sum of the components must be 100%TS, ash content – for SM, RH and FIW – and SSEDC content – for SHM, SBB, SR and BL – were calculated respectively with Equations 4.3 and 4.4:

$$ASH = 100 - (LIP + PROT + SSEDC + LIG + CELL + HCELL) \quad (4.3)$$

$$SSEDC = 100 - (LIP + PROT + LIG + CELL + HCELL + ASH) \quad (4.4)$$

2) After having obtained the missing values, the attention was shifted to the other substrates to normalize their organic components percentages to make their sum be equal to 100%TS, imposing Equation 4.5.

$$LIP + PROT + SSEDC + LIG + CELL + HCELL + ASH = 100 \quad (4.5)$$

This was done by applying a simple relationship that allows to preserve the relative ratios between the component contents and to obtain a global sum of 100%TS. Supposing to refer to a generic organic component (i.e., LIP, PROT, SSEDC, LIG, CELL, HCELL or ASH) simply as $COMP$, the formula to calculate the normalized percentage of that component is given by Equation 4.6.

$$COMP_{normalized} = \frac{100 \cdot COMP_{original}}{(LIP + PROT + LIG + CELL + HCELL + ASH)_{original}} \quad (4.6)$$

The final version of the Primary Averaged Database is shown in Table 4.30 (standard deviations are not reported in this case). In this final averaged database, no missing values are observed, and all the constraints are respected.

FIS is not reported since it has not been possible to collect enough data about it; the line concerning EKO is highlighted in yellow because it was decided not to consider it during the following data analysis, being this substrate composed almost completely of lipids and having a mean EBMP significantly higher than the other substrates, then it has been considered as an *"outlier"*.

Substrate	TS [%]	VS [%TS]	C/N [-]	LIP [%TS]	PROT [%TS]	SSEDC [%TS]	LIG [%TS]	CELL [%TS]	HCELL [%TS]	ASH [%TS]	TBMP [mL/gVS]	EBMP [mL/gVS]	BD [-]
DM	18.24	73.56	18.15	3.88	9.09	23.07	10.17	15.36	12.49	25.94	486.33	224.66	0.46
PM	19.15	72.73	11.62	5.85	15.74	31.99	3.37	7.97	13.88	21.20	573.50	388.33	0.68
SM	25.03	78.36	10.30	9.40	12.81	25.32	7.38	15.08	14.36	15.65	531.50	244.56	0.46
CM	30.60	72.26	8.93	0.34	20.98	13.36	3.50	21.37	17.06	23.39	485.96	289.71	0.60
CL	63.24	64.69	9.99	0.94	23.64	19.47	7.83	13.18	20.82	14.12	544.05	265.27	0.49
SHM	35.05	74.12	13.30	1.26	10.18	26.74	11.90	14.15	19.70	16.08	426.77	197.18	0.46
GM	64.79	77.64	17.91	3.05	7.81	33.33	11.93	12.55	16.98	14.36	301.70	202.63	0.67
ST	89.62	91.56	70.54	0.00	4.20	4.72	10.32	45.42	29.40	5.94	427.75	176.12	0.41
RH	90.10	81.75	74.18	0.00	2.50	20.80	14.40	34.05	18.45	9.80	485.00	49.00	0.10
SBB	38.11	82.03	26.92	1.38	11.10	9.05	9.90	26.40	19.50	22.68	452.45	421.92	0.93
DG	90.03	93.85	69.40	0.00	1.78	3.96	8.61	47.10	34.63	3.91	423.91	224.83	0.53
MR	36.67	96.36	59.55	2.92	6.57	33.14	1.79	20.87	30.48	4.23	447.10	388.40	0.87
CS	86.84	92.72	67.26	2.17	3.58	16.41	7.18	36.43	27.23	7.00	490.20	242.08	0.49
PW	13.45	93.20	36.09	0.73	13.27	72.32	0.84	8.67	0.00	4.17	422.00	344.13	0.82
VR	93.20	92.35	21.83	0.00	11.87	11.17	10.20	25.64	34.22	6.89	458.43	233.20	0.51
YW	60.10	87.31	53.24	2.44	7.52	28.38	11.83	20.05	18.17	11.61	501.97	189.26	0.38
FW	24.75	87.66	18.70	24.35	15.15	29.21	2.78	7.34	7.77	13.40	548.59	411.98	0.75
FVFW	6.53	87.02	15.22	2.82	19.41	32.52	4.57	26.15	3.42	11.11	436.57	347.79	0.80
OFMSW	32.00	82.16	22.90	15.67	13.70	33.20	7.10	12.45	5.67	12.20	494.46	351.10	0.71
FIW	36.89	81.94	25.40	27.61	24.99	9.81	1.08	0.25	0.52	35.74	580.00	412.67	0.71
SR	23.14	86.46	14.95	15.65	19.42	1.16	8.80	14.68	22.65	17.65	580.50	328.01	0.57
BL	18.26	86.71	3.23	1.14	92.53	4.60	0.00	0.00	0.00	1.73	457.50	293.20	0.64
PCW	40.65	93.08	22.68	6.02	16.61	68.95	0.00	0.00	0.00	8.42	473.43	321.15	0.68
EKO	93.45	98.64	48.50	99.86	0.00	0.00	0.00	0.00	0.00	0.14	804.50	705.38	0.88
SS	13.55	66.50	8.57	6.50	21.71	4.06	6.54	2.22	8.29	50.68	424.10	242.05	0.57

Table 4.30: Final version of the Primary Averaged Database

4.2.3 Secondary Averaged Database

The Secondary Averaged Database was simply obtained by averaging the mean values of the substrates for each macro-category, so to obtain mean values for Manure, Agro-Industrial Waste, Organic Waste and Sludges.

Macro-Category	Calculated Quantity	TS [%]	VS [%TS]	C/N [-]	LIP [%TS]	PROT [%TS]	SSEDC [%TS]	LIG [%TS]	CELL [%TS]	HCELL [%TS]	ASH [%TS]	TBMP [mL/gVS]	EBMP [mL/gVS]	BD [-]
Manure	AVG	36.59	73.34	12.88	3.53	14.32	24.75	8.01	14.24	16.47	18.68	478.54	258.90	0.54
	SD	18.20	4.15	3.49	2.98	5.64	6.44	3.32	3.71	2.85	4.42	84.67	61.06	-
Agro-Industrial Waste	AVG	63.11	89.85	57.15	1.21	6.31	23.60	8.11	29.87	22.23	8.67	456.30	254.47	0.56
	SD	29.07	5.17	19.57	7.67	4.72	19.69	4.63	12.86	10.78	5.99	40.43	122.16	-
Organic Waste	AVG	41.03	87.87	21.34	23.39	24.64	15.21	4.32	10.81	9.28	12.36	545.07	384.29	0.71
	SD	31.35	5.10	12.09	30.52	26.56	13.26	3.75	10.19	11.72	10.43	111.41	132.74	-
Sludges	AVG	13.55	66.50	8.57	6.50	21.71	4.06	6.54	2.22	8.29	50.68	424.10	242.05	0.57
	SD	0.00	0.00	0.00	0.00	0.00	0.00	0.00	0.00	0.00	0.00	0.00	0.00	-

Table 4.31: Secondary Averaged Database

The SD of Sludges is equal to zero since, after having removed FIS from the database, only one substrate (SS) has remained.

4.3 Data Analysis

The Primary Averaged Database shown in Table 4.30 was analysed to understand which are the correlations between parameters and why certain substrates are characterized by a higher EBMP than others. First, two-dimensional plots were created in Excel to search dependencies on single variables, then three-dimensional plots were created in MATLAB – using a multi-dimensional regression tool – when a certain parameter seemed to depend on more variables. Finally, a four-dimensional function for the EBMP was also developed on MATLAB.

4.3.1 2D Plots

4.3.1.1 C/N ratio

First, the attention was focused on the search of the dependencies of the C/N ratio on other parameters by plotting the C/N ratios of the substrates of the Primary Averaged Database as function of the other parameters: in particular, C/N ratio was found to have a clear correlation with the content of proteins, since – together with eventual free ammonia – they represent the main nitrogen carrier. The C/N ratio as function of the proteins content is represented in Figure 4.2, where the points represent the single

substrates – characterized by a certain C/N and PROT, according to the Primary Averaged Database – and the curve represents the data trendline.

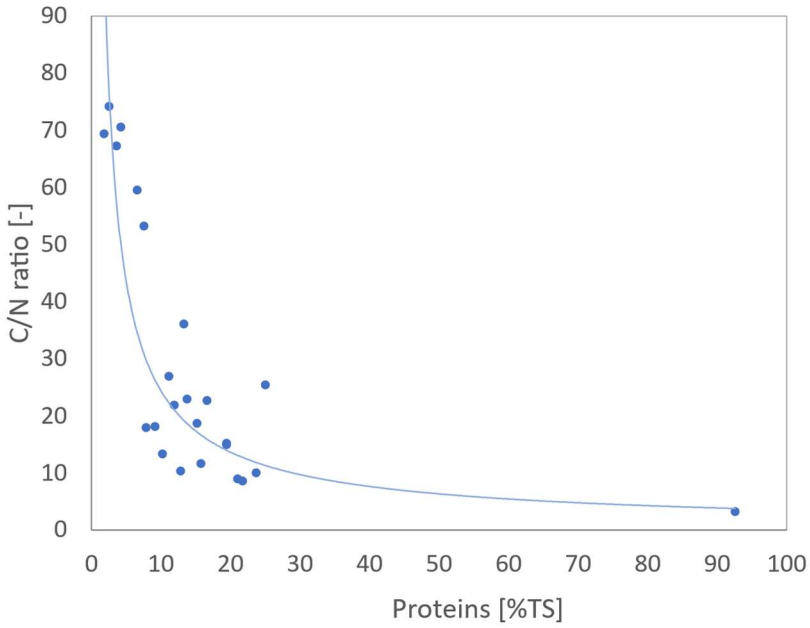

Figure 4.2: C/N ratio as function of Proteins content; the points represent the substrates of the database, and the curve represents the data trendline

As it can be observed in Figure 4.2, increasing the proteins content, the C/N ratio decreases due to the increase of nitrogen content. In particular, the substrate with the lowest C/N ratio is blood, which is on average composed of 92.5 %TS of proteins, while the substrate with highest C/N ratio is rice husk, which contains 2.50 %TS of proteins.

4.3.1.2 Biodegradability (BD)

Dependencies of BD on other parameters were searched to validate the importance of this parameter and to better understand its meaning.

As shown in Figure 4.3, the first dependency found for BD is on the lignin content. Indeed, BD decreases at increasing the amount of lignin because it represents the main hardly degradable component of substrates, reducing the organic content available for degradation.

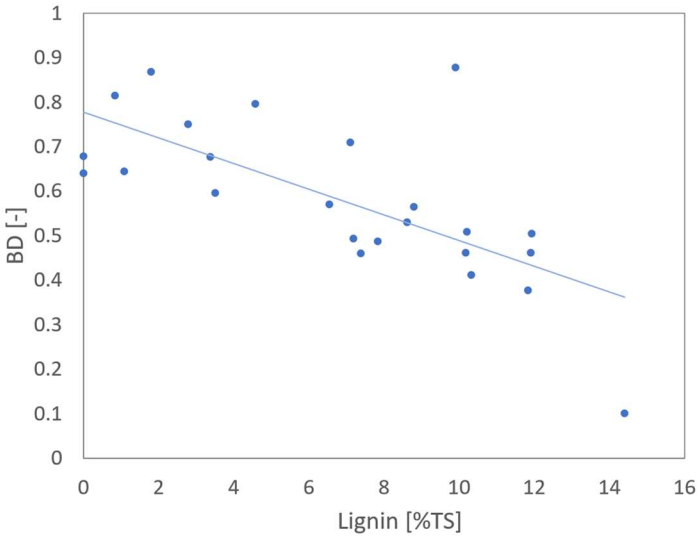

Figure 4.3: Biodegradability as function of Lignin content

Furthermore, BD also depends on the C/N ratio (Figure 4.4), showing a maximum when the C/N ratio is comprised between the optimal range: this stresses the importance of optimizing the C/N ratio when performing AcoD.

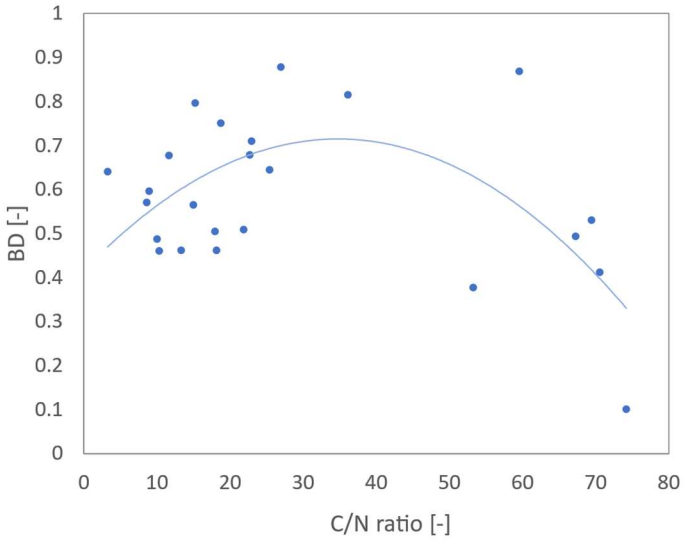

Figure 4.4: Biodegradability as function of the C/N ratio

4.3.1.3 Experimental Biomethane Potential (EBMP)

Lastly, the dependencies of EBMP were analysed to understand how parameters influence the methane production of the substrates.

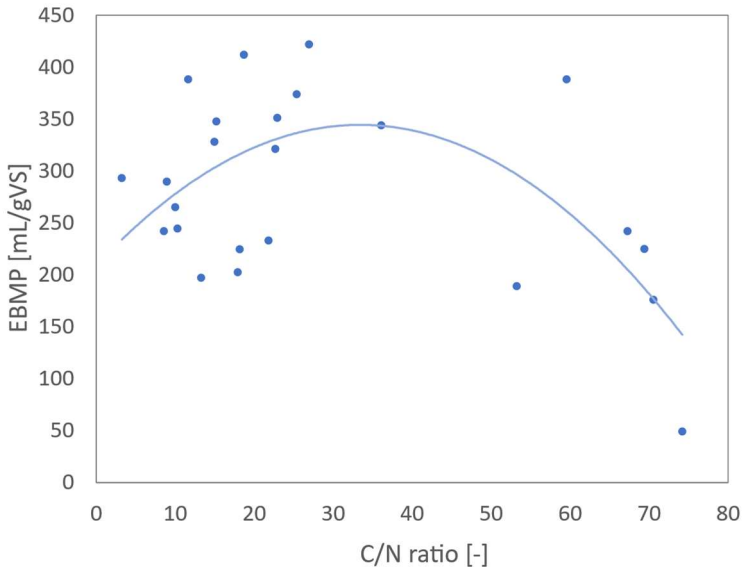

Figure 4.5: EBMP as function of the C/N ratio

The 2D plot of the EBMP as function of the C/N ratio (Figure 4.5) confirms again that the optimal range of C/N is between 20 and 40, where the EBMP shows a maximum. The fitting is however quite poor, and this suggests that the EBMP depends on other parameters too.

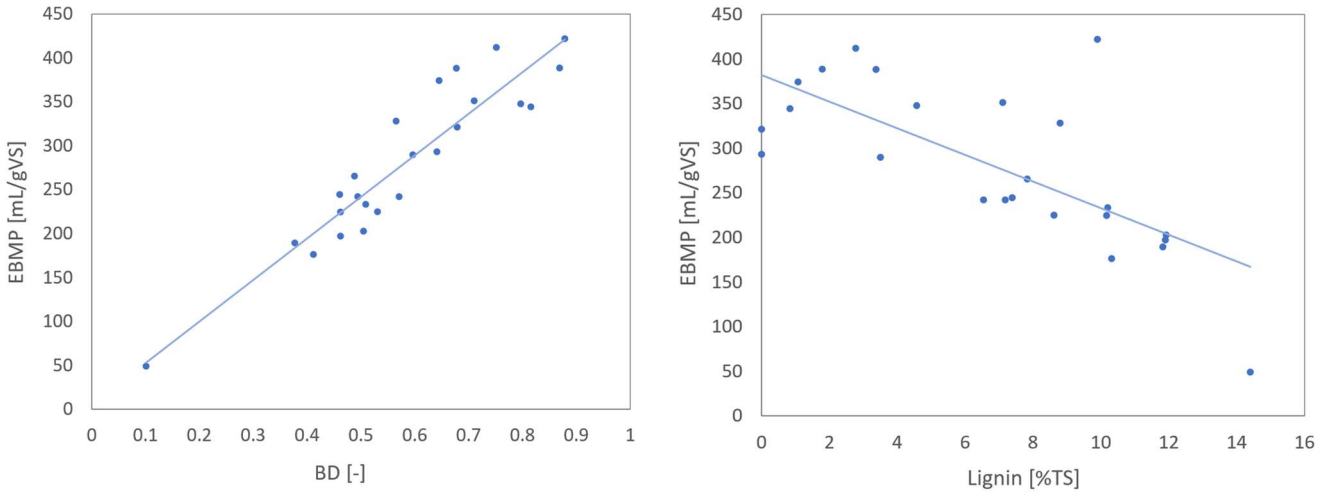

(a) (b)

Figure 4.6: EBMP as function of Biodegradability (a) and on Lignin content (b)

As predictable from the definition of Biodegradability, the EBMP increases at increasing the BD of the substrates, and highly degradable substrates generally show high EBMPs too (Figure 4.6 (a)). Furthermore, since BD decreases with the lignin content, the EBMP is characterized a similar trend, as shown in Figure 4.6 (b).

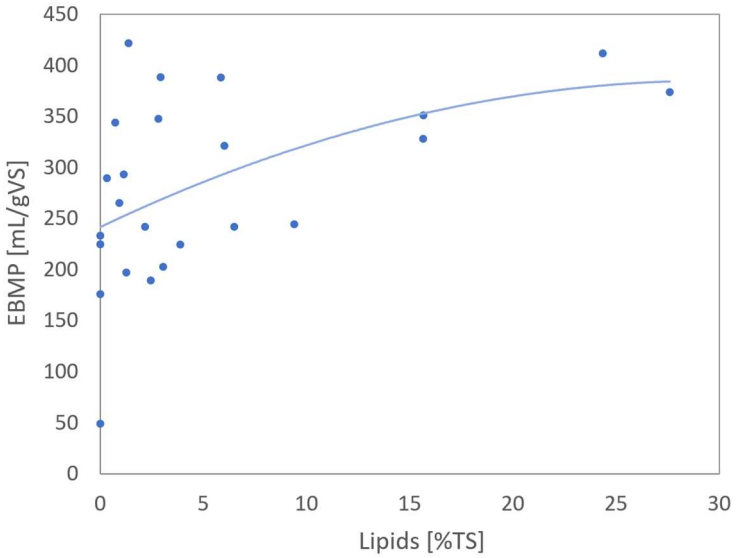

Figure 4.7: EBMP as function of Lipids content

In Figure 4.7, the trend of EBMP as function of lipids is reported. The fitting in this case is quite poor, but it shows how, increasing the lipids content, the EBMP increases too reaching a sort of plateau. Actually, in literature it has been demonstrated that the EBMP should reach a maximum as function of lipids content, since too high amounts of lipids lead to inhibition by VFA accumulation [93].

Finally, the dependence of EBMP on VS was analysed. In Figure 4.8 (a), it apparently seems that there is no correlation between EBMP and VS: this because the VS represents the overall organic content of the TS, without considering the real amount of VS that can be actually degraded. Therefore, it has been defined a parameter representing the available fraction of TS, named *corrected VS* (VS_{corr}), that is calculated by multiplying the VS for the BD of the substrate:

$$VS_{corr} = VS \cdot BD \tag{4.7}$$

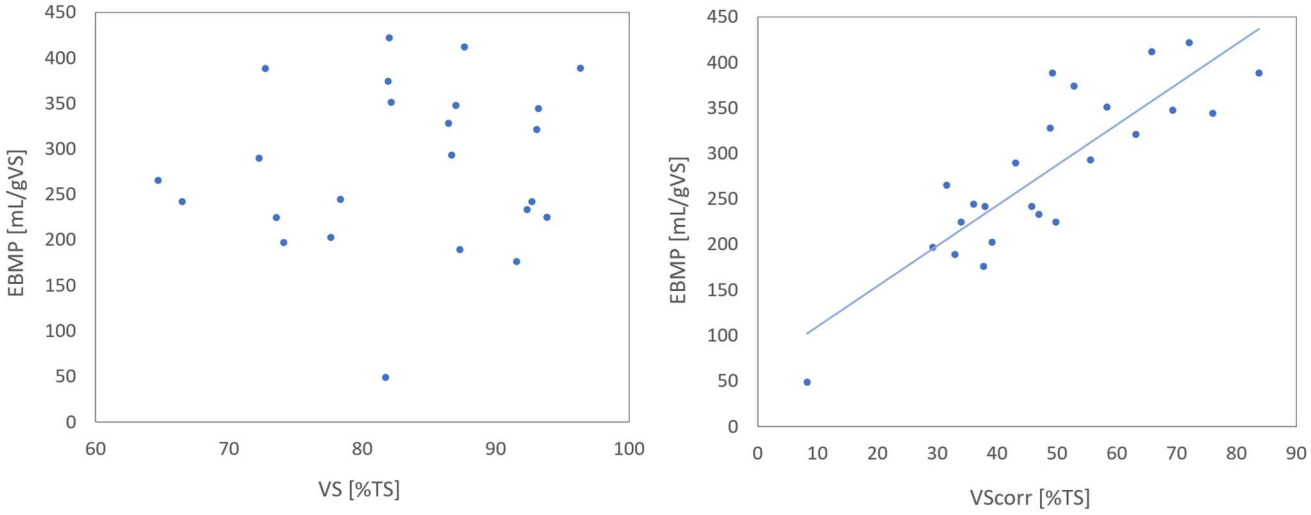

(a) (b)

Figure 4.8: EBMP as function of VS (a) and VS_{corr} (b)

By plotting the EBMP as function of VS_{corr} (Figure 4.8 (b)) an almost linear fitting is observed, showing an actual dependence on this parameter.

4.3.2 3D Plots

Starting from the 2D plots described in Section 4.3.1, 3D plots expressing the dependence of BD and EBMP on two variables at a time can be obtained by using regression tools. Once having selected a dependent variable Y (e.g., EBMP) and two independent variables x_1 and x_2 (e.g., C/N ratio and BD), 3D surfaces were obtained by performing a multi-dimensional regression analysis using the MATLAB tool `rstool`. This tool allows to calculate the coefficients β_i of the surface that better interpolates the points, giving the possibility of choosing between four possible models:

- *Linear* model: constant and linear terms

$$Y = \beta_0 + \beta_1 \cdot x_1 + \beta_2 \cdot x_2 \tag{4.8}$$

- *Pure Quadratic* model: constant, linear, and squared terms

$$Y = \beta_0 + \beta_1 \cdot x_1 + \beta_2 \cdot x_2 + \beta_3 \cdot {x_1}^2 + \beta_4 \cdot {x_2}^2 \tag{4.9}$$

- *Interaction* model: constant, linear, and interaction terms

$$Y = \beta_0 + \beta_1 \cdot x_1 + \beta_2 \cdot x_2 + \beta_3 \cdot x_1 \cdot x_2 \tag{4.10}$$

- *Full Quadratic* model: constant, linear, interaction, and squared terms

$$Y = \beta_0 + \beta_1 \cdot x_1 + \beta_2 \cdot x_2 + \beta_3 \cdot x_1 \cdot x_2 + \beta_4 \cdot {x_1}^2 + \beta_5 \cdot {x_2}^2 \tag{4.11}$$

4.3.2.1 Biodegradability (BD)

The first 3D plot describes the biodegradability as function of the C/N ratio and of the lignin content, merging the two correlations shown in Section 4.3.1.2. In this case, a *Pure Quadratic* model was chosen with the `rstool`, obtaining the surface represented in Figure 4.9 (a), that is described by Equation 4.12.

$$BD = \beta_0 + \beta_1 \cdot \left(\frac{C}{N}\right) + \beta_2 \cdot Lignin + \beta_3 \cdot \left(\frac{C}{N}\right)^2 + \beta_4 \cdot Lignin^2 \tag{4.12}$$

$$\begin{cases} \beta_0 = 0.4955 \\ \beta_1 = 0.0177 \\ \beta_2 = 0.0071 \\ \beta_3 = -0.0002 \\ \beta_4 = -0.0023 \end{cases}$$

In Figure 4.9 (b), the `rstool` graphical user interface for interactively investigating one-dimensional contours of the multidimensional response surface is also reported: here, the 2D projections of the surface at two fixed values of the C/N ratio and lignin content (that in this case are chosen by default by the tool and are 29.2019 for the C/N ratio and 6.7507 %TS for the lignin content) are represented. Furthermore, the dotted lines represent the confidence band of the prediction.

The plots in Figure 4.10 show that BD depends both on the C/N ratio and the biodegradability: BD shows indeed a maximum with respect to the C/N ratio and decreases by increasing the content of lignin.

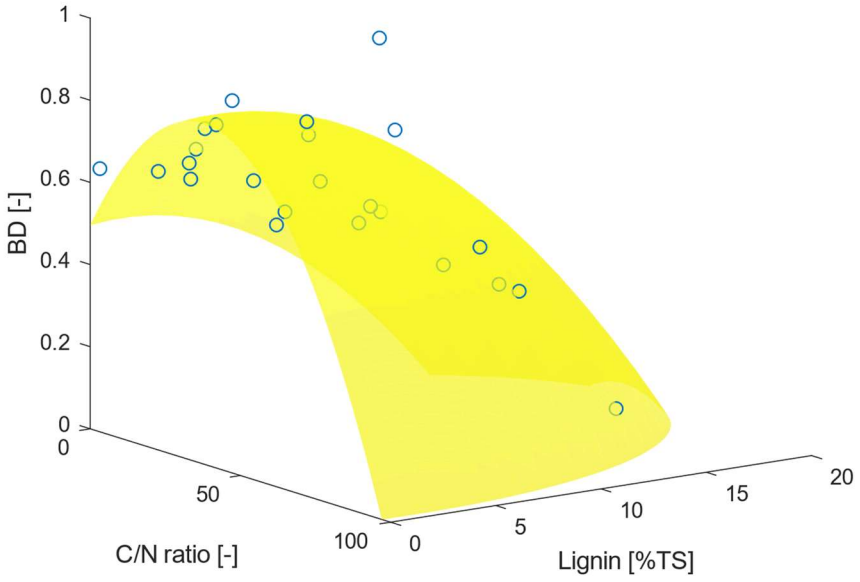

(a)

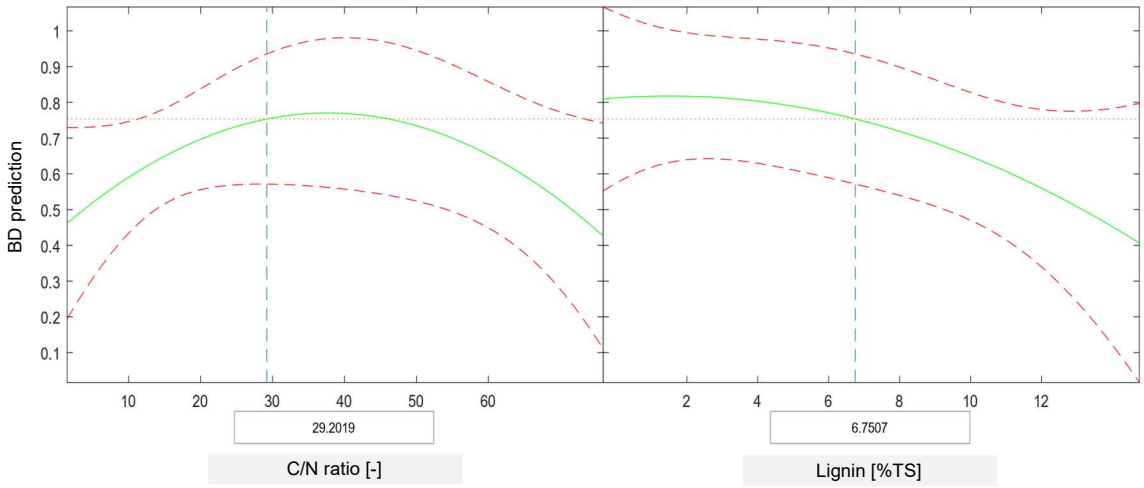

(b)

Figure 4.9: (a) Surface plot of BD as function of C/N ratio and lignin content; (b) graphical user interface of `rstool` with 2D projections of the surface

4.3.2.2 Experimental Biomethane Potential (EBMP)

Since the EBMP depends on a high number of variables, as demonstrated in Section 4.3.1.3, several 3D plots can be obtained, representing each the EBMP as function of two variables at a time.

- EBMP as function of C/N ratio and Biodegradability

The first relationship that was considered is the EBMP as function of the C/N ratio and BD. The surface model was obtained by choosing a *Pure Quadratic* model and the obtained 3D plot is shown in Figure 4.10 (a), which is represented by Equation 4.13.

$$EBMP = \beta_0 + \beta_1 \cdot \left(\frac{C}{N}\right) + \beta_2 \cdot BD + \beta_3 \cdot \left(\frac{C}{N}\right)^2 + \beta_4 \cdot BD^2 \tag{4.13}$$

$$\begin{cases} \beta_0 = 21.6613 \\ \beta_1 = 1.2558 \\ \beta_2 = 445.7076 \\ \beta_3 = -0.0223 \\ \beta_4 = -7.8201 \end{cases}$$

Figure 4.10 (b) represents the `rstool` interface showing the 2D projections of the EBMP at fixed values of its variables, chosen by default by the tool. The dotted lines represent the uncertainty of the prediction.

At fixed BD, the EBMP shows a maximum as function of the C/N ratio, and the value of such maximum increases by increasing the biodegradability. This confirms the trends that were obtained in the 2D plots of Figures 4.5 and 4.6.

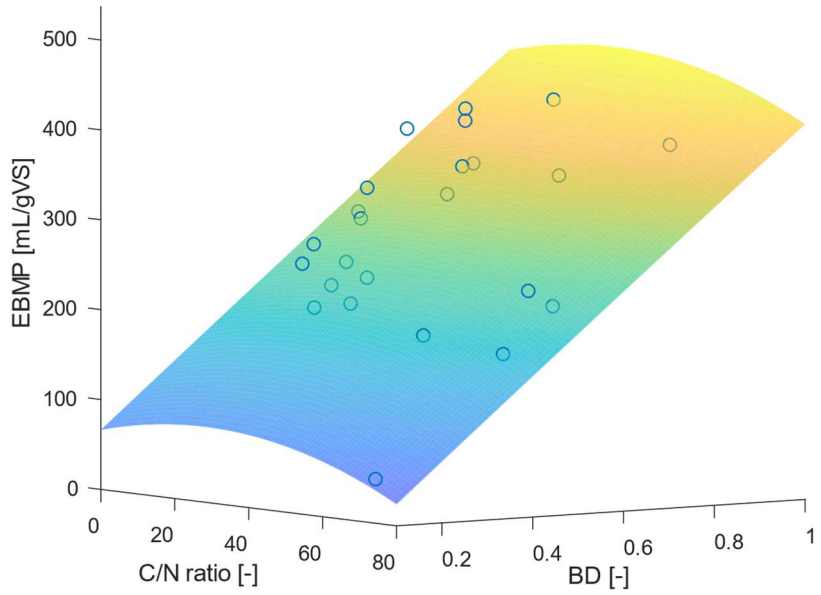

(a)

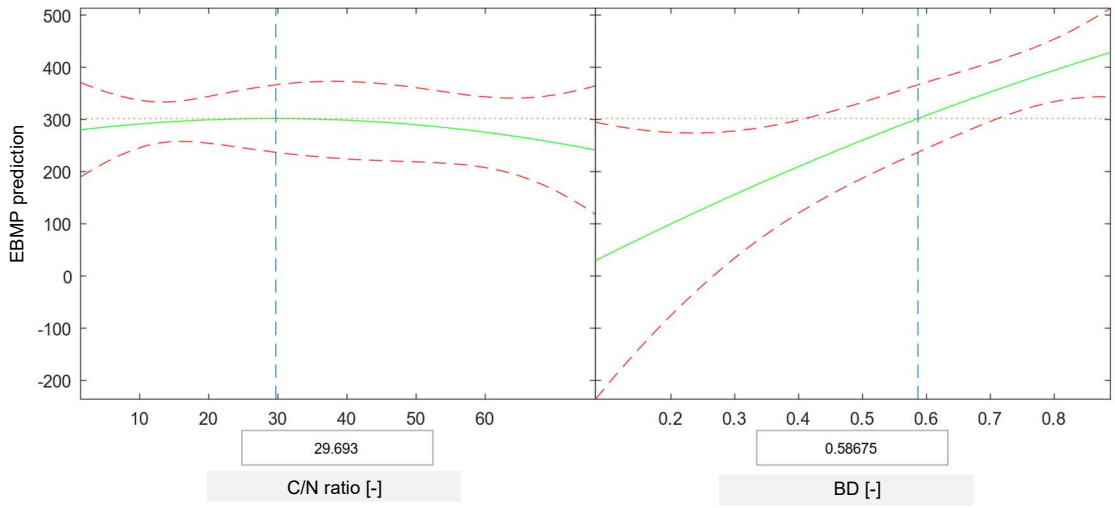

(b)

Figure 4.10: (a) Surface plot of EBMP as function of C/N ratio and BD; (b) graphical user interface of `rstool` with 2D projections of the surface

○ EBMP as function of C/N ratio and lignin content

Since BD decreases by increasing lignin content, a similar plot has been obtained by considering the EBMP as function of the C/N ratio and of the lignin content, represented in Figure 4.11 (a). In this case, the EBMP shows a maximum with respect to the C/N ratio and decreases at increasing lignin content, since the biodegradability is reduced.

For this surface, a *Full Quadratic* model on `rstool` was chosen, which is described by Equation 4.14.

$$EBMP = \beta_0 + \beta_1 \cdot \left(\frac{C}{N}\right) + \beta_2 \cdot Lignin + \beta_3 \cdot \left(\frac{C}{N}\right) \cdot Lignin + \beta_4 \cdot \left(\frac{C}{N}\right)^2 + \beta_5 \cdot Lignin^2 \quad (4.14)$$

$$\begin{cases} \beta_0 = 277.1885 \\ \beta_1 = 5.8153 \\ \beta_2 = 4.3002 \\ \beta_3 = -0.0110 \\ \beta_4 = -0.0776 \\ \beta_5 = -1.4598 \end{cases}$$

Figure 4.11 (b) represents the 2D projections obtained with `rstool` along with the confidence band for the fitted response surface.

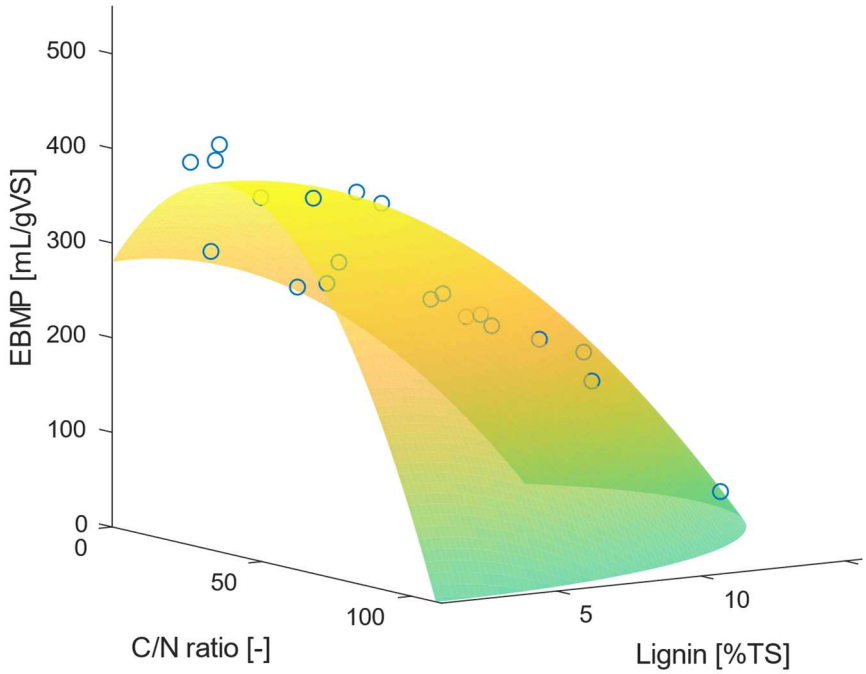

(a)

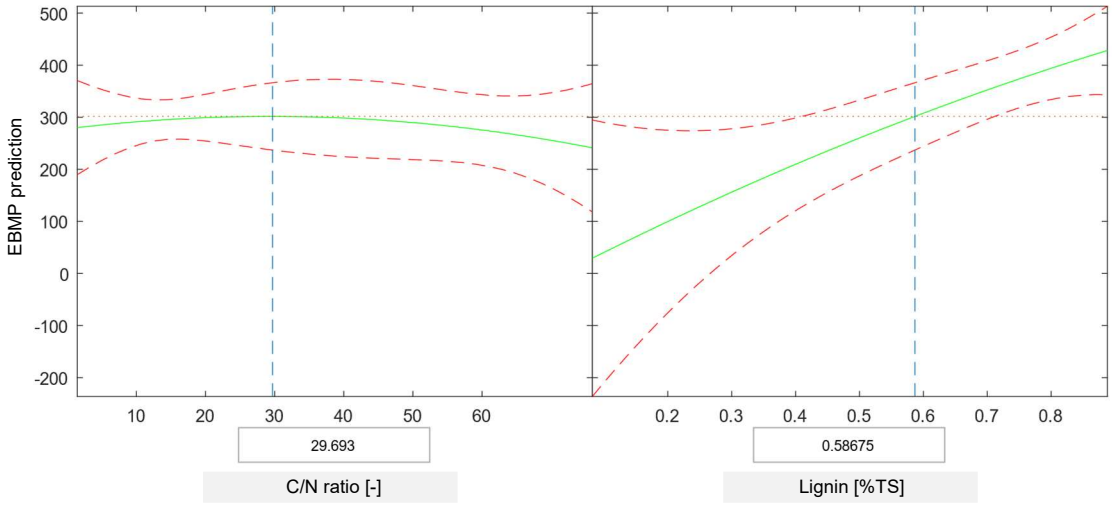

(b)

Figure 4.11: (a) Surface plot of EBMP as function of C/N ratio and lignin content; (b) graphical user interface of `rstool` with 2D projections of the surface

○ EBMP as function of lipids and lignin contents

Another interesting surface plot is the one representing the EBMP as function of lignin and lipids content, which is found with `rstool` using a *Pure Quadratic* model (Figure 4.12 (a) and (b)). As shown in Figure 4.12 (a), the EBMP is characterized by a maximum with respect to the lipids content, and the value of such maximum increases when the lignin content gets lower. This confirms that when the lipids content is too high, the methane production is reduced due to VFA accumulation, therefore an optimal range for the lipids content exists.

The surface represented in Figure 4.12 (a) is described by Equation 4.15.

$$EBMP = \beta_0 + \beta_1 \cdot Lipids + \beta_2 \cdot Lignin + \beta_3 \cdot Lipids^2 + \beta_4 \cdot Lignin^2 \qquad (4.15)$$

$$\begin{cases} \beta_0 = 315.7248 \\ \beta_1 = 6.1546 \\ \beta_2 = 2.1954 \\ \beta_3 = -0.1194 \\ \beta_4 = -1.2959 \end{cases}$$

.

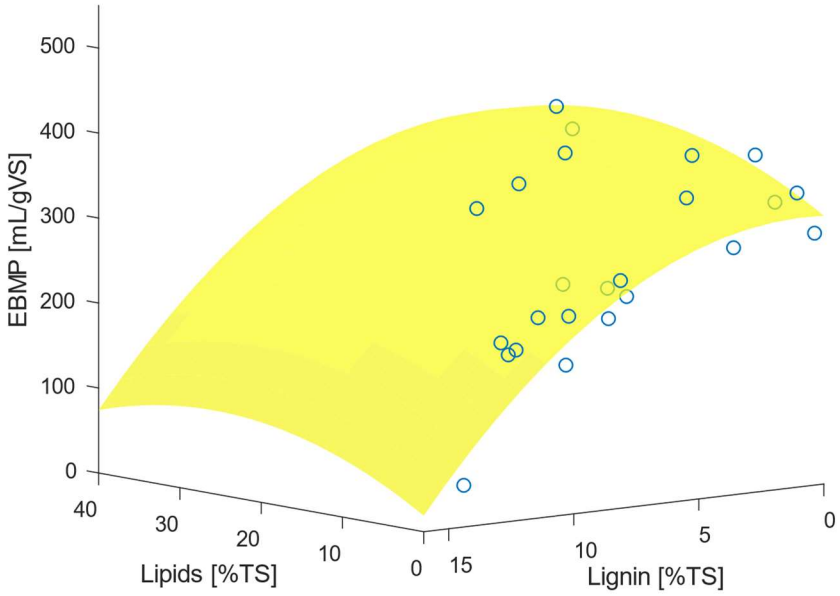

(a)

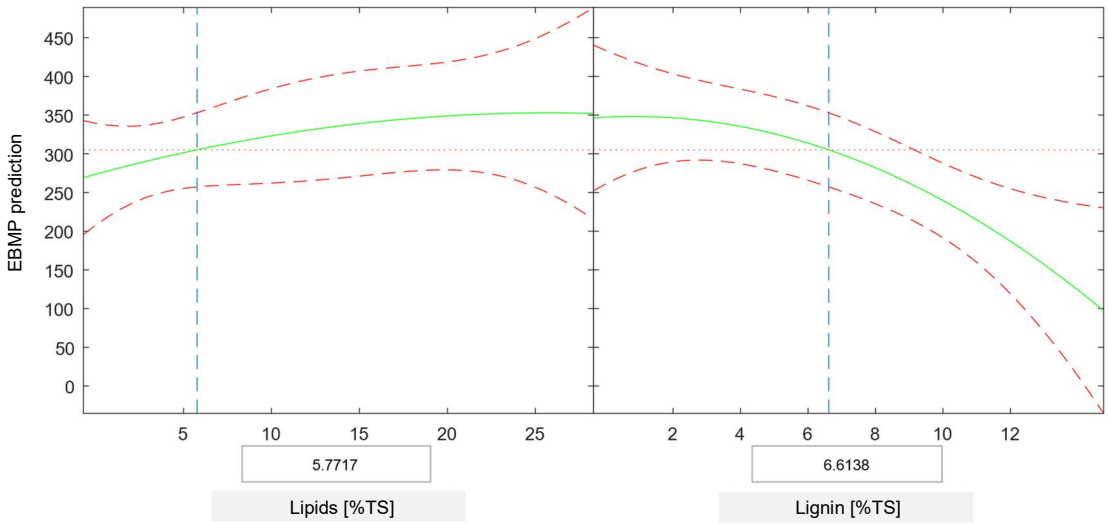

(b)

Figure 4.12: (a) Surface plot of EBMP as function of lipids and lignin content; (b) graphical user interface of `rstool` with 2D projections of the surface

○ EBMP as function of Biodegradability and Volatile Solids

Lastly, the dependence of EBMP on VS and BD (whose product is the so-called parameter VS_{corr}, defined by Equation 4.7) has been investigated.

In this case a *Linear* model was chosen with the `rstool` and the resulting surface is shown in Figure 4.13 (a), while in Figure 4.13 (b) the 2D projections given by the user interface of `rstool` at fixed values of BD and VS are reported. From Figure 4.12 (a) it can be observed that the points distribute themselves on a surface that increases linearly with the BD, while the dependence on VS is almost negligible. The surface is described by Equation 4.16.

$$EBMP = \beta_0 + \beta_1 \cdot VS + \beta_2 \cdot BD \tag{4.16}$$

$$\begin{cases} \beta_0 = 74.2090 \\ \beta_1 = -0.9394 \\ \beta_2 = 489.3507 \end{cases}$$

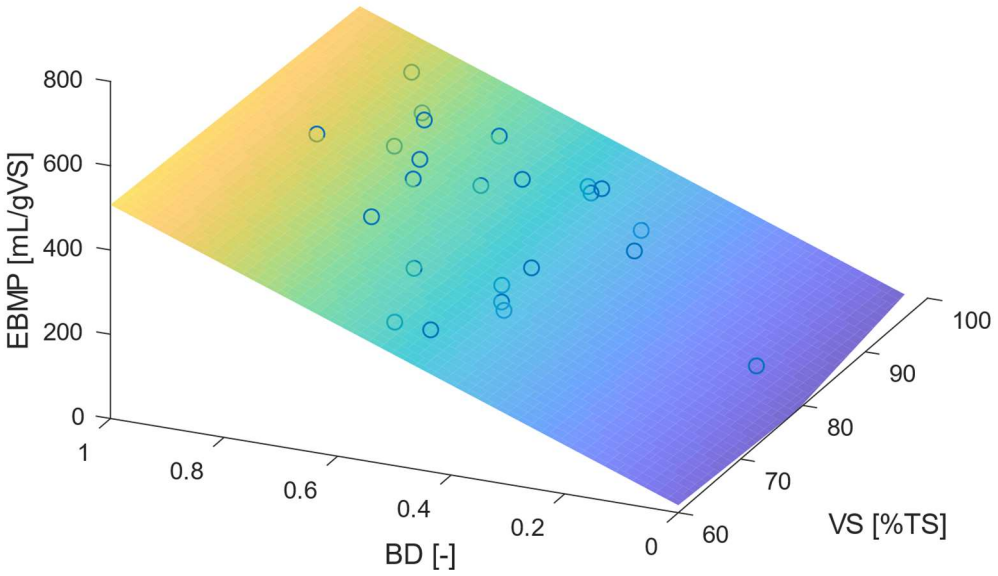

(a)

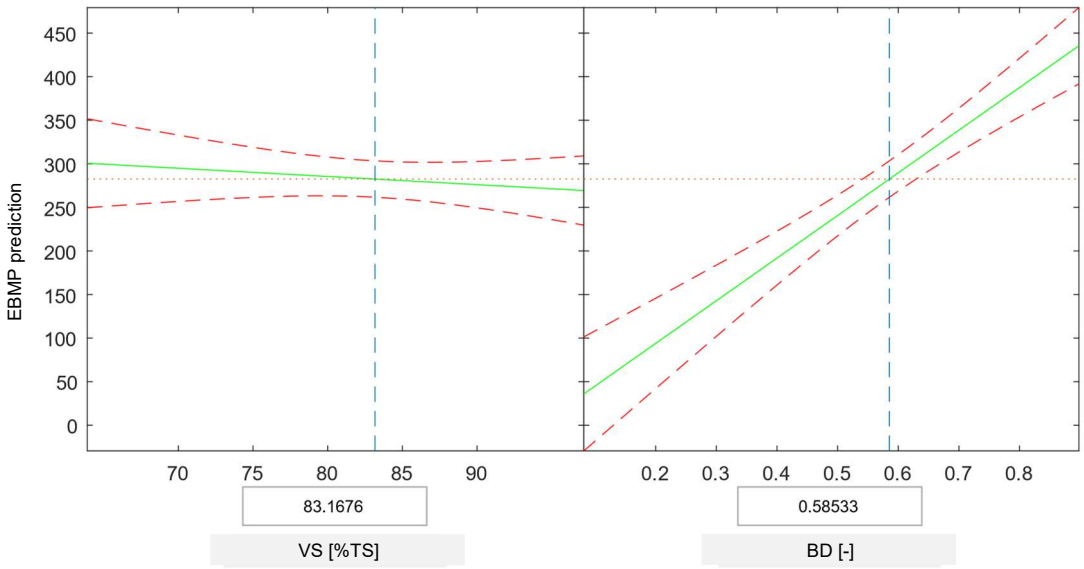

(b)

Figure 4.13: (a) Surface plot of EBMP as function of BD and VS; (b) graphical user interface of `rstool` with 2D projections of the surface

4.3.3 4D EBMP Function

Finally, a function of the EBMP depending on three variables was developed, that are the C/N ratio and the contents of lignin and lipids. This function was obtained still with `rstool` by choosing a full quadratic model for a three-variables function, which can be expressed as Equation 4.17:

$$Y = \beta_0 + \beta_1 \cdot x_1 + \beta_2 \cdot x_2 + \beta_3 \cdot x_3 + \beta_4 \cdot x_1 \cdot x_2 + \beta_5 \cdot x_1 \cdot x_3 + \beta_6 \cdot x_2 \cdot x_3 \ + \beta_7 \cdot {x_1}^2 + \beta_8 \cdot {x_2}^2 + \beta_9 \cdot {x_3}^2 \quad (4.17)$$

Assuming Y as EBMP, x_1 as the C/N ratio, x_2 as the lignin content, x_3 as the lipids content and applying the `rstool`, the obtained coefficients are reported in Equation 4.18.

$$EBMP = \beta_0 + \beta_1 \cdot \left(\frac{C}{N}\right) + \beta_2 \cdot Lignin + \beta_3 \cdot Lipids + \beta_4 \cdot \left(\frac{C}{N}\right) \cdot Lignin + \beta_5 \cdot \left(\frac{C}{N}\right) \cdot Lipids + \beta_6 \cdot Lignin \cdot Lipids \ + \beta_7 \cdot \left(\frac{C}{N}\right)^2 + \beta_8 \cdot Lignin^2 + \beta_9 \cdot Lipids^2 \quad (4.18)$$

$$\begin{cases} \beta_0 = 249.3464 \\ \beta_1 = 7.6699 \\ \beta_2 = 5.8635 \\ \beta_3 = -2.0732 \\ \beta_4 = 0.0041 \\ \beta_5 = -0.0901 \\ \beta_6 = 0.3424 \\ \beta_7 = -0.1014 \\ \beta_8 = -1.5273 \\ \beta_9 = 0.1586 \end{cases}$$

In this case a four-dimensional function is obtained, therefore it cannot be represented in a plot. The 2D projections returned by `rstool` user interface are shown in Figure 4.14 to understand how the EBMP varies as function of the three variables.

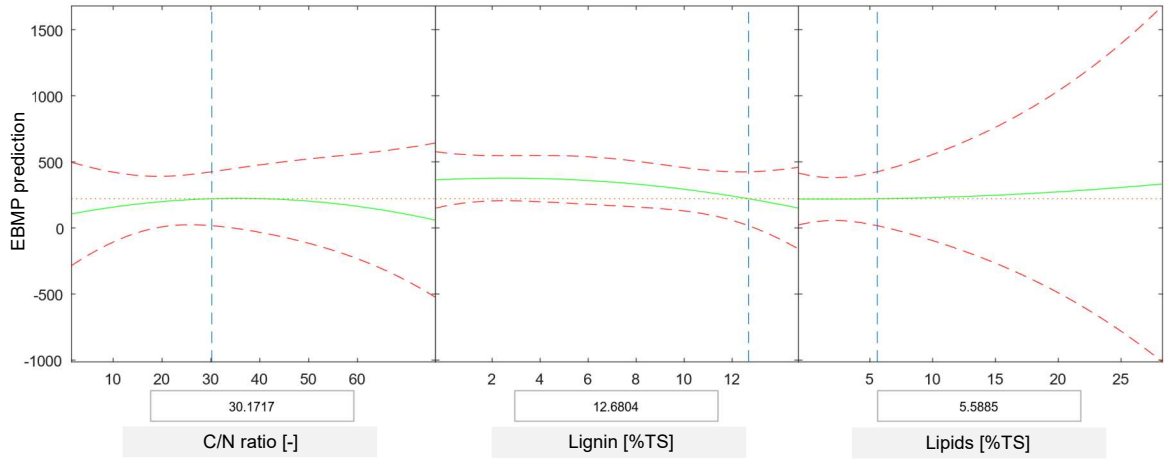

Figure 4.14: Graphical user interface of `rstool` with 2D projections of the function at fixed values of its variables

In Figure 4.14 it can be observed that the EBMP still shows a maximum with respect to the C/N ratio and a decreasing trend with respect to the lignin content; it doesn't show instead a maximum with respect to the lipids content probably due to numerical reasons and due to the high number of variables involved in the regression.

5. Blending Optimization Model

This chapter is dedicated to the development of the optimization algorithm that permits to calculate the optimal blending of substrates, aiming at maximizing the methane yield of the co-digestion.

The blending optimization consists of the maximization of an objective function representing the BMP of a mixture of substrates; when maximized, this function returns the highest possible BMP and the corresponding optimal mass fractions of the substrates. Such function should depend on the properties of the single and blended substrates and on their mass fractions and should take into account eventual synergistic effects deriving from the co-digestion. Moreover, it must be subjected to appropriate constraints when maximized.

The development of this tool represents a great innovation since it could be useful for industries that are interested in increasing their methane production by adopting better blending strategies, therefore a suitable programming environment has been chosen to make it accessible to the industrial world.

5.1 Optimization Algorithm Structure

The structure of the optimization algorithm developed in this project is shown in the block diagram in Figure 5.1.

When two or three substrates are co-digested, this algorithm is able to return the best mass fractions of these substrates to obtain the maximum possible methane yield: after having defined a first guess composition, the algorithm maximizes the objective function to obtain the optimized composition and the corresponding optimal BMP, calculated by the objective function itself. At the same time, the maximization must respect certain constraints, therefore the algorithm will find a solution that complies to them.

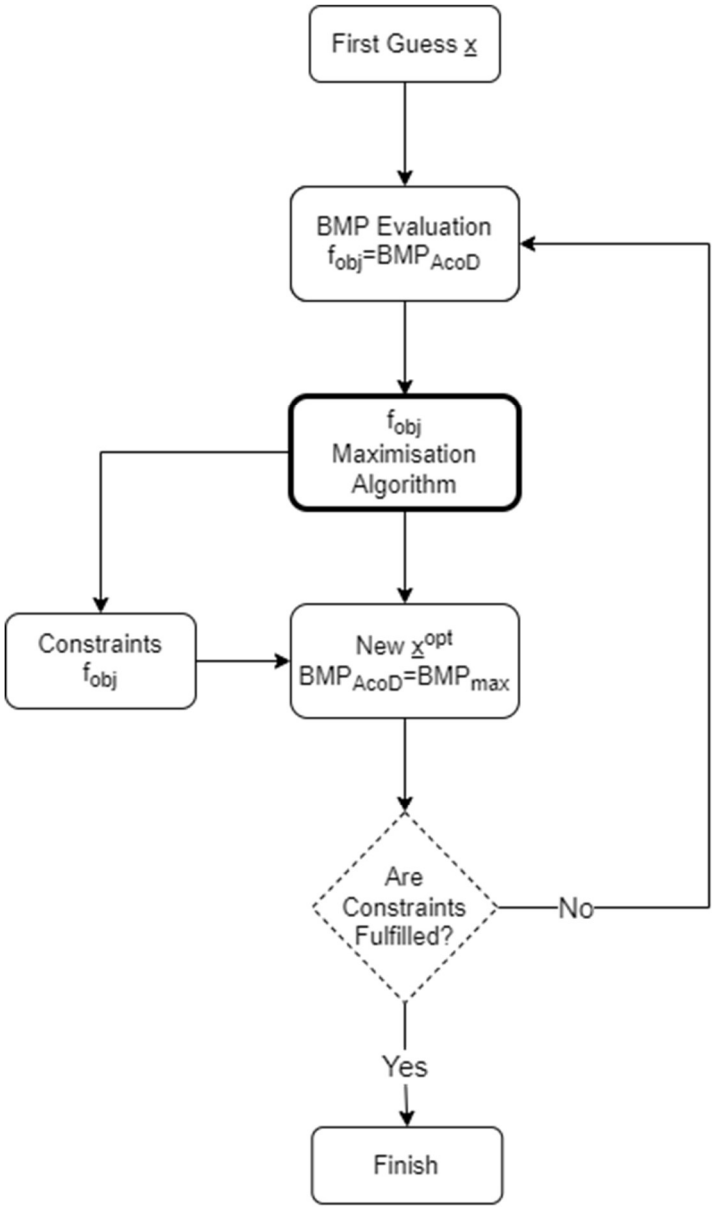

Figure 5.1: Block diagram of the blending optimization algorithm

5.2 Objective Function Definition – AcoD of Two Substrates

A considerable work was done to define an objective function that represents the BMP of a mixture of substrates and that shows a maximum in correspondence of the optimal blending composition.

5.2.1 Objective Function Structure

To define the objective function some considerations were done concerning its boundary conditions, considering at first the co-digestion of only two substrates: since the objective function should represent the co-digestion BMP, then when a mono-digestion is performed, it should be equal to the EBMP of the single substrate. Therefore, the conditions 5.1 should hold.

$$\begin{cases} x_1 = 1,\ x_2 = 0 & f_{obj} = EBMP_1 \\ x_1 = 0,\ x_2 = 1 & f_{obj} = EBMP_2 \end{cases} \tag{5.1}$$

Consequently, the objective function was defined in a way that these two boundary conditions would be respected, assuming a structure of the type in Equation 5.2.

$$f_{obj,NC=2} = BMP_{AcoD} = x_1 \cdot EBMP_1 + x_2 \cdot EBMP_2 + x_1 \cdot x_2 \cdot BMP_{mix} \tag{5.2}$$

The last term of Equation 5.2 represents the *interaction term* of the two substrates: when one of the two mass fractions is zero, this term zeroes too; when the two mass fractions are nonzero, this term represents the synergy of the co-digestion, that makes the actual BMP_{AcoD} higher than the weighted average of the EBMPs of the single substrates. Therefore, a definition for BMP_{mix} is necessary.

BMP_{mix} has been defined as the BMP of a pseudo-single substrate representing the blended mixture. In fact, after several trials, it has been decided to calculate this parameter by using the EBMP correlations obtained from the database analysis: BMP_{mix} is indeed calculated as the EBMP of a substrate characterized by weighted parameters with respect to the composition of the mixture, through the data-driven correlations shown in Chapter 4. In particular, two EBMP correlations have been identified as suitable for the definition of BMP_{mix}: the one depending on C/N ratio and BD (Equation 4.13) and the one depending on C/N ratio, lignin content and lipids content (Equation 4.14). These two definitions have both been used to maximize the objective function during tests and have been compared to determine which one works best.

5.2.2 First BMP_{mix} Definition: $BMP_{mix}\left(\frac{C}{N}, BD\right)$

This definition is obtained by taking advantage of the mathematical correlation of the EBMP with the C/N ratio and the BD shown in Section 4.3.2.2.

$$BMP_{mix}\left(\frac{C}{N}, BD\right) = \beta_0 + \beta_1 \cdot \left(\frac{C}{N}\right)_{mix} + \beta_2 \cdot BD_{mix} + \beta_3 \cdot \left(\frac{C}{N}\right)^2_{mix} + \beta_4 \cdot BD^2_{mix} \quad (5.3)$$

$$\begin{cases} \beta_0 = 21.6613 \\ \beta_1 = 1.2558 \\ \beta_2 = 445.7076 \\ \beta_3 = -0.0223 \\ \beta_4 = -7.8201 \end{cases}$$

In Equation 5.3 the BMP_{mix} is calculated with the same expression of the EBMP as function of the C/N ratio and the biodegradability, however in this case these parameters are calculated as weighted average of the ones of the substrates composing the blend, as shown in Equations 5.4 and 5.5.

$$\left(\frac{C}{N}\right)_{mix} = \sum_{i=1}^{NC} x_i \cdot \left(\frac{C}{N}\right)_i \quad (5.4)$$

$$BD_{mix} = \sum_{i=1}^{NC} x_i \cdot BD_i \quad (5.5)$$

In these equations, i represents the *i-th* substrate, NC represents the number of substrates (i.e., 2 in this case), x_i is the mass fraction of substrate i, and $\left(\frac{C}{N}\right)_i$ and BD_i are the C/N ratio and the biodegradability of substrate i, respectively.

5.2.3 Second BMP_{mix} Definition: $BMP_{mix}\left(\frac{C}{N}, Lignin, Lipids\right)$

The second definition of BMP_{mix} aims at considering the dependency of the EBMP on the C/N ratio and on the content of two important organic components of substrates – lignin and lipids content. The function used in this case is the one of Section 4.3.3, that is the BMP_{mix} calculated as function of the weighted values of the C/N ratio, lignin, and lipids content.

$$BMP_{mix}\left(\frac{C}{N}, Lignin, Lipids\right) = \beta_0 + \beta_1 \cdot \left(\frac{C}{N}\right)_{mix} + \beta_2 \cdot Lignin_{mix} + \beta_3 \cdot Lipids_{mix}$$
$$+ \beta_4 \cdot \left(\frac{C}{N}\right)_{mix} \cdot Lignin_{mix} + \beta_5 \cdot \left(\frac{C}{N}\right)_{mix} \cdot Lipids_{mix} + \beta_6 \cdot Lignin_{mix} \cdot Lipids_{mix}$$
$$+\beta_7 \cdot \left(\frac{C}{N}\right)_{mi}^{2} + \beta_8 \cdot Lignin_{mix}{}^{2} + \beta_9 \cdot Lipids_{mix}{}^{2} \quad (5.6)$$

$$\begin{cases} \beta_0 = 249.3464 \\ \beta_1 = 7.6699 \\ \beta_2 = 5.8635 \\ \beta_3 = -2.0732 \\ \beta_4 = 0.0041 \\ \beta_5 = -0.0901 \\ \beta_6 = 0.3424 \\ \beta_7 = -0.1014 \\ \beta_8 = -1.5273 \\ \beta_9 = 0.1586 \end{cases}$$

The *mix* parameters are calculated as:

$$\left(\frac{C}{N}\right)_{mix} = \sum_{i=1}^{NC} x_i \cdot \left(\frac{C}{N}\right)_i \quad (5.7)$$

$$Lignin_{mix} = \sum_{i=1}^{NC} x_i \cdot Lignin_i \quad (5.8)$$

$$Lipids_{mix} = \sum_{i=1}^{NC} x_i \cdot Lipids_i \quad (5.9)$$

Both these expressions of BMP_{mix} were used and compared during tests on experimental data.

5.3 Objective Function Definition – AcoD of Three Substrates

Since often biogas plants treat more than two substrates, an extension to the case of the co-digestion of three substrates was done, making hypothesis on the possible structure of the objective function. Also in this case, boundary conditions were first considered:

$$\begin{cases} x_1 = 1,\ x_2 = 0,\ x_3 = 0 & f_{obj} = EBMP_1 \\ x_1 = 0,\ x_2 = 1,\ x_3 = 0 & f_{obj} = EBMP_2 \\ x_1 = 0,\ x_2 = 0,\ x_3 = 1 & f_{obj} = EBMP_3 \end{cases} \tag{5.10}$$

After some trials, it was decided that the function that better represents the co-digestion of three substrates is the one reported in Equation 5.11.

$$f_{obj,NC=3} = BMP_{AcoD} = x_1 \cdot EBMP_1 + x_2 \cdot EBMP_2 + x_3 \cdot EBMP_3 + (x_1 \cdot x_2 + x_1 \cdot x_3 + x_2 \cdot x_3 + x_1 \cdot x_2 \cdot x_3) \cdot BMP_{mix} \tag{5.11}$$

Here, three binary interaction terms and one ternary interaction term are present, representing the synergy between the different substrates two by two and between the three of them. BMP_{mix} can be still calculated with the two expressions shown in Sections 5.2.2 and 5.2.3.

Several trials about this function were done to demonstrate its validity – with both the definitions of BMP_{mix}.

	f_{obj}	BMP_{mix}
Two Substrates	$f_{obj} = x_1 \cdot EBMP_1 + x_2 \cdot EBMP_2 + x_1 \cdot x_2 \cdot BMP_{mix}$	$BMP_{mix}\left(\frac{C}{N}, BD\right)$ $BMP_{mix}\left(\frac{C}{N}, Lignin, Lipids\right)$
Three Substrates	$f_{obj} = x_1 \cdot EBMP_1 + x_2 \cdot EBMP_2 + x_3 \cdot EBMP_3 + (x_1 \cdot x_2 + x_1 \cdot x_3 + x_2 \cdot x_3 + x_1 \cdot x_2 \cdot x_3) \cdot BMP_{mix}$	$BMP_{mix}\left(\frac{C}{N}, BD\right)$ $BMP_{mix}\left(\frac{C}{N}, Lignin, Lipids\right)$

Table 5.1: Summary table of the four versions of the objective function

5.4 Maximization Constraint

In Table 5.1 all the possible versions of the objective function are reported. When maximizing the objective function, whatever the number of substrates or the BMP_{mix} definition, proper constraints must be applied to obtain reasonable results.

In particular, the fundamental constraint that must always be imposed during this optimization is that the sum of the mass fractions composing the blend must be equal to one (Equation 5.12).

$$\sum_{i=1}^{NC} x_i = 1 \tag{5.12}$$

Maximizing the function by varying the mass fractions x_i, it is possible to calculate the compositions ${x_i}^{opt}$ that maximize the co-digestion BMP.

5.5 AcoD of Non-Synergistic Substrates

Sometimes it may happen that two or more substrates, due to the lack of complementarity, do not show synergy during co-digestion; therefore, another model was developed for this eventuality. In this case no interaction terms are present, and the BMP_{AcoD} is calculated as the weighted average of the EBMPs of the single substrates (Equation 5.13). This holds for any number NC of substrates.

$$BMP_{AcoD} = \sum_{i=1}^{NC} x_i \cdot EBMP_i \tag{5.13}$$

By calculating the BMP_{AcoD} with this formula, the resulting value will be always intermediate between the EBMPs of the involved substrates, thus no synergy is observed. Therefore, in this case the optimization cannot be performed since no maximum exists. Additional tests were done to validate this model.

6. Tests on Literature Data

This chapter aims at presenting the findings of the tests carried out to validate the objective functions described in Chapter 5, during which the model results have been compared to experimental data available in scientific journals. In particular, eight experimental studies performing BMP tests on mixtures of two or three substrates at varying blending ratios were selected in literature and analysed.

6.1 AcoD of Synergistic Substrates

In case of synergistic substrates, to compare the model results to the experimental results some operations were done for each trial:

1) The objective function (i.e., BMP_{AcoD}) was first maximized to obtain the optimized composition and the corresponding BMP.
2) The BMP_{AcoD} was also calculated at varying compositions.
3) The calculated and experimental BMPs were compared in plots.
4) Root Mean Square Error between the experimental and the corresponding calculated values was calculated according to Equation 6.1.

$$RMSE = \sqrt{\frac{\sum_i^N \left(BMP_{exp,i} - BMP_{calc,i}\right)^2}{N}} \tag{6.1}$$

N is the number of experimental blending ratios i at which BMP tests are performed, $BMP_{exp,i}$ is the experimental Biomethane Potential obtained at a certain blending ratio i, and $BMP_{calc,i}$ is the corresponding Biomethane Potential calculated with the objective function.

The tests were performed with both the definitions of BMP_{mix} shown in Sections 5.2.2 and 5.2.3, however in this chapter only the results obtained with the best version are shown (i.e., the one that shows on average lower RMSEs).

6.1.1 Choice of BMP_{mix} Definition

The eight tests were carried out with both the two definitions of BMP_{mix} reported in the previous chapter, however the one that depends on the $\left(\frac{C}{N}\right)_{mix}$ and BD_{mix} demonstrated to lead to lower RMSEs most of the times. In Table 6.1 the RMSEs obtained with the two definitions are shown.

		RMSE [mL/g_{VS}]	
		$BMP_{mix,1}$	$BMP_{mix,2}$
1°	[94]	15.60	18.36
2°	[95]	15.36	18.19
3°	[96]	19.88	29.06
4°	[97]	31.26	55.33
5°	[20]	15.69	30.14
6°	[98]	26.01	19.53
7°	[98]	20.11	26.77
8°	[98]	42.85	35.20

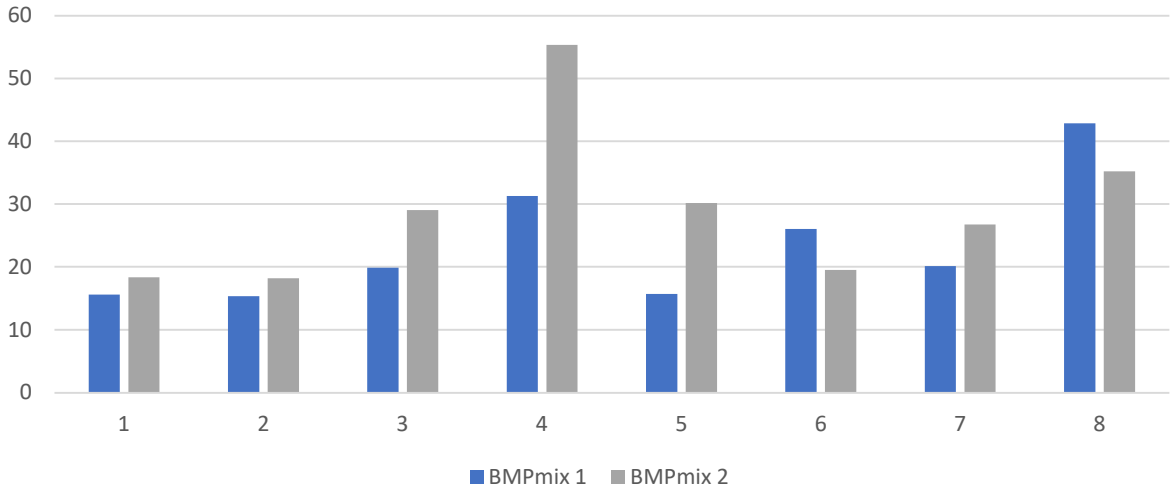

Figure 6.1: RMSEs associated with each trial with both the definitions of BMP_{mix}: $BMP_{mix}\left(\frac{C}{N}, BD\right)$ – indicated as $BMP_{mix,1}$ – and $BMP_{mix}\left(\frac{C}{N}, Lignin, Lipids\right)$ – indicated as $BMP_{mix,2}$

As observed in Figure 6.1, the RMSE obtained calculating f_{obj} with $BMP_{mix}\left(\frac{C}{N}, BD\right)$ is most of the times (six out of eight cases) lower than the other case, therefore it has been concluded that the first definition is more reliable. In addition, parameters such as the

$\frac{C}{N}$ ratio and the BD are more often available than others like lignin and lipids content, which are extremely variable and difficult to determine through analytical techniques.

6.1.2 Optimization Procedure

The tests were performed in Excel environment, defining the objective function as in Equations 6.2 and 6.3 for two and three substrates, respectively. Information about the EBMPs of the single substrates were usually given by the article.

$$f_{obj} = BMP_{AcoD} = x_1 \cdot EBMP_1 + x_2 \cdot EBMP_2 + x_1 \cdot x_2 \cdot BMP_{mix} \tag{6.2}$$

$$f_{obj} = BMP_{AcoD} = x_1 \cdot EBMP_1 + x_2 \cdot EBMP_2 + x_3 \cdot EBMP_3 + (x_1 \cdot x_2 + x_1 \cdot x_3 + x_2 \cdot x_3 + x_1 \cdot x_2 \cdot x_3) \cdot BMP_{mix} \tag{6.3}$$

BMP_{mix} is calculated as defined in Equation 6.4. Parameters such as the C/N ratios and the TBMPs of the substrates were taken from the paper if available, otherwise data from the Primary Averaged Database were used.

$$BMP_{mix}\left(\frac{C}{N}, BD\right) = \beta_0 + \beta_1 \cdot \left(\frac{C}{N}\right)_{mix} + \beta_2 \cdot BD_{mix} + \beta_3 \cdot \left(\frac{C}{N}\right)^2_{mix} + \beta_4 \cdot BD^2_{mix} \tag{6.4}$$

$$\begin{cases} \beta_0 = 21.6613 \\ \beta_1 = 1.2558 \\ \beta_2 = 445.7076 \\ \beta_3 = -0.0223 \\ \beta_4 = -7.8201 \end{cases}$$

$$\left(\frac{C}{N}\right)_{mix} = \sum_{i=1}^{NC} x_i * \left(\frac{C}{N}\right)_i \tag{6.5}$$

$$BD_{mix} = \sum_{i=1}^{NC} x_i * BD_i \tag{6.6}$$

Once defined f_{obj}, it was firstly maximized with the Excel Solver (using the GRG Nonlinear Solving Method), then its trend as function of the composition of the blend was calculated, comparing it with the experimental points. Finally, the RMSE between the experimental and the corresponding calculated points was evaluated.

The maximization was performed by imposing the constraint in Equation 6.7.

$$\sum_{i=1}^{NC} x_i = 1 \tag{6.7}$$

6.1.3 AcoD of Two Substrates

6.1.3.1 Food Waste (FW) and Pig Manure (PM) - 1

In the work of [94], BMP tests were performed at six different mixing ratios of FW and PM, obtaining the methane yields shown in Table 6.1.

x_{FW} [-]	x_{PM} [-]	BMP [mL/gVS]
0	1	260
0.2	0.7	320
0.4	0.6	443
0.6	0.4	489
0.8	0.2	521
1	0	516

Table 6.1: Experimental co-digestion BMPs obtained at varying compositions

To calculate the objective function, the EBMPs of the two substrates have been considered equal to 260 mL/g_{VS} for PM and 516 mL/g_{VS} for FW. Other data about the two substrates weren't available in the article, therefore the average values of the C/N ratio and the TBMP of the substrates – that are needed to calculate the BMP_{mix} – were taken from the Primary Averaged Database and are reported in Table 6.2. The BD of substrates was calculated by dividing the EBMP reported in the article by the TBMP from the database.

	C/N [-]	TBMP [mL/gVS]	EBMP [mL/gVS]	BD [-]
PM	11.62	573.50	260	0.45
FW	18.70	548.59	516	0.94

Table 6.2: Main substrates data used for the optimization

Maximizing the objective function, the model prediction about the optimal co-digestion conditions is shown Figure 6.2; there, the plot representing the comparison between the objective function – calculated as function of the mass fraction of FW – and the experimental points is reported too.

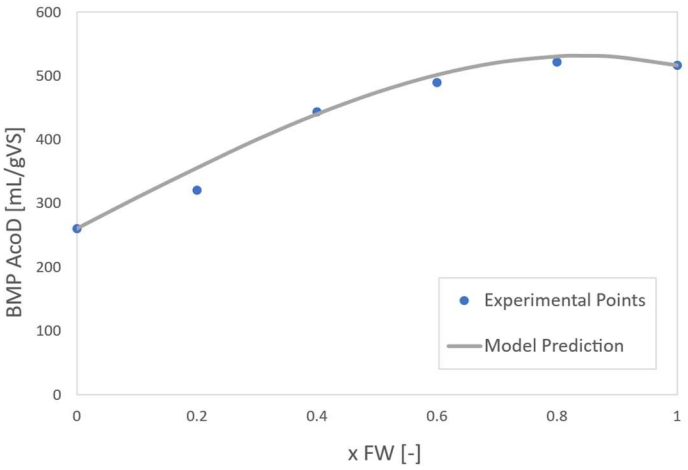

Model Optimal Conditions	
$x_{FW,opt}$ [-]	0.842
$x_{PM,opt} = 1 - x_{FW,opt}$ [-]	0.158
$\left(\frac{C}{N}\right)_{mix,opt}$ [-]	17.80
$BMP_{AcoD,opt}$ [mL/gVS]	530.89

Figure 6.2: Comparison between experimental points (blue points) and model prediction (grey line); the optimization results are reported in the table

As shown in Figure 6.2, the correspondence between experimental data and the model is very good, with a RMSE between experimental points and the corresponding predictions of 15.60 mL/g_{VS}. Therefore, in this case the model can accurately predict the BMP at every blending condition, allowing to calculate which blend is the best in terms of methane yield.

According to the model, the optimal mixture is composed of 84.2% of FW and 15.8% of PM: FW has a higher EBMP and BD than PM, moreover it is characterized by a higher C/N ratio, therefore it is the most abundant substrate in optimal conditions. For what concerns the C/N ratio, the optimal range should be in between 20 and 40, but in this case this range cannot be reached since both the substrates fall below it. The fact that the mixture shows a higher BMP than both the single substrates is due to the synergy that is often observed between two or more substrates.

6.1.3.2 Food Waste (FW) and Pig Manure (PM) - 2

Another test about the co-digestion of FW and PM was performed by [95]. The paper reported experimental data about BMP tests at different ratios of FW and PM, obtaining the results reported in Table 6.3.

x_{FW} [-]	x_{PM} [-]	BMP [mL/gVS]
0	1	248.14
0.167	0.833	314.38
0.250	0.750	641.64
0.500	0.500	398.95
0.750	0.250	415.49
0.833	0.167	411.19
1	0	386.80

Table 6.3: Experimental co-digestion BMPs obtained at varying compositions

According to these data, in this case the EBMPs of FW and PM are equal to 386.80 and 248.14 mL/g_{VS}, respectively. The paper also gives in this case information about the C/N ratios and the TBMPs of the two substrates, therefore there was no need to get those data from the database.

	C/N [-]	TBMP [mL/gVS]	EBMP [mL/gVS]	BD [-]
PM	10.63	406.82	248.14	0.61
FW	18.88	545.33	386.80	0.71

Table 6.4: Main substrates data used for the optimization

The maximization results and the objective function calculated as function of the mass fraction of FW are reported in Figure 6.3.

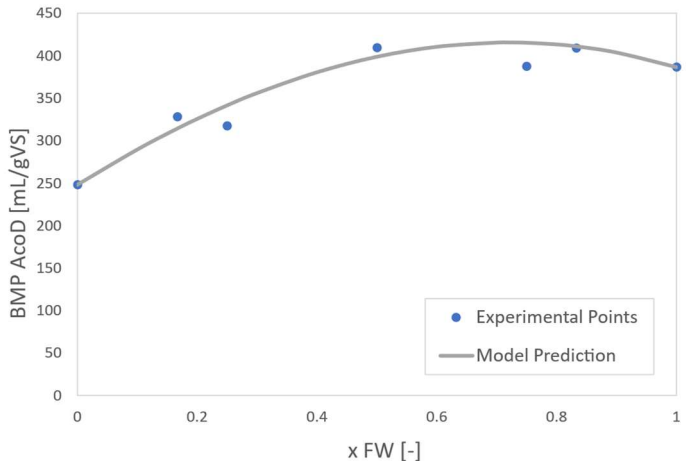

Model Optimal Conditions	
$x_{FW,opt}$ [-]	0.720
$x_{PM,opt} = 1 - x_{FW,opt}$ [-]	0.280
$\left(\frac{C}{N}\right)_{mix,opt}$ [-]	16.57
$BMP_{AcoD,opt}$ [mL/gVS]	415.81

Figure 6.3: Comparison between experimental points (blue points) and model prediction (grey line); the optimization results are reported in the table

Also in this case, it can be concluded that the objective function is able to estimate the BMP of the mixtures in a quite precise way, with a RMSE of 15.36 mL/g_{VS}. The optimal composition calculated by the model is similar to the one obtained in the previous test, indeed the mixed substrates are the same, while the optimal BMP is lower because the EBMPs used in this case – given by the article – are lower too.

6.1.3.3 Dairy Manure (DM) and Straw (ST)

In the work of [96] the co-digestion of dairy manure and straw was analysed, performing BMP tests on different blends of these two substrates with the results shown in Table 6.5.

x_{DM} [-]	x_{ST} [-]	BMP [mL/gVS]
0	1	151.80
0.167	0.833	189.44
0.250	0.750	205.26
0.500	0.500	237.60
0.750	0.250	242.31
0.833	0.167	237.09
1	0	216.00

Table 6.5: Experimental co-digestion BMPs obtained at varying composition

The EBMPs of DM and ST are equal to 216.0 and 151.8 mL/g_{VS}, respectively. The values of the C/N ratios of DM and ST are available in the paper, while the TBMPs are taken from the Primary Averaged Database.

	C/N [-]	TBMP [mL/gVS]	EBMP [mL/gVS]	BD [-]
PM	16.70	483.33	216.00	0.44
ST	55.40	427.75	151.80	0.35

Table 6.6: Main substrates data used for the optimization

Calculating the objective function by varying the mass fraction of DM and maximizing it, the obtained results are shown in Figure 6.4.

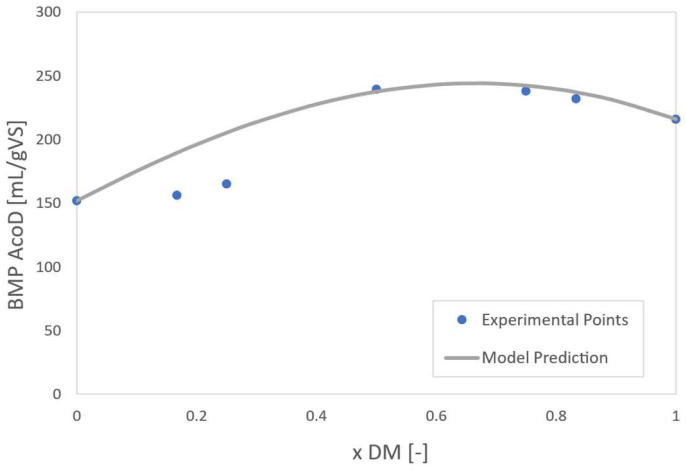

Model Optimal Conditions	
$x_{DM,opt}$ [-]	0.665
$x_{ST,opt} = 1 - x_{DM,opt}$ [-]	0.335
$\left(\frac{C}{N}\right)_{mix,opt}$ [-]	29.66
$BMP_{AcoD,opt}$ [mL/gVS]	244.08

Figure 6.4: Comparison between experimental points (blue points) and model prediction (grey line); the optimization results are reported in the table

Also in this case, the objective function is effectively able to predict the mixing ratio that produces the highest methane yield, in accordance with the experimental data, with a RMSE equal to 19.88 mL/g_{VS}. According to the model, the optimal composition is 33.5% ST and 66.5% DM: this can be explained by the fact that straw contributes to increasing the C/N ratio to make it fall inside the optimal range, but at the same time it is characterized by a lower biodegradability due to the high lignocellulosic content, therefore the main substrate of the optimal blend should be DM to have a good overall degradability.

6.1.3.4 Fruit and Vegetable Food Waste (FVFW) and Sewage Sludge (SS)

The anaerobic co-digestion of FVFW and SS is studied by [97] at different mixing ratios, obtaining the results in Table 6.7.

x_{FVFW} [-]	x_{SS} [-]	BMP [mL/gVS]
0	1	119
0.3	0.7	135
0.5	0.5	141
0.7	0.3	119
0.8	0.2	107
1	0	134

Table 6.7: Experimental co-digestion BMPs obtained at varying composition

The paper doesn't give information about the C/N ratios and TBMPs of the two substrates, therefore these parameters were taken from the Primary Averaged Database and used for the numerical tests.

	C/N [-]	TBMP [mL/gVS]	EBMP [mL/gVS]	BD [-]
FVFW	15.22	436.57	134.00	0.31
SS	8.57	424.10	119.00	0.28

Table 6.8: Main substrates data used for the optimization

These data were used to maximize the objective function and to represent it in a plot as function of the mass fraction of FVFW, as shown in Figure 6.5.

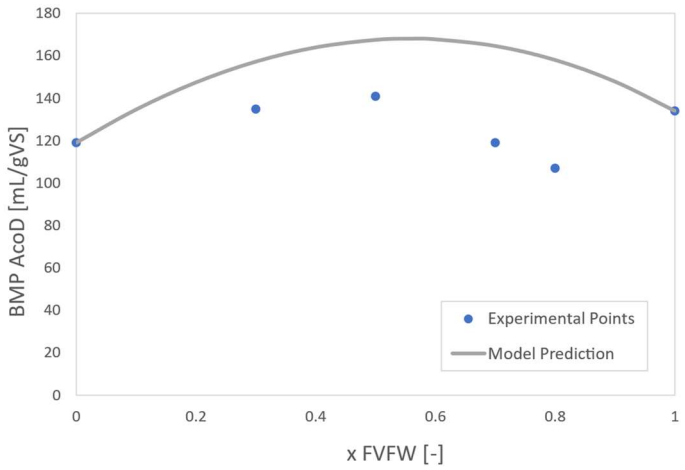

Model Optimal Conditions	
$x_{FVFW,opt}$ [-]	0.558
$x_{SS,opt} = 1 - x_{FVFW,opt}$ [-]	0.442
$\left(\frac{C}{N}\right)_{mix,opt}$ [-]	12.28
$BMP_{AcoD,opt}$ [mL/gVS]	167.98

Figure 6.5: Comparison between experimental points (blue points) and model prediction (grey line); the optimization results are reported in the table

The correspondence between experimental data and the objective function prediction is worse than in the previous cases, with a RMSE equal to 31.36 mL/g_{VS}. Indeed, an overestimation of the real BMP is observed: this could be due to the overestimation of the synergistic effect that the two substrates have together. On the other hand, the prediction of the optimal composition, that is 55.8% FVW and 44.2% SS, is in accordance with experimental data, therefore the model is able to successfully predict the best mixing ratio – which is the main goal of the project.

6.1.3.5 Organic Fraction of Municipal Solid Waste (OFMSW) and Sewage Sludge (SS)

In the work of [20], the co-digestion of the OFMSW and SS is analysed at various mixing ratios, obtaining the results in Table 6.9.

x_{OFMSW} [-]	x_{SS} [-]	BMP [mL/gVS]
0	1	164.50
0.2	0.8	200.20
0.4	0.6	212.30
0.6	0.4	217.50
0.8	0.2	220.60
1	0	201.50

Table 6.9: Experimental co-digestion BMPs obtained at varying composition

The article gives information about all the needed parameters for the optimization, therefore no data were taken from the database.

	C/N [-]	TBMP [mL/gVS]	EBMP [mL/gVS]	BD [-]
OFMSW	51.8	494.3	201.5	0.41
SS	8.9	333.9	164.5	0.49

Table 6.10: Main substrates data used for the optimization

The optimization results and the comparison between the model and the experimental points are reported in Figure 6.6.

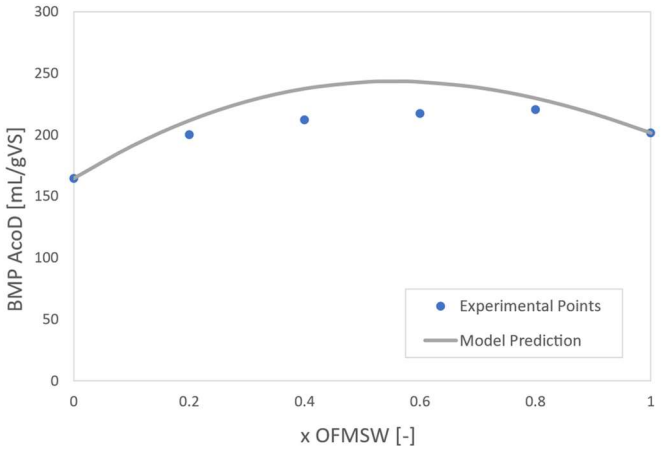

Model Optimal Conditions

$x_{OFMSW,opt}$ [-]	0.554
$x_{SS,opt} = 1 - x_{OFMSW,opt}$ [-]	0.446
$\left(\frac{C}{N}\right)_{mix,opt}$ [-]	32.68
$BMP_{AcoD,opt}$ [mL/gVS]	243.30

Figure 6.6: Comparison between experimental points (blue points) and model prediction (grey line); the optimization results are reported in the table

In this case it can be noted that the difference between predicted and experimental values is quite low, indeed the RMSE is equal to 15.69 mL/g_{VS}, however the model optimal composition predicted by the model is different from the experimental one: experimentally, the highest methane yield is obtained at a concentration of OFMSW of 80%, while the model predicts an optimal composition of 55.4% OFMSW. Moreover, a general overestimation of the BMP is observed. These problems could be caused by some possible reasons:

- The overestimation of the BMP by the model could be due to a wrong estimation of the synergy between the two substrates, which may also lead to a wrong prediction of the optimal mixture composition.
- The experimental BMP obtained at $x_{OFMSW} = 0.8$ could be wrong due to failure of analytical techniques or altered experimental conditions.

6.1.4 AcoD of Three Substrates

6.1.4.1 Dairy Manure (DM), Chicken Manure (CM) and Straw (ST)

The co-digestion of DM, CM and ST was tested in the work of [98] by varying the composition of the blend and measuring the BMP for each case. In particular, the results in Table 6.11 were obtained.

x_{DM} [-]	x_{CM} [-]	x_{ST} [-]	BMP [mL/gVS]
1	0	0	261
0	1	0	176
0	0	1	123
0.5	0.5	0	252
0.5	0	0.5	247
0	0.5	0.5	222
0.667	0.167	0.167	310
0.167	0.667	0.167	244
0.167	0.167	0.667	239
0.333	0.333	0.333	302

Table 6.11: Experimental co-digestion BMPs obtained at varying composition

The article gives information about the C/N ratios and the EBMPs of the substrates – 261, 176 and 123 mL/g_{VS} for DM, CM and ST, respectively – while the TBMPs were extrapolated from the Primary Averaged Database.

	C/N [-]	TBMP [mL/gVS]	EBMP [mL/gVS]	BD [-]
DM	23.50	486.33	261.00	0.54
CM	9.02	485.96	176.00	0.36
RS	51.70	427.75	123.00	0.29

Table 6.12: Main substrates data used for the optimization

In this case, the objective function was calculated with Equation 6.3 and its representation as function of the mass fractions of DM and CM is plotted together with the experimental points in Figure 6.7. The optimization results are also reported in the dedicated table in Figure 6.7.

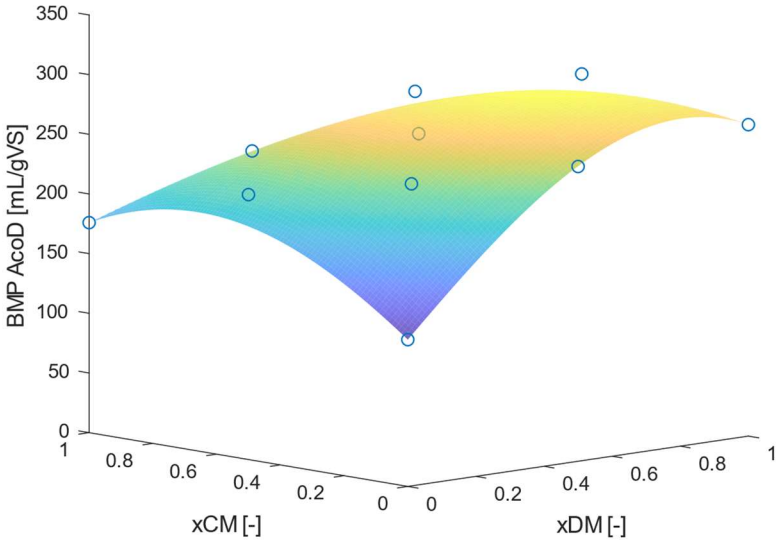

Model Optimal Conditions	
$x_{DM,opt}$ [-]	0.645
$x_{CM,opt}$ [-]	0.251
$x_{ST,opt} = 1 - x_{DM,opt} - x_{CM,opt}$ [-]	0.104
$\left(\frac{C}{N}\right)_{mix,opt}$ [-]	22.81
$BMP_{AcoD,opt}$ [mL/gVS]	291.97

Figure 6.7: Comparison between experimental points (blue points) and model prediction (surface); the optimization results are reported in the table.

As shown in Figure 6.7, the model well approximates the experimental data, with a RMSE of 26.01 mL/g_{VS}. The objective function maximization indicates that the maximum possible BMP, equal to 291.97 mL/g_{VS}, is obtained with a mixture of 64.5% DM, 25.1% CM and 10.4% ST. This is in accordance with experimental data since the experimental maximum BMP is recorded at 66.7% DM, 16.7% CM and 16.7% RS.

6.1.4.2 Dairy Manure (DM), Pig Manure (PM) and Straw (ST)

In the work of [98], various mixtures of DM, PM and ST were tested, and results are shown in Table 6.13.

x_{DM} [-]	x_{PM} [-]	x_{ST} [-]	BMP [mL/gVS]
1	0	0	261
0	1	0	188
0	0	1	123
0.5	0.5	0	247
0.5	0	0.5	231
0	0.5	0.5	231
0.667	0.167	0.167	301
0.167	0.667	0.167	259
0.167	0.167	0.667	228
0.333	0.333	0.333	287

Table 6.13: Experimental co-digestion BMPs obtained at varying composition

As in the previous case, data about C/N ratios and EBMPs of the single substrates are present in the article, while data about TBMPs are taken from the database.

	C/N [-]	TBMP [mL/gVS]	EBMP [mL/gVS]	BD [-]
DM	23.50	486.33	261.00	0.54
PM	13.00	573.50	188.00	0.33
RS	51.70	427.75	123.00	0.29

Table 6.14: Main substrates data used for the optimization

The optimization results and the comparison between experimental points and objective function are reported in Figure 6.8.

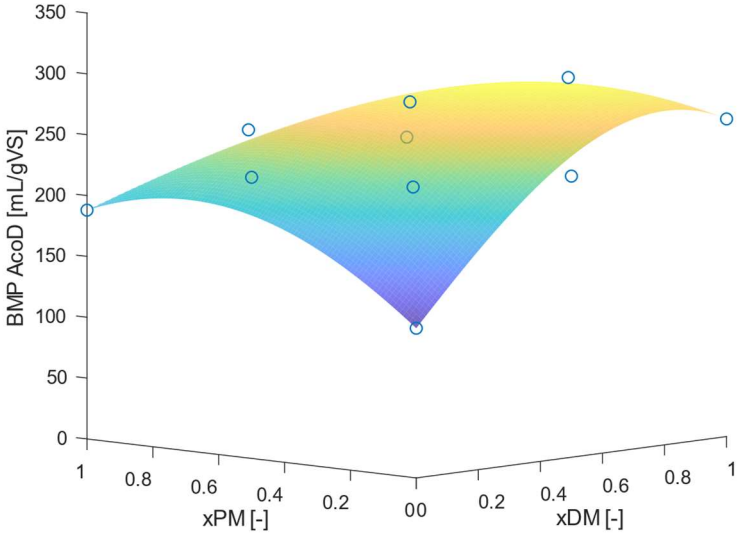

Model Optimal Conditions	
$x_{DM,opt}$ [-]	0.639
$x_{PM,opt}$ [-]	0.266
$x_{ST,opt} = 1 - x_{DM,opt} - - x_{PM,opt}$ [-]	0.095
$\left(\frac{C}{N}\right)_{mix,opt}$ [-]	23.39
$BMP_{AcoD,opt}$ [mL/gVS]	294.07

Figure 6.8: Comparison between experimental points (blue points) and model prediction (surface); the optimization results are reported in the table.

The RMSE between the model and the experimental data is 20.12 mL/g_{VS}, thus the approximation of experimental data is good. The optimization results are similar to the ones obtained experimentally: the highest experimental BMP was obtained with a mixture composed of 66.7%DM, 16.7% PM and 16.7% RS, while the optimization returns an optimal composition of 63.9% DM, 26.6% PM and 9.5% RS.

6.1.4.3 Chicken Manure (CM), Pig Manure (PM) and Straw (ST)

Mixtures of CM, PM and ST were also analysed by [98], obtaining the results in Table 6.15.

x_{CM} [-]	x_{PM} [-]	x_{ST} [-]	BMP [mL/gVS]
1	0	0	176
0	1	0	188
0	0	1	123
0.5	0.5	0	241
0.5	0	0.5	242
0	0.5	0.5	278
0.667	0.167	0.167	269
0.167	0.667	0.167	261
0.167	0.167	0.667	226
0.333	0.333	0.333	294

Table 6.15: Experimental co-digestion BMPs obtained at varying composition

The data used in the optimization process are shown in Table 6.16, where the C/N ratios and the EBMPs are furnished by the article while the TBMPs are taken from the database.

	C/N [-]	TBMP [mL/gVS]	EBMP [mL/gVS]	BD [-]
DM	23.50	486.33	261.00	0.54
PM	13.00	573.50	188.00	0.33
RS	51.70	427.75	123.00	0.29

Table 6.16: Main substrates data used during optimization

The optimization results and the comparison with experimental data are shown in Figure 6.9.

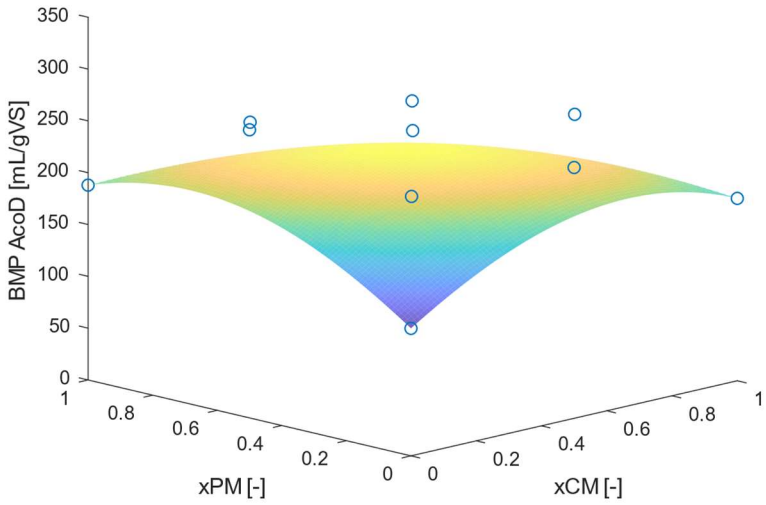

Model Optimal Conditions	
$x_{CM,opt}$ [-]	0.363
$x_{PM,opt}$ [-]	0.405
$x_{ST,opt} = 1 - x_{CM,opt} - x_{PM,opt}$ [-]	0.232
$\left(\frac{C}{N}\right)_{mix,opt}$ [-]	20.53
$BMP_{AcoD,opt}$ [mL/gVS]	235.30

Figure 6.9: Comparison between experimental points (blue points) and model prediction (surface); the optimization results are reported in the table

In this case the objective function underestimates the real biomethane potential, probably due to model issues concerning the synergy between substrates, showing a RMSE of 42.85 mL/g_{VS}. On the other hand, it succeeds in predicting the optimal composition – which is the main interest of this project – which is 36.3% CM, 40.5%

PM and 23.2% RS: this can be considered an acceptable result since the best experimental conditions are obtained with 33% CM, 33% PM and 33% RS.

6.2 AcoD of Non-Synergistic Substrates

In some cases, no synergy between substrates is observed during tests, and the BMP_{AcoD} is calculated as the weighted average of the EBMPs of the single substrates, as shown in Equation 6.8.

$$BMP_{AcoD} = \sum_{i=1}^{NC} x_i \cdot EBMP_i \tag{6.8}$$

When substrates don't show a synergistic effect, the optimization cannot be used to predict which blend maximizes the BMP, since the BMP_{AcoD} would always be comprised between the lowest and the highest EBMP of the involved substrates.

Therefore, in these cases, another type of test was done to validate the expression of BMP_{AcoD} shown in Equation 6.8:

1) BMP_{AcoD} was calculated as function of the composition of the blend.
2) If possible, the BMP_{AcoD} and the experimental points were represented in 2D or 3D plots.
3) The calculated BMP_{AcoD} were then compared with the experimental ones at each blending conditions and the RMSE between experimental and calculated values was found through Equation 6.1.

6.2.1 Tests on Non-Synergistic Mixtures

6.2.1.1 Food Waste (FW) and Dairy Manure (DM)

The co-digestion of DM and FW was analysed by [99], obtaining the results shown in Table 6.17.

x_{FW} [-]	x_{DM} [-]	BMP [mL/gVS]
0	1	144.3
0.50	0.50	297.0
0.67	0.33	310.3
0.75	0.25	318.7
1	0	362.2

Table 6.17: Experimental co-digestion BMPs obtained at varying composition

The EBMPs of FW and DM, in this case, are equal to 362.2 and 144.3 mL/g_{VS} respectively, and it can be noted that all the BMPs associated to their mixtures are intermediate between the EBMPs of the two single substrates, showing no synergy. In this situation the optimization tool cannot be used because the maximum BMP is achieved with food waste only. Therefore, the predicted BMP_{AcoD} was calculated with Equation 6.7. In Figure 6.10 the comparison between the prediction of Equation 6.7 and the experimental results is reported.

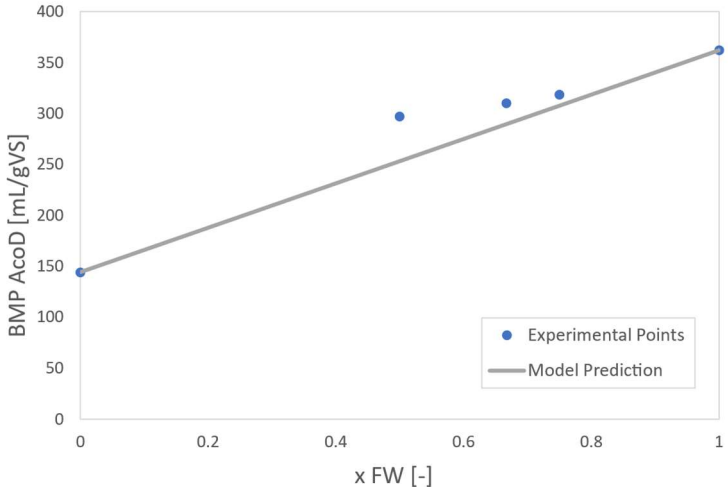

Figure 6.10: Comparison between experimental points (blue points) and model prediction (grey line)

In Figure 6.10 it is demonstrated that, since experimental values show no maximum, a linear model is suitable to represent the co-digestion BMP, with a RMSE between calculated and experimental values of 24.23 mL/g_{VS}.

In this case it cannot be decided which mixture is the best, however AcoD can successfully be used to improve the anaerobic digestion of dairy manure, whose EBMP is increased by adding food waste, and Equation 6.7 can be used to predict the co-digestion BMP.

6.2.1.2 Dairy Manure (DM), Pig Manure (PM) and Food Waste (FW)

In the case of [100], the co-digestion of three substrates was analysed, and the results are shown in Table 6.18.

x_{DM} [-]	x_{FW} [-]	x_{PM} [-]	BMP [mL/gVS]
1	0	0	176
0	1	0	188
0	0	1	123
0.5	0.5	0	241
0.5	0	0.5	242
0	0.5	0.5	278
0.667	0.167	0.167	269
0.167	0.667	0.167	261
0.167	0.167	0.667	226
0.333	0.333	0.333	294

Table 6.18: Experimental co-digestion BMPs obtained at varying composition

The EBMPs of DM, FW and PM in this case are equal to 176 mL/g_{VS}, 188 mL/g_{VS} and 123 mL/g_{VS}, respectively. In Figure 6.11 the comparison between the model's prediction and the experimental points is presented in a three-dimensional plot.

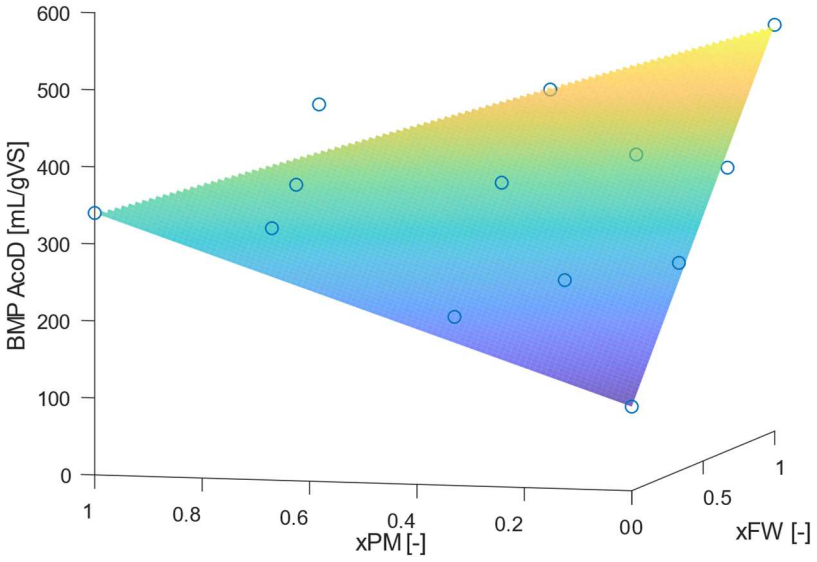

Figure 6.11: Comparison between experimental points (blue points) and model prediction (surface)

The model predicts the BMP of the mixture with good accuracy, with a RMSE of 35.82 mL/g_{VS}, and this confirms that it is suitable to describe substrates that undergo anaerobic digestion without synergy.

It is interesting to note that in this case the food waste doesn't show synergy with dairy manure, and neither with pig manure, contrarily to what shown in Sections 6.3.1 and 6.3.2. This could be caused by differences in the composition of these substrates from one test to another, showing a different synergy between each other. Therefore, a great improvement of the model could be given by the ability of predicting the *synergy level* of substrates depending on their composition and on their *complementarity*.

6.2.2 Future Development: Synergy Prediction

At this moment, it is not possible to predict when substrates do or do not show synergy, and therefore which of the two different BMP models apply. Furthermore, antagonistic effects are not considered at all by the objective function, and at times an over/underestimation of the real BMP is observed. The model should be improved to automatically predict these effects. This could be done, for example, by introducing *correction factors* inside the objective function able to modify its response according to the prediction of the synergy of substrates. This would require additional tests and model validation, and it represents one of the most important future developments of this project.

7. Tests on Industrial Data

The developed optimization tool was also applied to optimize industrial data provided by two companies.

7.1 Rota Guido s.r.l.

Rota Guido s.r.l. provided data about a 100 kW biogas plant, involving a CSTR anaerobic digester fed with 26.4 m^3/d of dairy manure (DM), 2.2 m^3/d of sorghum (SR) and 2.2 m^3/d of triticale (TR), with a total inlet volumetric flowrate of 30.8 m^3/d. Considering a density of 1000, 740 and 740 kg/m^3 for dairy manure, sorghum, and triticale respectively, it was also possible to calculate the mass fractions of the components of the inlet mixture.

	Volumetric Flow Rate $[m^3/d]$	Density $[kg/m^3]$	Mass Fraction [-]
DM	26.4	1000	0.890
SR	2.2	740	0.055
TR	2.2	740	0.055

Table 7.1: Inlet conditions at the anaerobic digester

Using the developed model, it was possible to calculate the optimal composition that would maximize the methane potential of the inlet mixture (i.e., the BMP), and thus would increase the methane production of the reactor.

In the documentation of Rota Guido s.r.l. it is indicated that dairy manure, sorghum and triticale are characterized by a mean EBMP of 260, 285 and 265 mL/g_{VS} respectively; no information about C/N ratios and TBMPs are available instead.

Therefore, missing data about DM were taken from the Primary Average Database, while for SR and TR mean values were obtained by gathering information from scientific papers (for sorghum [98–103] and for triticale [104–106]), and adopting the same averaging procedure used to obtain the Primary Averaged Database. The final data used for this optimization are shown in Table 7.2.

	C/N [-]	TBMP [mL/gVS]	EBMP [mL/gVS]	BD [-]
Dairy Manure	18.15	486.33	260.00	0.53
Sorghum	46.50	456.20	285.00	0.62
Triticale	38.45	415.79	265.00	0.64

Table 7.2: Dairy Manure, Sorghum and Triticale data used during optimization

These data can be used to calculate and maximize the objective function, obtaining the optimal inlet composition and the associated co-digestion BMP that are shown in Table 7.3.

Model Optimal Conditions	
$x_{DM,opt}$ [-]	0.289
$x_{SR,opt}$ [-]	0.377
$x_{TR,opt}$ [-]	0.334
$\left(\frac{C}{N}\right)_{mix,opt}$ [-]	35.63
$BMP_{AcoD,opt}$ [mL/gVS]	382.89

Table 7.3: Optimal inlet composition predicted by the objective function maximization

Table 7.3 shows that the optimal composition is very different from the actual inlet composition: the digester, indeed, is currently mainly fed with dairy manure, while the optimization tool suggests increasing the sorghum and triticale content at 37.7% and 33.4%, respectively. This increment should be coherent with the actual daily availability of these substrates, however data about the supply chain of the feedstocks were not available.

The $BMP_{AcoD,opt}$ represents the highest BMP associated with a mixture of CM, TR and ST, that is the cumulative methane production that would be obtained after a batch test. Actually, the methane is continuously withdrawn from the CSTR anaerobic digester, thus the BMP of the mixture cannot be considered as indicative of the actual methane production; however, since it represents the methane potential of the inlet mixture, even in a continuous reactor it can still be used to predict the best composition to be fed to the reactor.

Supposing a total inlet flowrate of 30.8 m^3/d, it is also possible to calculate the new, optimal inlet volumetric flowrates (shown in Table 7.4) by using the same densities of Table 7.1.

	Optimal Mass Fraction [-]	Density [kg/m3]	Optimal Volumetric Flow Rate [m^3/d]
Dairy Manure	0.289	1000	7.1
Sorghum	0.377	740	12.6
Triticale	0.334	740	11.1

Table 7.4: Optimized Inlet Conditions

7.2 Thöni s.r.l.

The data shared by Thöni s.r.l. record the inlet conditions of a CSTR anaerobic digester over the month of January 2022 and the related methane flux. Such biogas plant allows the generation of 1000 kW of electricity.

The substrates that enter the reactor can be included into the three categories of chicken manure (CM), fruit and vegetable food waste (FVFW) and straw (ST), and their daily massive flows are shown in Figure 7.1. In addition, in Figure 7.1 the total inlet mass flow rate and the outlet methane flow are reported.

In Figure 7.1 it can be observed that the CM supply is maintained constant at 5 ton/d during the whole month, and that the ST supply as well is almost constant except at the end when it decreases from an initial value of 13 ton/d to a final value of 11 ton/d. The most variable flow is the FVFW, which initially decreases from 12 ton/d to 7.5 ton/d, and then increases again to a final value of 15.50 ton/d. Summing up all the substrates, the total daily massive load varies between a minimum of 25 ton/d and a maximum of 33.5 ton/d. The total daily load, indeed, is chosen according both to the capacity of the reactor and to the amount of currently produced methane: indeed, since

the produced power must be maintained at 1000 kW, if a methane surplus is observed less load is added and vice versa. This is evident in Figure 7.1: when the methane flux starts to drop, the total daily load is slowly increased to increase methane production. Obviously, due to the high reaction times, some time is needed to observe a new increase of the methane production. Similarly, the effects of the inlet composition on the outlet gas production are observed with a certain lag time. Therefore, a certain delay between inlet and outlet conditions should be considered when analysing these industrial data.

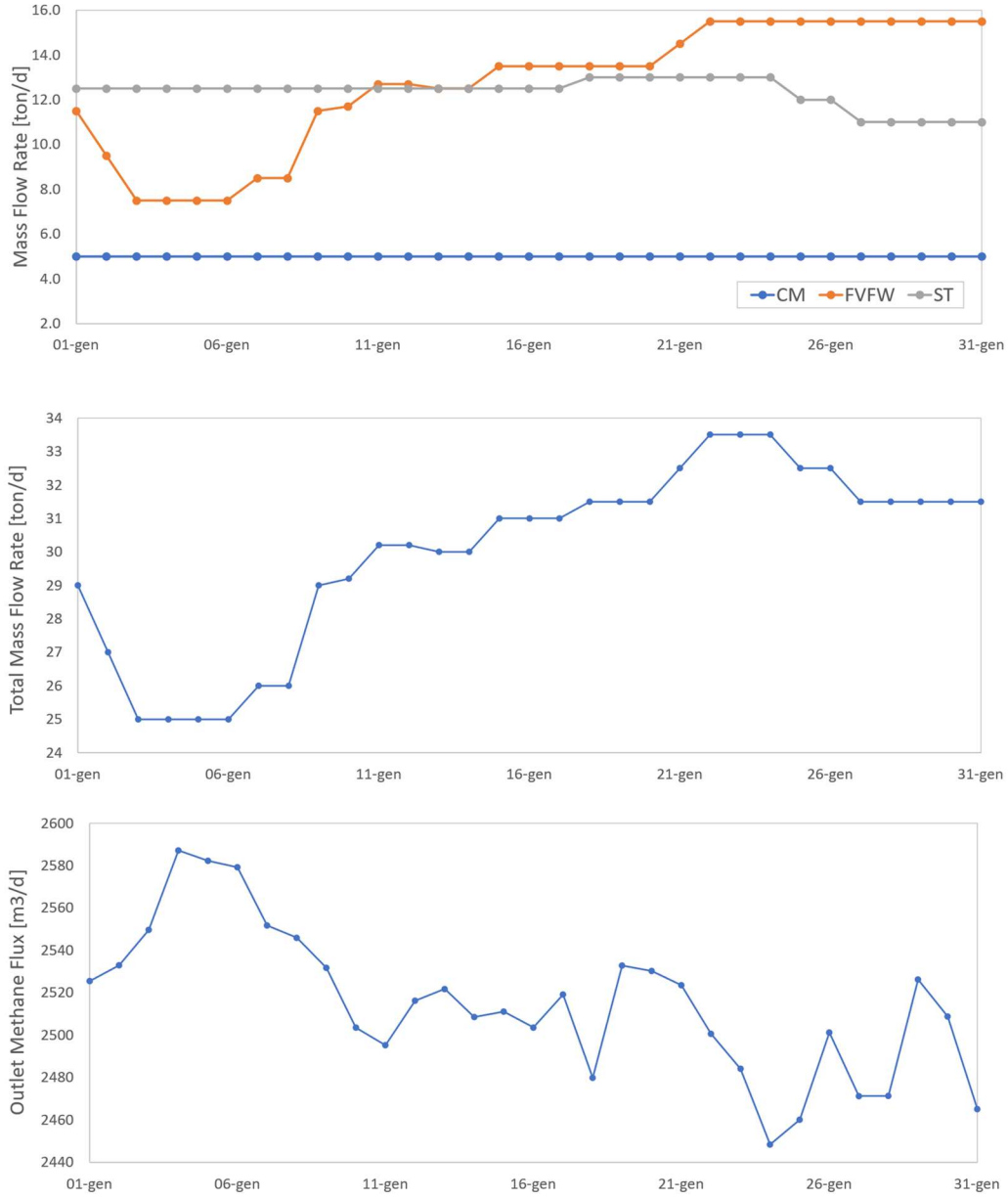

Figure 7.1: Industrial data about the inlet mixture and the methane production over the month of January 2022

To maximize the methane yield of the supplied load, the BMP of the inlet mixture should be maximized: knowing the categories of the substrates that are fed to the reactor, it is possible to use the optimization tool to calculate the composition that maximizes the BMP of the inlet blend.

To calculate the optimal inlet composition, data about CM, FVFW and ST were taken from the Primary Average Database, which are reported in Table 7.5.

	C/N [-]	TBMP [mL/gVS]	EBMP [mL/gVS]	BD [-]
CM	8.93	485.96	289.71	0.60
FVFW	15.22	436.57	347.79	0.80
ST	70.54	427.75	176.12	0.41

Table 7.5: CM, FVFW and ST data used for the optimization

These data can be used to maximize the objective function and calculate the optimal blending conditions (Table 7.6).

Model Optimal Conditions	
$x_{CM,opt}$ [-]	0.312
$x_{FVFW,opt}$ [-]	0.557
$x_{ST,opt}$ [-]	0.131
$\left(\frac{C}{N}\right)_{mix,opt}$ [-]	20.50
$BMP_{AcoD,opt}$ [mL/gVS]	420.80

Table 7.6: Optimal conditions for a mixture of CM, FVFW and ST calculated with the optimization tool.

In Table 7.6, the optimal conditions for the inlet mixture have been reported: the mixture of chicken manure, fruit and vegetable food waste and straw with the highest co-digestion BMP is a mixture of 31.2% CM, 55.7% FVFW and 13.1% ST.

Since the total mass flow that is fed to the reactor can vary between 25 and 33.5 ton/d (Figure 7.1), the associated mass flows of CM, FVFW and ST in optimal conditions can be calculated and represented as function of the total daily load (Figure 7.2).

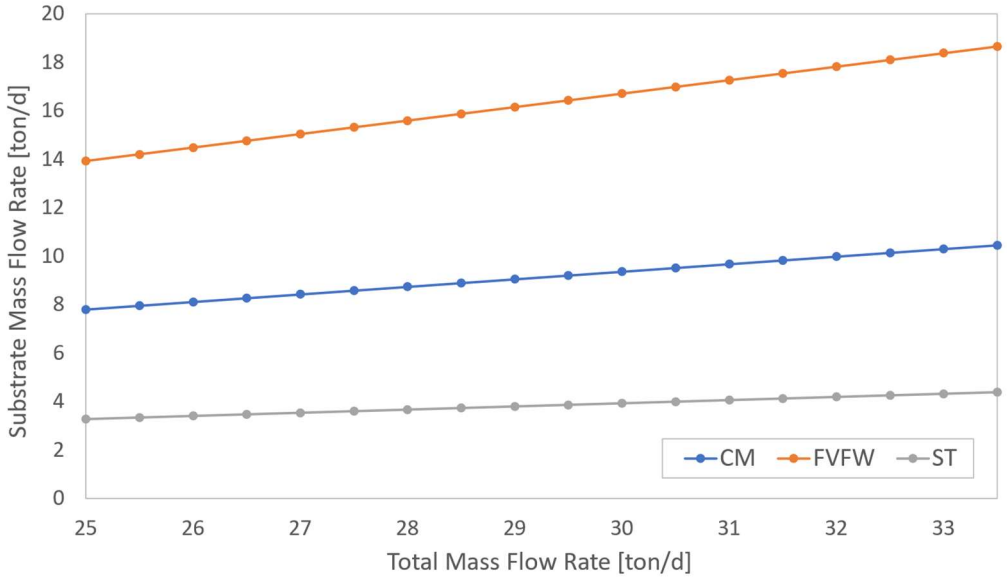

Figure 7.2: Optimal mass flow rates of CM, FVFW and ST depending on the value of the total mass flow rate.

Since the total mass flow rate is changed every day according to the current methane production, supposing to fix the daily total mass flow rates at the same values used by Thöni s.r.l. during the month, it is possible to plot the corresponding optimal substrates mass flow rates as function of time to make a comparison with the actual ones: the trend of the optimal massive loads as function of time is reported in Figure 7.3, where also a comparison between the BMPs of the optimal blends and the ones associated to the actual mixtures that are fed to the digester – that can be calculated by using the objective function – is reported. There, it can be observed that maintaining the optimal composition the BMP is maintained at its maximum value, therefore the methane production should increase with respect to the real case. On the downside, the optimized mass flow rates are significantly different from the actual ones, and do not take into account the real availabilities of the substrates and the storage capabilities of the plant: this will be the topic of the following chapter, in which the optimization tool will be modified to make it return feasible results taking into account supply chain factors.

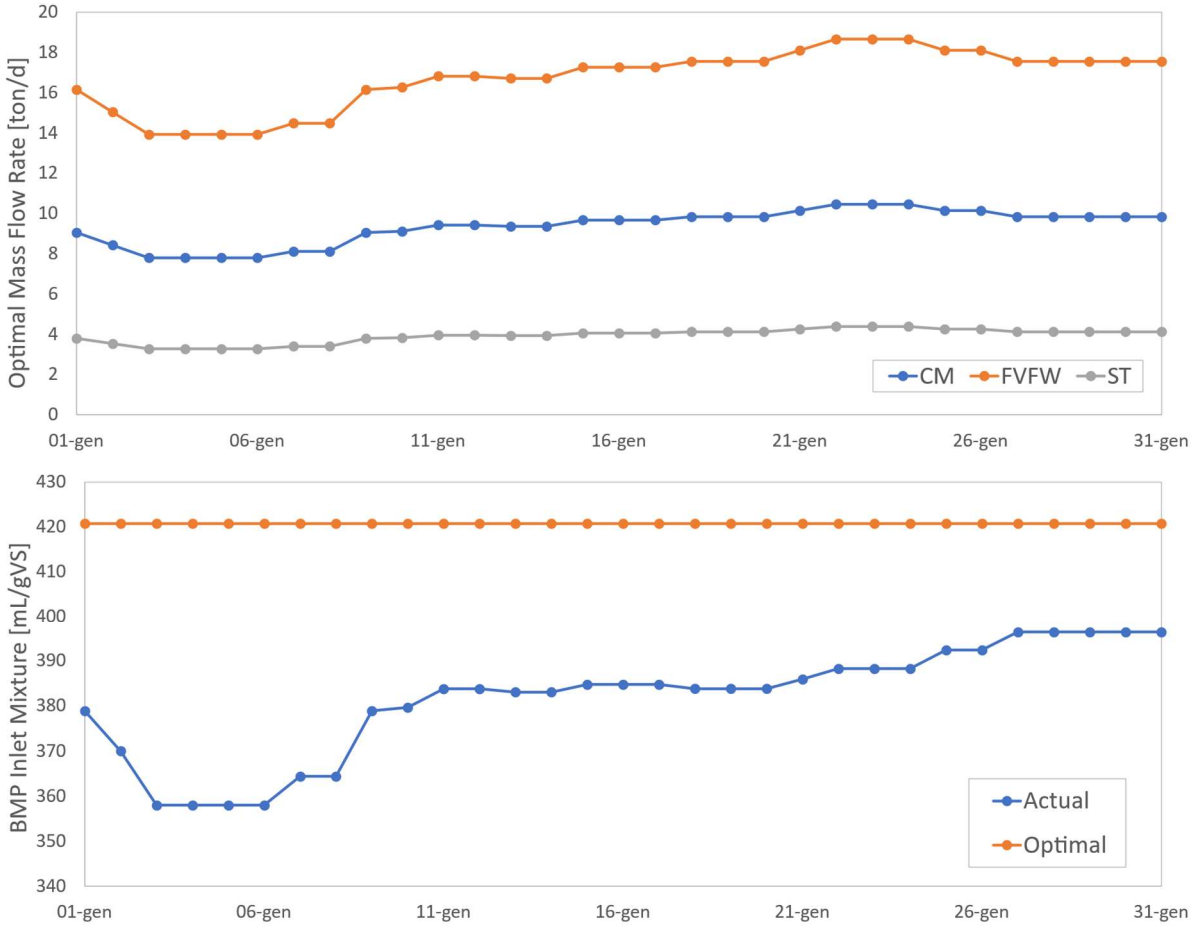

Figure 7.3: Mass flow rates associated to the optimal composition and comparison between optimal and actual feedstock BMP

8. Model Improvements for Industrial Applications

As anticipated in the previous chapter, when dealing with industrial scenarios, new factors must be considered with respect to lab-scale batch tests. In this chapter an improved version of the optimization model is proposed, and an industrial case study is also presented.

8.1 Model Improvements

In case of industrial realities, besides the composition of the optimal mixture in terms of highest methane potential, other issues must be faced, like the real availability of the substrates and the storage capability of the plant. Therefore, to consider these additional factors, the model presented in the previous chapters has been improved with new constraints both in case of batch and CSTR-based anaerobic digesters.

8.1.1 Batch Industrial Anaerobic Digester

In case of a batch anaerobic digester, besides the optimal composition of the mixture, other factors must be taken into account:

- The tons of available substrates for a certain batch cycle.
- The storage capability of the plant for those substrates, that determines the minimum quantity (in tons) of each substrate that must be necessarily disposed in the digester not to have excessive waste accumulation.
- The total capacity of the reactor.

The model that was previously developed is able to return the optimal composition of the mixture, but the corresponding massive loads might be incoherent with the aforementioned factors. To avoid that, the model has been modified adding new constraints in order to obtain feasible results.

Supposing to fix the total mixture quantity – measured in tons and named m_{TOT} – that can be loaded into the reactor (to which eventual water could be added to reach the desired solids concentration and volume), it is possible to calculate the optimal loads of the single substrates by performing an improved optimization. This can be done by imposing a lower and an upper threshold for each substrate load and imposing that their sum must be equal to the fixed total load. Such constraints can be written as:

$$m_{i,min} \leq m_i \leq m_{i,max} \tag{8.1}$$

$$m_{TOT} = \sum_{i=1}^{NC} m_i \tag{8.2}$$

Where i stands for the substrates i = 1…NC, $m_{i,min}$ represents the minimum quantity of substrate i that must be disposed in the digester and $m_{i,max}$ represents the maximum availability of substrate i.

The mass fraction of each substrate i can be then calculated by dividing the substrate load m_i for the total massive load m_{TOT}, as shown in Equation 8.3.

$$x_i = \frac{m_i}{m_{TOT}} \tag{8.3}$$

After having defined the new constraints and having calculated the mass fractions, it is possible to calculate f_{obj} and perform the optimization by varying the massive loads m_i of each substrate – instead of the mass fractions, as it was previously done – to maximize the BMP of the feedstock. This way the feedstock optimization is performed considering supply chain requirements and optimal values of m_i are obtained.

8.1.2 CSTR Industrial Anaerobic Digester

In case of an industrial CSTR digester, the reactor is fed with a continuous flowrate and a methane flux is continuously withdrawn. Therefore, in this case, the variables that have to be optimized are the substrates mass flow rates, generally measured in ton/d.

The continuous case is analogous to the batch one, however in this case different constraints have to be considered:

- The daily availability (in ton/d) of each substrate.
- The minimum daily quantity (in ton/d) of a certain substrate that must be necessarily disposed in the digester not to have excessive waste accumulation.
- The total mass flow rate of the mixture that is fed to the reactor, which is usually fixed depending on the reactor capacity or, as in the Thöni s.r.l. case, to maintain a constant electricity production.

Supposing to fix the total mass flow rate of the feedstock – measured in ton/d and named $\dot{m}_{TOT}$ – and the lower and higher limits of the substrates flow rates, it is possible to write analogous constraints with respect to the batch case:

$$\dot{m}_{i,min} \leq \dot{m}_i \leq \dot{m}_{i,max} \tag{8.4}$$

$$\dot{m}_{TOT} = \sum_{i=1}^{NC} \dot{m}_i \tag{8.5}$$

In order to calculate the objective function f_{obj}, the mass fractions can be calculated according to Equation 8.6.

$$x_i = \frac{\dot{m}_i}{\dot{m}_{TOT}} \tag{8.6}$$

Once having calculated f_{obj} the optimization can be performed by varying the massive flow rates $\dot{m}_i$, allowing to obtain the feedstock conditions that, complying to all the given constraints, maximize the inlet co-digestion BMP.

8.2 Interactive Dashboard Development

To perform the described optimization in an easy and immediate way, both for a batch and CSTR layout, a dedicated *software*, consisting of an interactive Excel dashboard, has been developed. Such dashboard, being connected with a Python™ algorithm, is able to return the optimization results by compiling it with the required inputs.

In Figures 8.1 and 8.2, two examples of usage of the dashboard are reported. In Figure 8.1 (a) the initialization conditions in case of the co-digestion of two substrates (e.g., chicken manure and OFMSW) are reported, while in Figure 8.1 (b) the compiled dashboard and are the results of the related optimization – whose inputs have been specifically elaborated for the sake of the example – are reported. Similarly, Figure 8.1 (a) represents the initialization conditions of the dashboard with three selected substrates (e.g., chicken manure, OFMSW and straw), and Figure 8.2 (b) shows the related results as an example.

The functioning of the software involves that, in the "Substrates Selection" section, the dashboard is linked through a Pivot Table to the database, allowing to select through a slicer the desired substrates and, automatically, their corresponding parameters used for the co-digestion optimization (the C/N ratio, the EBMP and the Biodegradability). The slicer allows the selection of two or three substrates since, up to now, the objective function has been defined in these two cases.

Once having selected the desired substrates, the data are transferred to the "Optimization Section", where the input data of a batch or CSTR-based digester have to be inserted in the dedicated cells – the ones marked with the words "add value". In particular, the required inputs are the pre-optimization conditions – used as first-guess values by the Python™ algorithm –, the two thresholds of each mass flow for a CSTR or of each load for a batch digester, and the desired total mass flow rate/load that must be fed to the digester.

Once having added the required values, by clicking the "Optimization" button, a macro connected to a Python™ algorithm allows to obtain in the dedicated cells – the ones marked with the word "result" – the optimal mass flow rates or loads for each substrate, and the related composition complying to the imposed constraints. The algorithm is able to distinguish the cases in which of two or three substrates are selected.

In addition, two pie charts and a histogram are present to compare the optimized and non-optimized compositions and feedstock BMPs, respectively.

The Python™ algorithm has been linked to the Excel sheet by using the package *PyWin32*, which allows to pick the input values from the desired cells to perform the optimization. Then, the Optimization macro has been built by creating a link to Python through the Visual Basic Advance language.

This dashboard allows to easily select the desired substrates and perform a blending optimization exploiting a reliable database.

Figure 8.1: Initialization of the Excel dashboard (a) and practical example (b) with two substrates

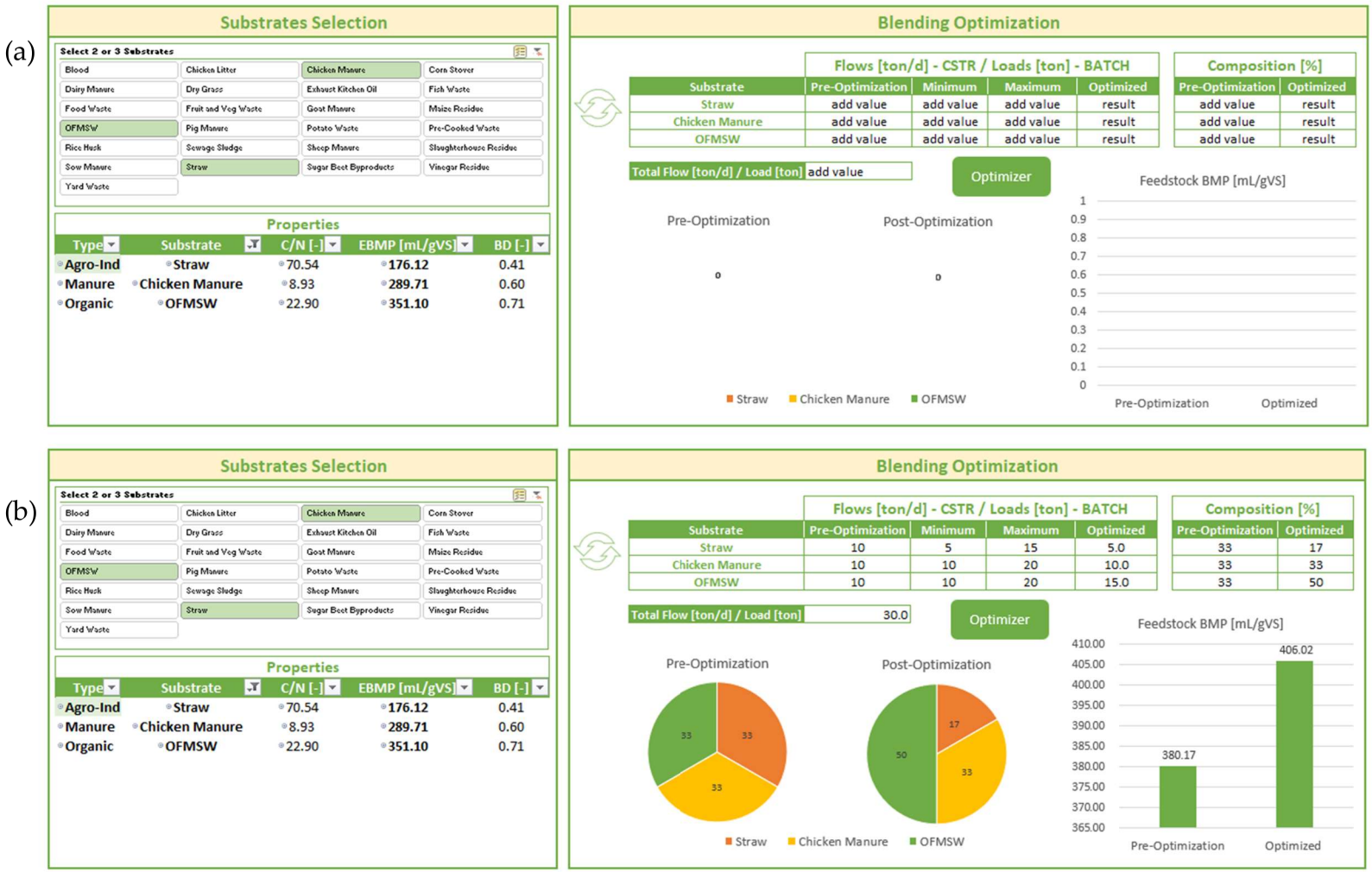

Figure 8.2: Initialization of the Excel dashboard (a) and practical example (b) with three substrates

8.3 Industrial Case Study – CSTR Model Validation

This case study aims at validating the improved version of the optimization tool for a CSTR reactor and is based on the data provided by Thöni s.r.l. – already presented in Chapter 7.

By looking at the experimental data shared by Thöni s.r.l., each substrate is characterized by a lower and a higher value between which the daily load varies during the month, that are shown in Table 8.1.

Mass Flow Rate [ton/d]	Minimum	Maximum
CM	5	5
FVFW	7.5	15.5
ST	11	13

Table 8.1: Lower thresholds (minimum required daily consumption) and higher threshold (daily maximum availability) of the daily loads

As it can be observed in Table 8.1, the lower and higher thresholds for CM are equal since the CM load is always equal to 5 ton/d; the thresholds of FVFW and ST are instead given by the lowest and highest amount of these substrates that have been fed during the month of January.

The total inlet flowrate of the plant is decided on a daily basis according to the current methane production: the total mass flow rate, indeed, is changed day by day in order to reduce or increase the methane output to maintain a constant electricity production. Therefore, to make a comparison between optimized and non-optimized data, in this case study the optimization is performed for each day considering the same total mass flow rate of the real case.

The aim of the study is then to optimize day by day, during the month of January, the daily substrate loads respecting the constraints given by the daily availabilities, the needed consumptions, and the total required mass flow rate.

To do that, the additional constraints must be imposed: each day, the substrates mass flow rates must be comprised between the two thresholds, and the total mass flow rate should be equal to the one assigned to that day. Thus, for each day j = 1…31 the following constraints are imposed:

$$4 \leq \dot{m}_{CM,j} \leq 5 \tag{8.7}$$

$$7.5 \leq \dot{m}_{FVFW,j} \leq 15.5 \tag{8.8}$$

$$11 \leq \dot{m}_{ST,j} \leq 13 \tag{8.9}$$

$$\dot{m}_{TOT,j} = \dot{m}_{CM,j} + \dot{m}_{FVFW,j} + \dot{m}_{ST,j} \tag{8.10}$$

Where $\dot{m}_{TOT,j}$ is fixed and stands for the total load assigned to day j depending on the gas production; the thresholds are assumed to be valid for any day j. It must be noted that $\dot{m}_{CM,j}$ is assumed as comprised between 4 and 5 ton/d in order to introduce a variability of this quantity.

The optimization tool proposes itself to optimize the inlet flow rates so that the inlet BMP is maximized, respecting at the same time the new constraints. Therefore, the mass fractions, that are needed to calculate the objective function, are now calculated as function of the mass flow rates as in Equation 8.11.

$$x_{i,j} = \frac{m_{i,j}}{m_{TOT,j}} \tag{8.11}$$

After that, the objective function f_{obj} can be calculated day by day and maximized to obtain the daily optimal mass flow rates of the substrates.

The optimal daily flow rates that are obtained are reported in Figure 8.3, where the flow rates before optimization are reported too.

As it can observed in Figure 8.3, the optimized mass flow rates now comply to the imposed thresholds, therefore it is here proposed a feasible way in which the methane production of the month of January could have been increased thanks to the maximization of the inlet BMP.

In Figure 8.4 a comparison between the BMP associated with the actual blends and to the optimized ones is presented: there it can be noted that the optimized BMP is significantly higher than the actual one until January 22, after which the optimized blends correspond to the actual ones and so the actual BMPs result to be already optimized.

The described calculations can be quickly performed by using the Excel-Python™ dashboard described in the previous section. The model results obtained using the dashboard for the first day of January are reported in Figure 8.5.

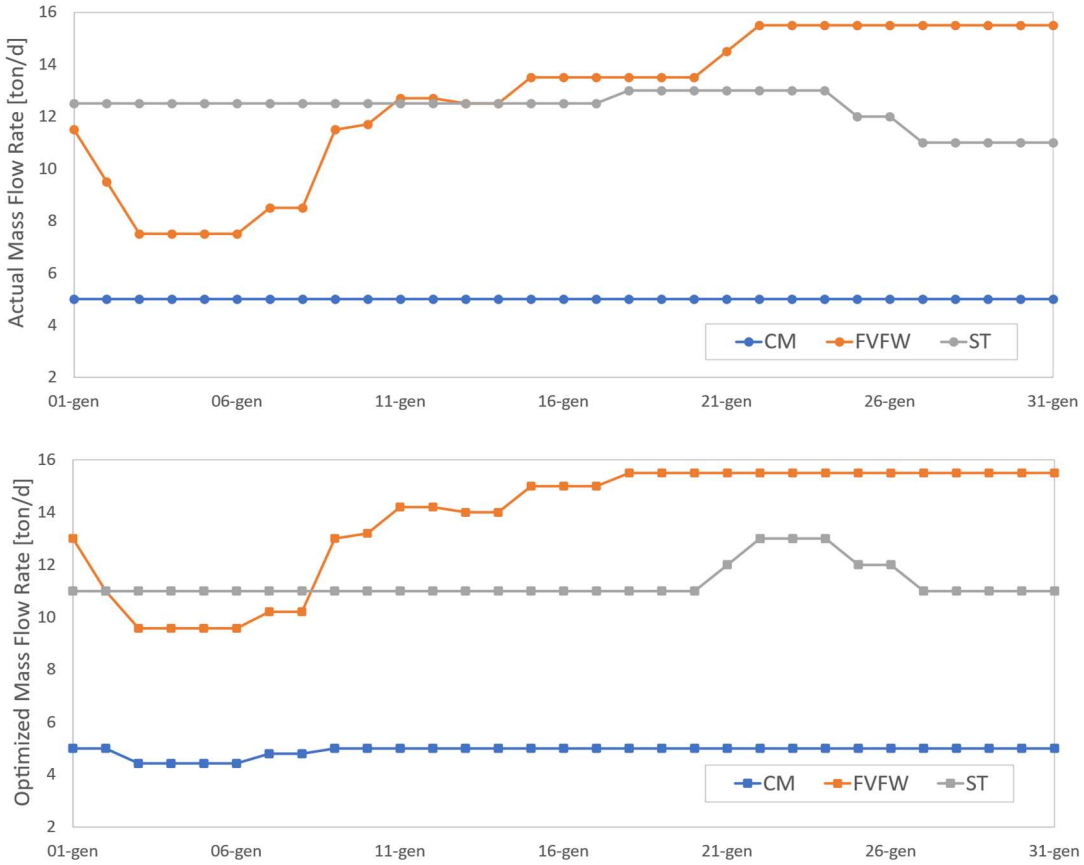

Figure 8.3: Actual mass flow rates and optimized mass flow rates over the month of January

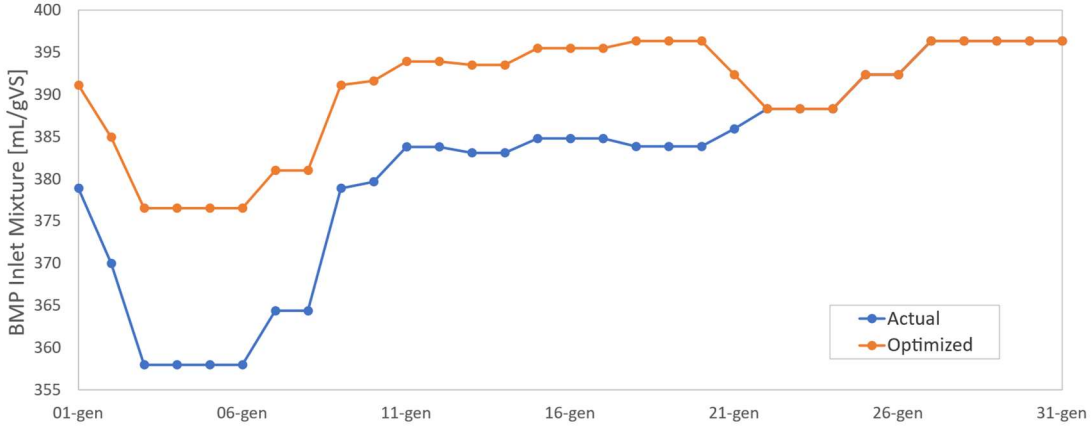

Figure 8.4: Comparison between the actual and optimized BMPs of the inlet mixtures over the month of January

Figure 8.5: Feedstock optimization using the Excel-Python™ dashboard for the day January 1st

Conclusions

The aim of the thesis was to lay the foundations and develop an optimization tool able to predict the optimal feedstock blending of anaerobic digesters, in order to improve biomethane production thanks to a better exploitation of raw materials.

The project started with wide bibliographic research, during which hundreds of scientific articles were carefully read and analysed to deeply understand the subject and to gather information about feedstock properties. During this phase, the main parameters characterizing the substrates were identified, and a parameter representing the biodegradability of the substrates was also defined.

After the bibliographic research, over eighty scientific papers were used to build a database, named *Complete Database*, where data about commonly used substrates were collected. By analysing this database, it was concluded that, even if substrates of the same nature may show differences in their compositions depending on their source, clear similarities could be observed: this allowed the building of another database, the *Primary Averaged Database*, where general values were proposed for the main parameters of substrates.

The data contained in the *Primary Averaged Database* were then analysed to understand if correlations between parameters did exist: the data analysis made it possible to develop mathematical relationships between parameters and also allowed to validate the definition of biodegradability that was previously proposed.

Thanks to the correlations emerged from the *Primary Average Database* analysis, an objective function representing the co-digestion BMP of mixtures of two or three substrates was then developed. The maximization of the objective function allows to calculate the composition of the mixture that maximizes the methane yield. This model was validated by comparing the model results with experimental batch co-digestion tests.

Afterwards, the optimization tool was tested on industrial data, however in this case problems related to the large-scale application had to be faced: because of that, an improvement of the model was proposed to make it suitable for industrial realities,

validating its results with an industrial case study based on the data provided by the company Thöni s.r.l.

The final version of the optimization model represents an efficient and simple way to understand at industrial level how to efficiently combine the different substrates that are supplied to anaerobic digesters, both in case of continuous and discontinuous layouts.

This data-driven model represents an innovative tool that could be helpful in the decision-making processes of biogas plants related to the feedstock management: indeed, it requires only a few, easily available input data to return how substrates should be combined to maximize their biomethane potential; moreover, it could also be used to predict the effect of adding new substrates to the ones that are already fed to an existing digester.

This project, however, is still at its beginnings, and an extremely higher number of factors could be considered to obtain even more realistic and flexible results. Improvements to this model could be given by:

- Enlarging the database with even more data and substrates.
- Adding information about the localization of the biogas plant and about the transport of the substrates, in order to consider not only the availability of substrates and storage capabilities, but also how they are brought from the source to the plant. This could be done by connecting this model to the ADPL (Anaerobic Digestion Plant Locator) software [110], which represents a decision support system for the optimization of the localization of anaerobic digestion plants.
- Connecting the optimization model to anaerobic digestion kinetic models such as ADE [111], that would allow to automatically compare the biogas production in optimized and non-optimized conditions.
- The introduction in the objective function of *correction factors* to improve the prediction of synergistic and antagonistic effects between substrates, since at times an over/under-estimation of the biomethane potential is observed; moreover, they should also allow to predict if substrates do not show synergy at all.
- Extending the objective function expression to an indefinite number of substrates.
- Validating the model results with dedicated experimental tests.

Even if improvements can be certainly done, it is interesting to see how a seemingly chaotic matter such as waste has been somehow rationalised throughout this project, and a tool able to propose how to efficiently combine different substrates has been

developed. Hopefully this technology, once properly improved and experimentally validated, could be made available for industries that are interested in improving their methane production by better exploiting their raw materials. The high practicality of this technology represents indeed its major point of strength.

Bibliography

[1] J. N. Meegoda, B. Li, K. Patel, and L. B. Wang, "A review of the processes, parameters, and optimization of anaerobic digestion," *Int. J. Environ. Res. Public Health*, vol. 15, no. 10, 2018, doi: 10.3390/ijerph15102224.

[2] S. Jain, S. Jain, I. T. Wolf, J. Lee, and Y. W. Tong, "A comprehensive review on operating parameters and different pretreatment methodologies for anaerobic digestion of municipal solid waste," *Renew. Sustain. Energy Rev.*, vol. 52, pp. 142–154, 2015, doi: 10.1016/j.rser.2015.07.091.

[3] F. Battista, "Caratterizzazione del biogas e del digestato in uscita dal reattore anaerobico partendo da diversi feedstock," *Prova Final.*, pp. 1–11, 2021.

[4] M. N. I. Siddique and Z. A. Wahid, "Achievements and perspectives of anaerobic co-digestion: A review," *J. Clean. Prod.*, vol. 194, no. 1, pp. 359–371, 2018, doi: 10.1016/j.jclepro.2018.05.155.

[5] R. Steffen, O. Szolar, and R. Braun, "Feedstocks for anaerobic digestion," *Inst. Agrobiotechnology Tulin, Univ. Agric. Sci. Vienna*, pp. 1–29, 1998.

[6] J. A. Álvarez, L. Otero, and J. M. Lema, "A methodology for optimising feed composition for anaerobic co-digestion of agro-industrial wastes," *Bioresour. Technol.*, vol. 101, no. 4, pp. 1153–1158, 2010, doi: 10.1016/j.biortech.2009.09.061.

[7] S. García-Gen, J. Rodríguez, and J. M. Lema, "Optimisation of substrate blends in anaerobic co-digestion using adaptive linear programming," *Bioresour. Technol.*, vol. 173, pp. 159–167, 2014, doi: 10.1016/j.biortech.2014.09.089.

[8] S. García-Gen, J. Rodríguez, and J. M. Lema, "Control strategy for maximum anaerobic co-digestion performance," *Water Res.*, vol. 80, pp. 209–216, 2015, doi: 10.1016/j.watres.2015.05.029.

[9] M. Verdaguer, M. Molinos-Senante, and M. Poch, "Optimal management of substrates in anaerobic co-digestion: An ant colony algorithm approach," *Waste Manag.*, vol. 50, pp. 49–54, 2016, doi: 10.1016/j.wasman.2016.01.047.

[10] D. Palma-Heredia, M. Verdaguer, M. Molinos-Senante, M. Poch, and M. Cugueró-Escofet, "Optimised blending for anaerobic co-digestion using ant colony approach: Besòs river basin case study," *Renew. Energy*, vol. 168, pp. 141–150, 2021, doi: 10.1016/j.renene.2020.12.064.

[11] A. Gil, M. Toledo, J. A. Siles, and M. A. Martín, "Multivariate analysis and biodegradability test to evaluate different organic wastes for biological treatments: Anaerobic co-digestion and co-composting," *Waste Manag.*, vol. 78, pp. 819–828, 2018, doi: 10.1016/j.wasman.2018.06.052.

[12] M. Ahmadi-Pirlou, M. Ebrahimi-Nik, M. Khojastehpour, and S. H. Ebrahimi, "Mesophilic co-digestion of municipal solid waste and sewage sludge: Effect of mixing ratio, total solids, and alkaline pretreatment," *Int. Biodeterior. Biodegrad.*, vol. 125, pp. 97–104, 2017, doi: 10.1016/j.ibiod.2017.09.004.

[13] X. Wang, G. Yang, Y. Feng, G. Ren, and X. Han, "Optimizing feeding composition and carbon-nitrogen ratios for improved methane yield during anaerobic co-digestion of dairy, chicken manure and wheat straw," *Bioresour. Technol.*, vol. 120, pp. 78–83, 2012, doi: 10.1016/j.biortech.2012.06.058.

[14] A. D. Dima, O. C. Pârvulescu, C. Mateescu, and T. Dobre, "Optimization of substrate composition in anaerobic co-digestion of agricultural waste using central composite design," *Biomass and Bioenergy*, vol. 138, no. March, pp. 8–10, 2020, doi: 10.1016/j.biombioe.2020.105602.

[15] M. Wang, W. Li, P. Li, S. Yan, and Y. Zhang, "An alternative parameter to characterize biogas materials: Available carbon-nitrogen ratio," *Waste Manag.*, vol. 62, pp. 76–83, 2017, doi: 10.1016/j.wasman.2017.02.025.

[16] J. Kainthola, A. S. Kalamdhad, and V. V. Goud, "Optimization of process parameters for accelerated methane yield from anaerobic co-digestion of rice straw and food waste," *Renew. Energy*, vol. 149, pp. 1352–1359, 2020, doi: 10.1016/j.renene.2019.10.124.

[17] D. Li *et al.*, "Effects of feedstock ratio and organic loading rate on the anaerobic mesophilic co-digestion of rice straw and cow manure," *Bioresour. Technol.*, vol. 189, pp. 319–326, 2015, doi: 10.1016/j.biortech.2015.04.033.

[18] M. Jabeen, Zeshan, S. Yousaf, M. R. Haider, and R. N. Malik, "High-solids anaerobic co-digestion of food waste and rice husk at different organic loading rates," *Int. Biodeterior. Biodegrad.*, vol. 102, pp. 149–153, 2015, doi: 10.1016/j.ibiod.2015.03.023.

[19] R. A. Labatut, L. T. Angenent, and N. R. Scott, "Biochemical methane potential and biodegradability of complex organic substrates," *Bioresour. Technol.*, vol. 102,

no. 3, pp. 2255–2264, 2011, doi: 10.1016/j.biortech.2010.10.035.

[20] A. Nielfa, R. Cano, and M. Fdz-Polanco, "Theoretical methane production generated by the co-digestion of organic fraction municipal solid waste and biological sludge," *Biotechnol. Reports*, vol. 5, no. 1, pp. 14–21, 2015, doi: 10.1016/j.btre.2014.10.005.

[21] K. Aboudi, C. J. Álvarez-Gallego, and L. I. Romero-García, "Influence of total solids concentration on the anaerobic co-digestion of sugar beet by-products and livestock manures," *Sci. Total Environ.*, vol. 586, pp. 438–445, 2017, doi: 10.1016/j.scitotenv.2017.01.178.

[22] S. S. V. Varsha, A. F. Soomro, Z. T. Baig, A. K. Vuppaladadiyam, S. Murugavelh, and E. Antunes, "Methane production from anaerobic mono- and co-digestion of kitchen waste and sewage sludge: synergy study on cumulative methane production and biodegradability," *Biomass Convers. Biorefinery*, 2020, doi: 10.1007/s13399-020-00884-x.

[23] Y. Li, R. Zhang, G. Liu, C. Chen, Y. He, and X. Liu, "Comparison of methane production potential, biodegradability, and kinetics of different organic substrates," *Bioresour. Technol.*, vol. 149, pp. 565–569, 2013, doi: 10.1016/j.biortech.2013.09.063.

[24] J. M. Triolo, S. G. Sommer, H. B. Møller, M. R. Weisbjerg, and X. Y. Jiang, "A new algorithm to characterize biodegradability of biomass during anaerobic digestion: Influence of lignin concentration on methane production potential," *Bioresour. Technol.*, vol. 102, no. 20, pp. 9395–9402, 2011, doi: 10.1016/j.biortech.2011.07.026.

[25] N. Sawyerr, C. Trois, and T. Workneh, "Identification and characterization of potential feedstock for biogas production in South Africa," *J. Ecol. Eng.*, vol. 20, no. 6, pp. 103–116, 2019, doi: 10.12911/22998993/108652.

[26] A. M. Buswell and H. F. Mueller, "Mechanism of Methane Fermentation," *Ind. Eng. Chem.*, vol. 44, no. 3, pp. 550–552, 1952, doi: 10.1021/ie50507a033.

[27] I. Angelidaki and W. Sanders, "Assessment of the anaerobic biodegradability of macropollutants," *Rev. Environ. Sci. Biotechnol.*, vol. 3, no. 2, pp. 117–129, 2004, doi: 10.1007/s11157-004-2502-3.

[28] T. Kunatsa and X. Xia, "A review on anaerobic digestion with focus on the role of biomass co-digestion, modelling and optimisation on biogas production and enhancement," *Bioresour. Technol.*, vol. 344, no. PB, p. 126311, 2022, doi: 10.1016/j.biortech.2021.126311.

[29] D. Hidalgo and J. M. Martín-Marroquín, "Biochemical methane potential of

livestock and agri-food waste streams in the Castilla y León Region (Spain)," *Food Res. Int.*, vol. 73, pp. 226–233, 2015, doi: 10.1016/j.foodres.2014.12.044.

[30] F. Raposo *et al.*, "Biochemical methane potential (BMP) of solid organic substrates: Evaluation of anaerobic biodegradability using data from an international interlaboratory study," *J. Chem. Technol. Biotechnol.*, vol. 86, no. 8, pp. 1088–1098, 2011, doi: 10.1002/jctb.2622.

[31] J. Ohemeng-Ntiamoah and T. Datta, "Perspectives on variabilities in biomethane potential test parameters and outcomes: A review of studies published between 2007 and 2018," *Sci. Total Environ.*, vol. 664, pp. 1052–1062, 2019, doi: 10.1016/j.scitotenv.2019.02.088.

[32] G. Yang *et al.*, "Biochemical methane potential prediction for mixed feedstocks of straw and manure in anaerobic co-digestion," *Bioresour. Technol.*, vol. 326, no. December 2020, p. 124745, 2021, doi: 10.1016/j.biortech.2021.124745.

[33] S. Achinas and G. J. W. Euverink, "Theoretical analysis of biogas potential prediction from agricultural waste," *Resour. Technol.*, vol. 2, no. 3, pp. 143–147, 2016, doi: 10.1016/j.reffit.2016.08.001.

[34] T. T. T. Cu *et al.*, "Biogas production from Vietnamese animal manure, plant residues and organic waste: Influence of biomass composition on methane yield," *Asian-Australasian J. Anim. Sci.*, vol. 28, no. 2, pp. 280–289, 2015, doi: 10.5713/ajas.14.0312.

[35] G. K. Kafle and L. Chen, "Comparison on batch anaerobic digestion of five different livestock manures and prediction of biochemical methane potential (BMP) using different statistical models," *Waste Manag.*, vol. 48, pp. 492–502, 2016, doi: 10.1016/j.wasman.2015.10.021.

[36] Y. Deng, L. Qiu, Y. Shao, and Y. Yao, "Process Modeling and Optimization of Anaerobic Co-Digestion of Peanut Hulls and Swine Manure Using Response Surface Methodology," *Energy and Fuels*, vol. 33, no. 11, pp. 11021–11033, 2019, doi: 10.1021/acs.energyfuels.9b02381.

[37] D. Li *et al.*, "Effects of feedstock ratio and organic loading rate on the anaerobic mesophilic co-digestion of rice straw and pig manure," *Bioresour. Technol.*, vol. 187, pp. 120–127, 2015, doi: 10.1016/j.biortech.2015.03.040.

[38] K. Aboudi, C. J. Álvarez-Gallego, and L. I. Romero-García, "Semi-continuous anaerobic co-digestion of sugar beet byproduct and pig manure: Effect of the organic loading rate (OLR) on process performance," *Bioresour. Technol.*, vol. 194, pp. 283–290, 2015, doi: 10.1016/j.biortech.2015.07.031.

[39] Á. Rodríguez-Abalde, X. Flotats, and B. Fernández, "Optimization of the

anaerobic co-digestion of pasteurized slaughterhouse waste, pig slurry and glycerine," *Waste Manag.*, vol. 61, pp. 521–528, 2017, doi: 10.1016/j.wasman.2016.12.022.

[40] B. Gunadi, C. A. Edwards, and C. Blount IV, "The influence of different moisture levels on the growth, fecundity and survival of Eisenia fetida (Savigny) in cattle and pig manure solids," *Eur. J. Soil Biol.*, vol. 39, no. 1, pp. 19–24, 2003, doi: 10.1016/S1164-5563(02)00005-5.

[41] W. Zhang, Q. Lang, S. Wu, W. Li, H. Bah, and R. Dong, "Anaerobic digestion characteristics of pig manures depending on various growth stages and initial substrate concentrations in a scaled pig farm in Southern China," *Bioresour. Technol.*, vol. 156, pp. 63–69, 2014, doi: 10.1016/j.biortech.2014.01.013.

[42] Z. Mei *et al.*, "Anaerobic Mesophilic Codigestion of Rice Straw and Chicken Manure: Effects of Organic Loading Rate on Process Stability and Performance," *Appl. Biochem. Biotechnol.*, vol. 179, no. 5, pp. 846–862, 2016, doi: 10.1007/s12010-016-2035-6.

[43] A. Babaee, J. Shayegan, and A. Roshani, "Anaerobic slurry co-digestion of poultry manure and straw: effect of organic loading and temperature," *J. Environ. Heal. Sci. Eng.*, vol. 11, no. 1, pp. 1–6, 2013, doi: 10.1186/2052-336x-11-15.

[44] M. A. Rahman, H. B. Møller, C. K. Saha, M. M. Alam, R. Wahid, and L. Feng, "Optimal ratio for anaerobic co-digestion of poultry droppings and lignocellulosic-rich substrates for enhanced biogas production," *Energy Sustain. Dev.*, vol. 39, pp. 59–66, 2017, doi: 10.1016/j.esd.2017.04.004.

[45] Y. Li *et al.*, "Evaluating methane production from anaerobic mono- and co-digestion of kitchen waste, corn stover, and chicken manure," *Energy and Fuels*, vol. 27, no. 4, pp. 2085–2091, 2013, doi: 10.1021/ef400117f.

[46] Y. Li, R. Zhang, C. Chen, G. Liu, Y. He, and X. Liu, "Biogas production from co-digestion of corn stover and chicken manure under anaerobic wet, hemi-solid, and solid state conditions," *Bioresour. Technol.*, vol. 149, pp. 406–412, 2013, doi: 10.1016/j.biortech.2013.09.091.

[47] Z. Zahan, M. Z. Othman, and T. H. Muster, "Anaerobic digestion/co-digestion kinetic potentials of different agro-industrial wastes: A comparative batch study for C/N optimisation," *Waste Manag.*, vol. 71, pp. 663–674, 2018, doi: 10.1016/j.wasman.2017.08.014.

[48] J. Shen and J. Zhu, "Optimization of methane production in anaerobic co-digestion of poultry litter and wheat straw at different percentages of total solid and volatile solid using a developed response surface model," *J. Environ. Sci.*

Heal. - Part A Toxic/Hazardous Subst. Environ. Eng., vol. 51, no. 4, pp. 325–334, 2016, doi: 10.1080/10934529.2015.1109395.

[49] J. C. Meneses-Reyes, G. Hernández-Eugenio, D. H. Huber, N. Balagurusamy, and T. Espinosa-Solares, "Biochemical methane potential of oil-extracted microalgae and glycerol in co-digestion with chicken litter," *Bioresour. Technol.*, vol. 224, pp. 373–379, 2017, doi: 10.1016/j.biortech.2016.11.012.

[50] S. M. Ashekuzzaman and T. G. Poulsen, "Optimizing feed composition for improved methane yield during anaerobic digestion of cow manure based waste mixtures," *Bioresour. Technol.*, vol. 102, no. 3, pp. 2213–2218, 2011, doi: 10.1016/j.biortech.2010.09.118.

[51] D. W. Hamilton, "Anaerobic Digestion of Animal Manures: Methane Production Potential of Waste Materials," *Bae 1762*, no. 2, pp. 4–7, 2012, [Online]. Available: pods.dasnr.okstate.edu/docushare/dsweb/Get/Document-8544/BAE-1762web.pdf

[52] K. C. Das, M. Garcia-Perez, B. Bibens, and N. Melear, "Slow pyrolysis of poultry litter and pine woody biomass: Impact of chars and bio-oils on microbial growth," *J. Environ. Sci. Heal. - Part A Toxic/Hazardous Subst. Environ. Eng.*, vol. 43, no. 7, pp. 714–724, 2008, doi: 10.1080/10934520801959864.

[53] Y. Li, S. Achinas, J. Zhao, B. Geurkink, J. Krooneman, and G. J. Willem Euverink, "Co-digestion of cow and sheep manure: Performance evaluation and relative microbial activity," *Renew. Energy*, vol. 153, pp. 553–563, 2020, doi: 10.1016/j.renene.2020.02.041.

[54] W. Li *et al.*, "Methane production through anaerobic co-digestion of sheep dung and waste paper," *Energy Convers. Manag.*, vol. 156, no. May 2017, pp. 279–287, 2018, doi: 10.1016/j.enconman.2017.08.002.

[55] H. Kaur and R. R. Kommalapati, "Optimizing anaerobic co-digestion of goat manure and cotton gin trash using biochemical methane potential (BMP) test and mathematical modeling," *SN Appl. Sci.*, vol. 3, no. 8, 2021, doi: 10.1007/s42452-021-04706-1.

[56] A. Orangun, H. Kaur, and R. R. Kommalapati, "Batch anaerobic co-digestion and biochemical methane potential analysis of goat manure and food waste," *Energies*, vol. 14, no. 7, pp. 1–14, 2021, doi: 10.3390/en14071952.

[57] Y. Zhang, S. Kusch-Brandt, A. M. Salter, and S. Heaven, "Estimating the methane potential of energy crops: An overview on types of data sources and their limitations," *Processes*, vol. 9, no. 9, 2021, doi: 10.3390/pr9091565.

[58] M. S. Kalra and J. S. Panwar, "Anaerobic digestion of rice crop residues," *Agric.*

Wastes, vol. 17, no. 4, pp. 263–269, 1986, doi: 10.1016/0141-4607(86)90134-4.

[59] V. Kryvoruchko, A. Machmüller, V. Bodiroza, B. Amon, and T. Amon, "Anaerobic digestion of by-products of sugar beet and starch potato processing," *Biomass and Bioenergy*, vol. 33, no. 4, pp. 620–627, 2009, doi: 10.1016/j.biombioe.2008.10.003.

[60] A. H. Vazifehkhoran, J. M. Triolo, S. U. Larsen, K. Stefanek, and S. G. Sommer, "Assessment of the variability of biogas production from sugar beet silage as affected by movement and loss of the produced alcohols and organic acids," *Energies*, vol. 9, no. 5, 2016, doi: 10.3390/en9050368.

[61] W. Parawira, M. Murto, R. Zvauya, and B. Mattiasson, "Anaerobic batch digestion of solid potato waste alone and in combination with sugar beet leaves," *Renew. Energy*, vol. 29, no. 11, pp. 1811–1823, 2004, doi: 10.1016/j.renene.2004.02.005.

[62] M. U. Sieborg, B. D. Jønson, S. U. Larsen, A. H. Vazifehkhoran, and J. M. Triolo, "Co-ensiling of wheat straw as an alternative pre-treatment to chemical, hydrothermal and mechanical methods for methane production," *Energies*, vol. 13, no. 15, 2020, doi: 10.3390/en13164047.

[63] M. A. Abdoli, L. Amiri, A. Baghvand, J. Nasiri, and E. Madadian, "Methane Production from Anaerobic Co-Digestion of Maize and Cow Dung," *Environ. Prog. Sustain. Energy*, pp. 676–680, 2013.

[64] M. J. Cuetos, X. Gómez, E. J. Martínez, J. Fierro, and M. Otero, "Feasibility of anaerobic co-digestion of poultry blood with maize residues," *Bioresour. Technol.*, vol. 144, pp. 513–520, 2013, doi: 10.1016/j.biortech.2013.06.129.

[65] E. Bruni, A. P. Jensen, E. S. Pedersen, and I. Angelidaki, "Anaerobic digestion of maize focusing on variety, harvest time and pretreatment," *Appl. Energy*, vol. 87, no. 7, pp. 2212–2217, 2010, doi: 10.1016/j.apenergy.2010.01.004.

[66] R. Gao *et al.*, "Methane yield through anaerobic digestion for various maize varieties in China," *Bioresour. Technol.*, vol. 118, pp. 611–614, 2012, doi: 10.1016/j.biortech.2012.05.051.

[67] Q. Zhou *et al.*, "Minimizing asynchronism to improve the performances of anaerobic co-digestion of food waste and corn stover," *Bioresour. Technol.*, vol. 166, pp. 31–36, 2014, doi: 10.1016/j.biortech.2014.04.074.

[68] S. Achinas, Y. Li, V. Achinas, and G. J. W. Euverink, "Biogas potential from the anaerobic digestion of potato peels: Process performance and kinetics evaluation," *Energies*, vol. 12, no. 12, 2019, doi: 10.3390/en12122311.

[69] Y. Zhang, G. S. Caldwell, A. M. Zealand, and P. J. Sallis, "Anaerobic co-digestion of microalgae Chlorella vulgaris and potato processing waste: Effect of mixing ratio, waste type and substrate to inoculum ratio," *Biochem. Eng. J.*, vol. 143, no. August 2018, pp. 91–100, 2019, doi: 10.1016/j.bej.2018.12.021.

[70] L. Mu, L. Zhang, K. Zhu, J. Ma, M. Ifran, and A. Li, "Anaerobic co-digestion of sewage sludge, food waste and yard waste: Synergistic enhancement on process stability and biogas production," *Sci. Total Environ.*, vol. 704, p. 135429, 2020, doi: 10.1016/j.scitotenv.2019.135429.

[71] I. Naroznova, J. Møller, and C. Scheutz, "Characterisation of the biochemical methane potential (BMP) of individual material fractions in Danish source-separated organic household waste," *Waste Manag.*, vol. 50, pp. 39–48, 2016, doi: 10.1016/j.wasman.2016.02.008.

[72] L. Zhang, K. C. Loh, and J. Zhang, "Food waste enhanced anaerobic digestion of biologically pretreated yard waste: Analysis of cellulose crystallinity and microbial communities," *Waste Manag.*, vol. 79, pp. 109–119, 2018, doi: 10.1016/j.wasman.2018.07.036.

[73] D. Brown and Y. Li, "Solid state anaerobic co-digestion of yard waste and food waste for biogas production," *Bioresour. Technol.*, vol. 127, pp. 275–280, 2013, doi: 10.1016/j.biortech.2012.09.081.

[74] L. Feng *et al.*, "Biochemical methane potential (BMP) of vinegar residue and the influence of feed to inoculum ratios on biogas production," *BioResources*, vol. 8, no. 2, pp. 2487–2498, 2013, doi: 10.15376/biores.8.2.2487-2498.

[75] J. Feng *et al.*, "Enhanced methane production of vinegar residue by response surface methodology (RSM)," *AMB Express*, vol. 7, no. 1, 2017, doi: 10.1186/s13568-017-0392-3.

[76] L. Li *et al.*, "Anaerobic digestion performance of vinegar residue in continuously stirred tank reactor," *Bioresour. Technol.*, vol. 186, pp. 338–342, 2015, doi: 10.1016/j.biortech.2015.03.086.

[77] T. Xie, S. Xie, M. Sivakumar, and L. D. Nghiem, "Relationship between the synergistic/antagonistic effect of anaerobic co-digestion and organic loading," *Int. Biodeterior. Biodegrad.*, vol. 124, pp. 155–161, 2017, doi: 10.1016/j.ibiod.2017.03.025.

[78] L. Wang *et al.*, "Anaerobic co-digestion of kitchen waste and fruit/vegetable waste: Lab-scale and pilot-scale studies," *Waste Manag.*, vol. 34, no. 12, pp. 2627–2633, 2014, doi: 10.1016/j.wasman.2014.08.005.

[79] J. Jiang *et al.*, "Anaerobic digestion of kitchen waste: The effects of source,

concentration, and temperature," *Biochem. Eng. J.*, vol. 135, pp. 91–97, 2018, doi: 10.1016/j.bej.2018.04.004.

[80] V. Cabbai, M. Ballico, E. Aneggi, and D. Goi, "BMP tests of source selected OFMSW to evaluate anaerobic codigestion with sewage sludge," *Waste Manag.*, vol. 33, no. 7, pp. 1626–1632, 2013, doi: 10.1016/j.wasman.2013.03.020.

[81] G. Carucci, F. Carrasco, K. Trifoni, M. Majone, and M. Beccari, "Anaerobic Digestion of Food Industry Wastes: Effect of Codigestion on Methane Yield," *J. Environ. Eng.*, vol. 131, no. 7, pp. 1037–1045, 2005, doi: 10.1061/(asce)0733-9372(2005)131:7(1037).

[82] S. Panigrahi and B. K. Dubey, "A critical review on operating parameters and strategies to improve the biogas yield from anaerobic digestion of organic fraction of municipal solid waste," *Renew. Energy*, vol. 143, pp. 779–797, 2019, doi: 10.1016/j.renene.2019.05.040.

[83] G. Silvestre, A. Bonmatí, and B. Fernández, "Optimisation of sewage sludge anaerobic digestion through co-digestion with OFMSW: Effect of collection system and particle size," *Waste Manag.*, vol. 43, pp. 137–143, 2015, doi: 10.1016/j.wasman.2015.06.029.

[84] Y. Zhang and C. J. Banks, "Co-digestion of the mechanically recovered organic fraction of municipal solid waste with slaughterhouse wastes," *Biochem. Eng. J.*, vol. 68, pp. 129–137, 2012, doi: 10.1016/j.bej.2012.07.017.

[85] L. Alibardi and R. Cossu, "Composition variability of the organic fraction of municipal solid waste and effects on hydrogen and methane production potentials," *Waste Manag.*, vol. 36, pp. 147–155, 2015, doi: 10.1016/j.wasman.2014.11.019.

[86] J. D. Browne and J. D. Murphy, "Assessment of the resource associated with biomethane from food waste," *Appl. Energy*, vol. 104, pp. 170–177, 2013, doi: 10.1016/j.apenergy.2012.11.017.

[87] C. Fonseca, L. M. Frare, L. D'avila, and T. Edwiges, "Influence of different waste compositions from tilapia fish on methane production," *J. Clean. Prod.*, vol. 265, 2020, doi: 10.1016/j.jclepro.2020.121795.

[88] Y. M. Yoon, S. H. Kim, K. S. Shin, and C. H. Kim, "Effects of substrate to inoculum ratio on the biochemical methane potential of piggery slaughterhouse wastes," *Asian-Australasian J. Anim. Sci.*, vol. 27, no. 4, pp. 600–607, 2014, doi: 10.5713/ajas.2013.13537.

[89] A. R. Vidal *et al.*, "Extraction and characterization of collagen from sheep slaughter by-products," *Waste Manag.*, vol. 102, pp. 838–846, 2020, doi:

10.1016/j.wasman.2019.12.004.

[90] J. H. Jeung, D. H. Moon, and S. W. Chang, "Methane Potential of Various Organic Wastes: Study of Biochemical Methane Potential (BMP) Test Before Co-Digestion," no. 2008, pp. 283–288, 2016, doi: 10.1142/9789814723039_0038.

[91] T. H. Nazifa, N. M. Cata Saady, C. Bazan, S. Zendehboudi, A. Aftab, and T. M. Albayati, "Anaerobic digestion of blood from slaughtered livestock: A review," *Energies*, vol. 14, no. 18, pp. 1–25, 2021, doi: 10.3390/en14185666.

[92] Y. Yoon, S. Lee, K. H. Kim, T. Jeon, and S. Shin, "Study of anaerobic co-digestion on wastewater treatment sludge and food waste leachate using BMP test," *J. Mater. Cycles Waste Manag.*, vol. 20, no. 1, pp. 283–292, 2018, doi: 10.1007/s10163-017-0581-9.

[93] Y. Sun, D. Wang, J. Yan, W. Qiao, W. Wang, and T. Zhu, "Effects of lipid concentration on anaerobic co-digestion of municipal biomass wastes," *Waste Manag.*, vol. 34, no. 6, pp. 1025–1034, 2014, doi: 10.1016/j.wasman.2013.07.018.

[94] C. Dennehy *et al.*, "Synergism and effect of high initial volatile fatty acid concentrations during food waste and pig manure anaerobic co-digestion," *Waste Manag.*, vol. 56, pp. 173–180, 2016, doi: 10.1016/j.wasman.2016.06.032.

[95] H. Tian, N. Duan, C. Lin, X. Li, and M. Zhong, "Anaerobic co-digestion of kitchen waste and pig manure with different mixing ratios," *J. Biosci. Bioeng.*, vol. 120, no. 1, pp. 51–57, 2015, doi: 10.1016/j.jbiosc.2014.11.017.

[96] M. Jugal Sukhesh and P. Venkateswara Rao, "Synergistic effect in anaerobic co-digestion of rice straw and dairy manure - a batch kinetic study," *Energy Sources, Part A Recover. Util. Environ. Eff.*, vol. 41, no. 17, pp. 2145–2156, 2019, doi: 10.1080/15567036.2018.1550536.

[97] M. Elsayed, A. Diab, and M. Soliman, "Methane production from anaerobic co-digestion of sludge with fruit and vegetable wastes: effect of mixing ratio and inoculum type," *Biomass Convers. Biorefinery*, vol. 11, no. 3, pp. 989–998, 2021, doi: 10.1007/s13399-020-00785-z.

[98] X. Wang, G. Yang, F. Li, Y. Feng, G. Ren, and X. Han, "Evaluation of two statistical methods for optimizing the feeding composition in anaerobic co-digestion: Mixture design and central composite design," *Bioresour. Technol.*, vol. 131, pp. 172–178, 2013, doi: 10.1016/j.biortech.2012.12.174.

[99] R. Li, S. Chen, and X. Li, "Anaerobic co-digestion of kitchen waste and cattle manure for methane production," *Energy Sources, Part A Recover. Util. Environ. Eff.*, vol. 31, no. 20, pp. 1848–1856, 2009, doi: 10.1080/15567030802606038.

[100] G. Baek, D. Kim, J. Kim, H. Kim, and C. Lee, "Treatment of cattle manure by anaerobic co-digestion with food waste and pig manure: Methane yield and synergistic effect," *Int. J. Environ. Res. Public Health*, vol. 17, no. 13, pp. 1–13, 2020, doi: 10.3390/ijerph17134737.

[101] Z. Zhang, G. Zhang, W. Li, C. Li, and G. Xu, "Enhanced biogas production from sorghum stem by co-digestion with cow manure," *Int. J. Hydrogen Energy*, vol. 41, no. 21, pp. 9153–9158, 2016, doi: 10.1016/j.ijhydene.2016.02.042.

[102] W. Cao, C. Sun, X. Li, J. Qiu, and R. Liu, "Methane production enhancement from products of alkaline hydrogen peroxide pretreated sweet sorghum bagasse," *RSC Adv.*, vol. 7, no. 10, pp. 5701–5707, 2017, doi: 10.1039/c6ra25798d.

[103] M. E. Adrover, I. Cotabarren, E. Madies, M. Rayes, S. B. Rodriguez Reartes, and M. Pedernera, "Anaerobic co-digestion of rabbit manure and sorghum crops in a bench-scale biodigester," *Bioresour. Bioprocess.*, vol. 7, no. 1, 2020, doi: 10.1186/s40643-020-00327-5.

[104] H. Ma, Y. Hu, T. Kobayashi, and K. Q. Xu, "The role of rice husk biochar addition in anaerobic digestion for sweet sorghum under high loading condition," *Biotechnol. Reports*, vol. 27, p. e00515, 2020, doi: 10.1016/j.btre.2020.e00515.

[105] Y. Hu, H. Ma, C. Shi, T. Kobayashi, and K. Q. Xu, "Nutrient augmentation enhances biogas production from sorghum mono-digestion," *Waste Manag.*, vol. 119, pp. 63–71, 2021, doi: 10.1016/j.wasman.2020.09.041.

[106] E. Bellini and E. Giordani, "Advances in Horticultural Science: Foreword," *Adv. Hortic. Sci.*, vol. 22, no. 4, p. 231, 2008.

[107] A. Teghammar, K. Karimi, I. Sárvári Horváth, and M. J. Taherzadeh, "Enhanced biogas production from rice straw, triticale straw and softwood spruce by NMMO pretreatment," *Biomass and Bioenergy*, vol. 36, pp. 116–120, 2012, doi: 10.1016/j.biombioe.2011.10.019.

[108] M. Heiermann, M. Plöchl, B. Linke, H. Schelle, and C. Herrmann, "Biogas Crops - Part I : Specifications and Suitability of Field Crops for Anaerobic Digestion," *Agric. Eng. Int. CIGR Ejournal*, vol. XI, 2009.

[109] I. A. Nges, F. Escobar, X. Fu, and L. Björnsson, "Benefits of supplementing an industrial waste anaerobic digester with energy crops for increased biogas production," *Waste Manag.*, vol. 32, no. 1, pp. 53–59, 2012, doi: 10.1016/j.wasman.2011.09.009.

[110] A. Tagliabue, "Sviluppo di un Decision Support System per l'Ottimizzazione di Impianti di Digestione Anaerobica," 2020.

[111] F. Moretta, E. Rizzo, F. Manenti, and G. Bozzano, "Enhancement of anaerobic digestion digital twin through aerobic simulation and kinetic optimization for co-digestion scenarios," *Bioresour. Technol.*, vol. 341, no. August, p. 125845, 2021, doi: 10.1016/j.biortech.2021.125845.

List of Figures

List of Tables